

Nanoscale multiphase phase field approach for stress- and temperature-induced martensitic phase transformations with interfacial stresses at finite strains

Anup Basak¹ and Valery I. Levitas^{1,2,3*}

¹ *Department of Aerospace Engineering, Iowa State University, Ames, IA 50011, USA.*

² *Departments of Mechanical Engineering, and Material Science and Engineering, Iowa State University, Ames, IA 50011, USA.*

³ *Ames Laboratory, Division of Materials Science and Engineering, Ames, IA 50011, USA.*

A thermodynamically consistent, novel multiphase phase field approach for stress- and temperature-induced martensitic phase transformations at finite strains and with interfacial stresses has been developed. The model considers a single order parameter to describe the austenite \leftrightarrow martensitic transformations, and another N order parameters describing N variants and constrained to a plane in an N -dimensional order parameter space. In the free energy model coexistence of three or more phases at a single material point (multiphase junction), and deviation of each variant-variant transformation path from a straight line have been penalized. Some shortcomings of the existing models are resolved. Three different kinematic models (KMs) for the transformation deformation gradient tensors are assumed: (i) In KM-I the transformation deformation gradient tensor is a linear function of the Bain tensors for the variants. (ii) In KM-II the natural logarithms of the transformation deformation gradient is taken as a linear combination of the natural logarithm of the Bain tensors multiplied with the interpolation functions. (iii) In KM-III it is derived using the twinning equation from the crystallographic theory. The instability criteria for all the phase transformations have been derived for all the kinematic models, and their comparative study is presented. A large strain finite element procedure has been developed and used for studying the evolution of some complex microstructures in nanoscale samples under various loading conditions. Also, the stresses within variant-variant boundaries, the sample size effect, effect of penalizing the triple junctions, and twinned microstructures have been studied. The present approach can be extended for studying grain growth, solidifications, para \leftrightarrow ferro electric transformations, and diffusive phase transformations.

Keywords: Multiphase phase field approach; Martensitic transformation; Variant-variant boundary; Twinning; Multiphase junction; Instability of phase; Interfacial stress; Finite strain; Size effect.

1. Introduction

Multivariant martensitic transformations (crystallographic theory). Martensitic phase transformation (PT) plays the central role in exhibiting some important phenomena, such as shape memory effect, pseudoelasticity, and pseudoplasticity (Bhattacharya (2004); Pitteri and Zanzotto (2003)). Such transformations usually result in complex microstructures, including austenite-twinned martensites, wedge, twins within twins etc. (Ball and James (1987); Bhattacharya (2004); Pitteri and Zanzotto (2003); Schryvers (1993); Wayman (1964)). In this paper we denote the austenite phase (parent phase) by A , the martensite (product phase) by M , and the N variants of martensites by $M_1, M_2, \dots, M_i, M_j, \dots, M_N$. In actual microstructures we seldom see interface between A and a single martensite variant, as the lattices of stress-free A and a single M_i are not geometrically compatible in the sense of Hadamard's compatibility. The system rather prefers to form microstructures consisting of mixture of austenite and twinned martensite, which are laminated microstructures with planar interfaces, and are minimizer of the total elastic energy of the system (Ball and James (1987); Bhattacharya (2004); Pitteri and Zanzotto (2003)). The interface between A and twinned martensite in such microstructures is diffused, i.e. has a finite width. The compatibility condition therein is satisfied in an average sense, and the local incompatibility is accommodated by elastic strains. However, away from the A - M interface the elastic stresses vanish. On the other hand, twin boundaries are compatible sharp interfaces, and hence the elastic stresses are vanishing, both within the variants and twin boundaries.

Multiphase phase field approach to martensitic PTs. Besides various continuum studies of multivariant martensitic PTs within a sharp interface approach (Ball and James (1987); Levitas and Ozsoy (2009a,b); Petryk and Stupkiewicz (2010a,b); Roytburd (1974); Roytburd and Slutsker (2001)), the phase field approaches (also known as the Ginzburg-Landau approaches) have been widely used for studying microstructure evolution during martensitic PTs (Artemev et al. (2000, 2001, 2005); Chen (2002); Clayton and Knap (2011a,b); Hildebrand and Miehe (2012); Idesman et al. (2008); Jin et al. (2001); Lei et al. (2010); Levin et al. (2013); Levitas and Javanbakht (2011); Levitas and Lee (2007); Levitas and Preston (2002a,b); Levitas et al. (2003, 2013, 2009); Li et al. (2001); Seol et al. (2002, 2003); Tůma and Stupkiewicz (2016); Tůma et al. (2016)). The central idea in all the phase field approaches is to introduce the order parameters for describing the PTs in a continuous way. The free energy of the system and the transformation strains are functions of the order parameters. These

functions include interpolation of all material properties between their values in each phase, the energy barrier between phases, and the terms related to the gradient of the order parameters penalizing interfaces between phases. The interfaces are therefore of finite width and their structures are also resolved.

The evolution of the order parameters is governed by a system of Ginzburg-Landau equations. Here we consider the transformation strain related order parameters, (see, e.g. Artemev et al. (2001); Levitas (2014); Levitas and Preston (2002b); Levitas et al. (2003)), in contrast to the total strain related order parameters in Barsch and Krumhansl (1984); Falk (1983); Jacobs (1992). The latter cannot be used to satisfy some important requirements formulated in Levitas (2013a); Levitas and Preston (2002a,b); Levitas and Roy (2016).

A critical analysis of the multiphase phase field approaches (MPFA) to PTs is now presented, highlighting their main features and drawbacks (see also Levitas and Roy (2015, 2016); Tóth et al. (2015)).

MPFA-I: In this approach N volume fraction related order parameters η_i along with a single constraint $\sum_{i=1}^N \eta_i = 1$ are considered for a system with $N + 1$ phases; see Refs. Ankit et al. (2013); Bollada et al. (2012); Garcke et al. (1999); Kim et al. (2006); Moelans et al. (2008, 2009); Nestler (2005); Steinbach et al. (1996); Steinbach and Pezzolla (1999); Tóth et al. (2011a,b, 2015). The models have been mostly used for studying solid \leftrightarrow liquid transformations and grain growth without mechanics, as well as for PTs between solid phases with mechanics (Schneider et al. (2015); Steinbach and Apel (2006)). The constraint plane is schematically shown in η_i - η_j - η_k space in Fig. 1(a), and all the liquid \leftrightarrow solid (or $A \leftrightarrow M_i$) transformation paths belong to this plane. This single constraint alone cannot ensure that each of the PTs can be described by a single order parameter, which is an important condition for calibrating the model parameters, and also to prevent the appearance of a third (if spurious) phase between two others (Levitas and Roy (2015, 2016)). A specialized model for a three phase system was derived by Folch and Plapp (Folch and Plapp (2003, 2005)) which successfully prevents the spurious phase, but yields a restriction on the kinetic coefficients. Also, it is not clear how to generalize the model for a system with more phases. Conversely, there can be instances where a third phase can actually nucleate between two others and plays an important role; see, e.g. solid-solid PT via intermediate (virtual) melt (Levitas et al. (2004, 2012)). Hence a robust model should have a provision to control the nucleation of a third phase between two others and also the quantity. The disadvantages of imposing the constraint using the Lagrangian multipliers (used in Folch and Plapp (2003, 2005)) are analyzed and overcome in Ref. Bollada

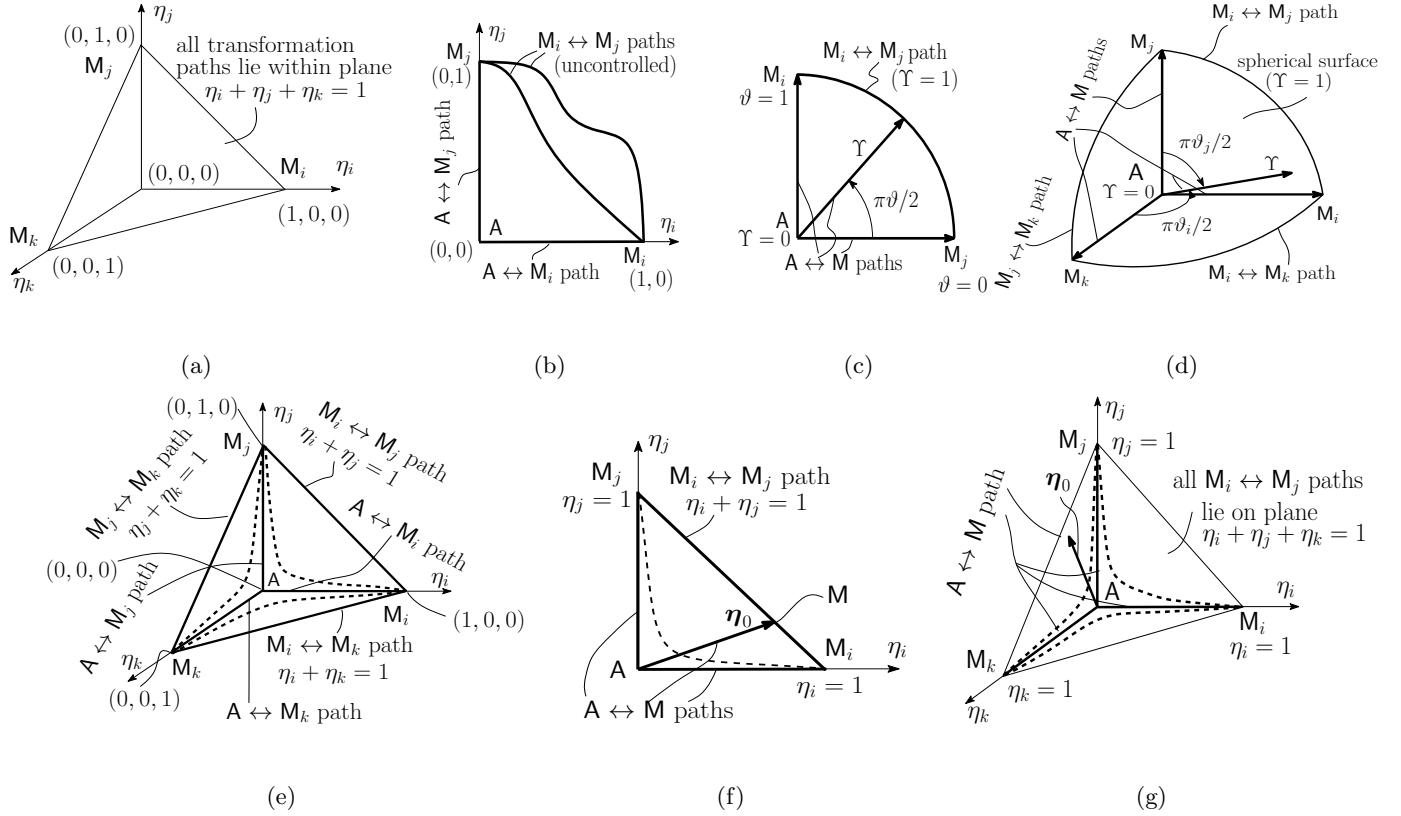


Figure 1: Schematics of the order parameter space and the transformation paths from various models. (a) Models used in Ankit et al. (2013); Bollada et al. (2012); Garcke et al. (1999); Kim et al. (2006); Moelans et al. (2008, 2009); Nestler (2005); Steinbach et al. (1996); Steinbach and Pezzolla (1999); Tóth et al. (2011a,b, 2015) where all the transformation paths lie within the $\eta_i + \eta_j + \eta_k = 1$ plane. (b) Model used in Artemev et al. (2000, 2001); Jin et al. (2001); Levitas (2013a); Levitas and Preston (2002a,b); Li et al. (2001); Seol et al. (2002, 2003), for which variant \leftrightarrow variant transformation paths cannot be described with a single order parameter and are not controlled. (c) & (d) Models with polar (c) and hyperspherical (d) order parameters (Levitas et al. (2003, 2013)). (e) Model developed in Levitas and Roy (2015, 2016), for which transformation paths between martensitic variants are controlled by penalizing the energy term. (f) & (g) Present model with two variants and three variants, respectively.

et al. (2012). Further improvement of the model is presented in Tóth et al. (2015) where the drawbacks of the previous models are analyzed in detail. The last model was analyzed in Levitas and Roy (2016). Note that none of these models containing the constraint describe the instability criteria, which are very important in PTs.

In this context, we also mention that the volume fraction related order parameters have also been used

to study martensitic PTs, e.g. in Refs. Idesman et al. (2005); Lei et al. (2010); Levitas et al. (2004); Tůma and Stupkiewicz (2016); Tůma et al. (2016), where all the interpolation functions are linear and represent the simple mixture rule. Such models work well in microscale modelings, in which the interface width is either artificially increased from its actual size of one to a few nanometers by one to several orders of magnitude. At the nanoscale, when one mimics actual processes practically at the atomistic scale, the interpolation functions must be smooth. The first derivative of the interpolation functions must vanish within the bulk – a criterion imposed by the thermodynamic equilibrium condition (Levitas (2013a); Levitas and Preston (2002a,b)). We will focus here on the nanoscale models.

MPFA-II: The authors in Refs. Artemev et al. (2000, 2001); Jin et al. (2001); Li et al. (2001); Seol et al. (2002, 2003) considered N order parameters η_i for a system with N variants, where each η_i describes $A \leftrightarrow M_i$ transformations ($\eta_i = 0$ in A and $\eta_i = 1$ in M_i). Additional conditions for such a choice have been imposed in Levitas (2013a); Levitas and Preston (2002a,b) for small and large strains, which in particular include lattice instability conditions, and lead to more complex thermodynamic potentials and expressions for the transformation strains. These functions are designed in such a way that the instability criteria for $A \leftrightarrow M_i$ and $M_i \leftrightarrow M_j$ transformations yield the expected phase transformation conditions. Since $A \leftrightarrow M_i$ PTs are described with the single order parameter η_i (Fig. 1(b)), the analytical solution for static and propagating A - M_i interface exists, which allows one to calibrate the energy, width, and mobility of the A - M_i interfaces. However, $M_i \leftrightarrow M_j$ transformations cannot be described by a single order parameter, because they occur along some curvilinear path within the η_i - η_j plane (Fig. 1(b)), which depend in some way on temperature and stresses and thus are uncontrolled. That is why an analytical solution for M_i - M_j interface cannot be obtained. The numerically determined energy and width of M_i - M_j interfaces therefore depend on the stresses and temperature in an artificial way. As a result, the parameters for these interfaces cannot be calibrated, and also, interfacial stresses cannot be introduced consistently within the theory. Also, there is no treatment for the multiphase junctions.

MPFA-III: A phase field model based on hyperspherical order parameters was developed in Levitas et al. (2003, 2013) for N -variant martensitic PTs (see Figs. 1(d)). In Levitas and Momeni (2014); Momeni and Levitas (2014, 2015), a similar model for three phases was developed with polar order parameters and applied

to transformations between two solid phases and melt, namely, for solid-solid PT via intermediate melt Figs. 1(c). Here A (or melt) was considered to be located at the center and all N martensitic variants (or solid phases) are placed at the intersection of the Cartesian axes and the N -dimensional hypersphere. The radial coordinate Υ was used as the order parameter for $A \leftrightarrow M$ transformations and N angles $\pi\vartheta_i/2$ between the radius vector Υ and N Cartesian axes related to M_i were utilized as angular order parameters describing $M_i \leftrightarrow M_j$ transformations. Obviously, all the ϑ_i satisfy a nonlinear constraint $\sum_{i=1}^N \cos^2(\pi\vartheta_i/2) = 1$ (Levitas et al. (2013)). The radial lines along the Cartesian axes represent the $A \leftrightarrow M_i$ transformation paths, and the $M_i \leftrightarrow M_j$ transformation paths belong to the quarter circle. Thus, each transformation path is described by a single order parameter; analytical solutions for all the order parameters exist; all interfacial parameters can be calibrated; the interfacial stresses can be introduced in consistent manner. The desired lattice instability conditions for hyperspherical order parameters have been proved in Levitas et al. (2003) using local Cartesian order parameters η_i . However, the constraint equation has infinite derivatives at M_i , which does not allow to extend the proof for the hyperspherical order parameters. Thus, the lattice instability conditions cannot be non-contradictorily implemented for the hyperspherical order parameters. Then, the nonlinear constraint was replaced by a linear constraint (Levitas et al. (2013)), which is simpler but has the same problem with instability conditions like in *MPFA-I*. However, only for a two variant system or three-phase system in polar coordinate with single angular order parameter, the constraint was eliminated and all the issues were resolved.

MPFA-IV: The models recently developed in Levitas and Roy (2015, 2016) operate with the traditional Cartesian order parameters η_i like in *MPFA-II*, see e.g. Artemev et al. (2000); Levitas (2013a); Seol et al. (2002). However, each variant-variant transformation path (or path between phases with one of the order parameter equal to unity) is regulated therein by penalizing the free energy for deviation of the transformation paths from the prescribed straight lines connecting two martensitic variants. More specifically, a controlling parameter is used within this penalizing term for each variant \leftrightarrow variant path. When the coefficient in the penalizing term, K , tends to infinity, the path for $M_i \leftrightarrow M_j$ transformation coincides with the straight line $\eta_i + \eta_j = 1$ (see Fig. 1(e)), and under such condition the third phase (A in this case) is strictly prohibited between two others. However, when the magnitude K is small, the third phase may coexist within an interface, and the variant \leftrightarrow variant transformation paths (or path between two phases) for such cases are indicated by

dashed curves belonging to the η_i - η_j plane. $A \leftrightarrow M_i$ transformation paths are along the Cartesian axes. Since for very large K all transformation paths can be described by a single order parameter, an analytical solution exists for all the interfaces, and all the interface parameters were consistently calibrated. Also, the model penalizes the junctions between the martensitic variants.

Although the model in Levitas and Roy (2015, 2016) is the most advanced and consistent, the following problems still persist:

(a) There is no free material parameter within the interpolation functions for all phases, and all the phases are thus equivalent. That means the interpolation functions are invariant with respect to interchange of phases. However, for martensitic PT the martensitic variants are indeed equivalent but not the austenite phase. That is why the interpolation functions for A - M_i transformations should not be invariant with respect to an exchange of phases, and should contain an additional material parameter to control this. Recent molecular dynamic simulations (Levitas et al. (2017)) show that such a parameter is needed to satisfy the lattice instability conditions under multiaxial loading. Note that in all the previous models except in Levitas (2013a); Levitas and Preston (2002a,b), the interpolation functions do not possess any free material parameters.

(b) Although the junctions between the martensitic variants were penalized, the junctions between A and the variants were not penalized.

(c) The effective kinetic coefficient for the variant-variant interfaces determined therein (Eq. (24)₂ in Levitas and Roy (2015)) is not symmetric about the diagonal elements of the original kinetic coefficient matrix which are basically the kinetic coefficients of the respective A - M_i interfaces. Hence it is an inappropriate expression.

(d) The model is presented for stress-free state in Levitas and Roy (2016) and small strain formulations in Levitas and Roy (2015); the finite strain formulation is still missing.

Interfacial stresses. The interfacial stresses can play a crucial role in the nucleation of phases and propagation of the A - M and variant-variant interfaces (Levitas and Javanbakht (2010, 2011)). Such stresses can significantly decrease the activation energy for intermediate melt within solid-solid interfaces (Momeni et al. (2015)), or result in PTs in nanoscale wires (Diao et al. (2003); Li et al. (2010)). Therefore, a complete phase field model must consider these stresses. We recall that the interfaces or material surfaces are always subjected to biaxial stresses $\bar{\sigma}^s$ (Gibbs (1948)), where $\bar{\sigma}^s$ is the surface Cauchy stress tensor which is a symmetric tensor tangential

to the interface (see Gurtin and Murdoch (1975) for details). For a solid-solid interface the interfacial stress tensor is given by the Shuttleworth equation $\bar{\boldsymbol{\sigma}}^s = \gamma(\mathbf{I} - \mathbf{n} \otimes \mathbf{n}) + \partial\gamma/\partial\bar{\boldsymbol{\varepsilon}}^s$, where $\bar{\boldsymbol{\varepsilon}}^s$ is the average surface strain tensor which is symmetric and tangential to the interface (Fischer et al. (2008); Gurtin and Murdoch (1975)). The part $\gamma(\mathbf{I} - \mathbf{n} \otimes \mathbf{n})$ is called the structural stress tensor, and $\partial\gamma/\partial\bar{\boldsymbol{\varepsilon}}^s$ is the elastic stress tensor within the surfaces. The elastic interfacial stresses appear automatically within the solution of coupled phase field and elasticity problems. An analytical solution for them within a variant-variant interface was found in Basak and Levitas (2017). Structural interfacial stresses, i.e. biaxial tensile stresses with the magnitude equal to the interface energy, were introduced in phase field for solid-solid PTs, first for small strains (Levitas and Javanbakht (2010, 2011)), and then in the most general form for large strains with isotropic (Levitas (2014)) and anisotropic (Levitas and Warren (2016)) interfacial energy. To introduce the interfacial stresses consistently, one needs to have the analytical solution for a propagating interface. Since for the analytical solution for the variant-variant interfaces was lacking for the most popular MPFA-II, the interfacial stresses were introduced therein at a best guess. The interfacial stresses were correctly introduced for a three-phase model in the polar order parameters (Momeni and Levitas (2016)) and the models with multivariant martensitic transformations in Levitas and Roy (2015); Levitas et al. (2013)) (without detailed derivations). However, these models have drawbacks as discussed above.

Goal and contribution of this paper. Our goal in this paper is to develop a thermodynamically consistent and non-contradictory multiphase phase field approach to stress- and temperature-induced martensitic transformations with interfacial stresses and at finite strains, in which all the shortcomings of the previous models MPFA-I to MPFA-IV are resolved. In particular,

- (i) All of the $A \leftrightarrow M_i$ and variant \leftrightarrow variant transformation paths are well controlled in the present approach, and the existence of a third phase between any two other phases is regulated as desired (compare with MPFA-I and II). The M_i - M_j interfacial energy, width, and kinetic coefficients have been calibrated.
- (ii) The interpolation functions for the $A \leftrightarrow M$ transformations contain a free material parameter for accommodating the non-equivalence of the austenite and martensite and providing the required flexibility in the lattice instability conditions (compare with MPFA I to IV).
- (iii) All possible multiphase junctions have been consistently penalized (compare with MPFA-I to IV).

(iv) The model is applicable for any number of variants (compare with MPFA-III).

(v) The desired instability criteria for all the phases are also established (compare with MPFA-I and II).

Our model considers $N + 1$ order parameters in a system with A and N martensitic variants. The key point is to describe $A \leftrightarrow M$ PTs separately from $M_i \leftrightarrow M_j$ PTs. The order parameter η_0 is introduced, which describes $A \leftrightarrow M$ transformations and is assumed to be 0 in A and 1 in M. To some extent η_0 is similar to radial order parameter Υ for hyperspherical order parameters, and shown as a vector $\boldsymbol{\eta}_0$ in Fig. 1(f) and (g). Other N order parameters η_i describe the martensitic variants such that $\eta_i = 1$ in M_i and $\eta_i = 0$ in M_j for all $j \neq i$. We constrain all η_i such that $\sum_i^N \eta_i = 1$, i.e. all the variant-variant transformation paths are constrained to a plane in the order parameter space η_i ; see the schematics in Fig. 1 for a two variant system in (f) and a three variant system in (g). Since η_0 is independent of η_i , the η_0 line does not belong to the order parameter space η_i and is just shown conventionally. It starts at 0 (A) where $\eta_0 = 0$ and ends at $\eta_0 = 1$ corresponding to M and shown conventionally at the martensitic plane $\sum_i^N \eta_i = 1$. The thermodynamic potential is designed in a way that $A \leftrightarrow M$ PTs occur at some $\eta_i = 1$ and $\eta_j = 0$ for all $j \neq i$. That is why the line η_0 may be conventionally directed along a Cartesian axis along which a specific martensitic variant transforms.

For controlling a third phase M_k ($k \neq i, j$) between two others, M_i and M_j , a similar idea from Refs. Levitas and Roy (2015, 2016) have been considered, i.e. the free energy is penalized for deviation of the $M_i \leftrightarrow M_j$ paths from $\eta_i + \eta_j = 1$, for all i, j and $i \neq j$. In order to prevent the third phase, the penalizing coefficient is assumed to tend to infinity, and to allow it the coefficient is taken to be small. Also, all possible multiphase junctions, including those made by A and various martensitic variants, have been penalized. Note that when there are two variants, the path $\eta_i + \eta_j = 1$ strictly follows from the constraint $\sum_{i=1}^N \eta_i = 1$.

Since the analytical solutions in our model exist for all interfaces, the interfacial stresses for all interfaces can be introduced in a manner similar to the case for a single order parameter in Levitas (2014). An appropriate expression for the Helmholtz free energy has been developed and the dissipation inequalities are derived. Based on these inequalities, the system of Ginzburg-Landau equations for the order parameters have been formulated. Three different kinematic models (KMs) are assumed for the transformation deformation gradient \boldsymbol{F}_t :

(i) In KM-I we express \boldsymbol{F}_t as a linear function of the Bain tensors of all the variants multiplied with the nonlinear interpolation functions, similar to Levitas (2013a); Levitas et al. (2013).

(ii) In KM-II we assume the natural logarithm of \mathbf{F}_t as a linear function of the natural logarithm of the Bain tensors multiplied with the interpolation functions, similar to Basak and Levitas (2017); Tůma and Stupkiewicz (2016); Tůma et al. (2016).

(iii) In KM-III we derive \mathbf{F}_t using the twinning equation from the crystallographic theory of martensite, similar to Clayton and Knap (2011a); Levitas and Preston (2002a, 2005).

It is to be noted that KM-II and III yield isochoric variant-variant transformations, but for KM-I the transformation is volume changing. The lattice instability criteria for $A \leftrightarrow M$ and $M_i \leftrightarrow M_j$ transformations have been established for all the kinematic models, and a comparative study of the role of \mathbf{F}_t in the transformation work and instability criteria has been presented.

A large strain finite element procedure has been developed and implemented using an open source deal.ii framework (Bangerth et al. (2016)). Several model problems, yielding complex microstructures, have been solved.

The effects of external loading, penalizing the triple junctions, and the size of the sample on microstructures have been studied. In some cases differences in the microstructures are observed for KM-I and II even when all other parameters and conditions are exactly identical. The normal elastic stress in the longitudinal direction for the variant-variant interfaces (including the twin boundaries) are significantly large for both KM-I and II; in fact, it is much larger for KM-II than that for KM-I, the reason for which has been investigated in Basak and Levitas (2017). The KM-III yields excess elastic stress-relaxed twin boundaries.

The paper has been organized in the following manner. In Section 2, the order parameters are described. In Section 3, the essential kinematic relations are enlisted. A general theory and the thermodynamic formalism of our multiphase phase field approach, including expression for the free energy density, derivation of the Ginzburg-Landau equations, constitutive relations for \mathbf{F}_t , and analysis of the transformation work for all the KMs have been presented in Section 4. The thermodynamic instability criteria for the phase transformations are established and analyzed in Section 5. All the governing equations for the model are summarized in Section 6. The analytical solutions of our Ginzburg-Landau equations and the material parameters for NiAl alloy are listed in Section 7. The finite element results for some model problems have been presented in Section 8. Finally, the paper is concluded in Section 9.

Notation: We denote the inner product and multiplication of two second order tensors as $\mathbf{A} : \mathbf{B} = A_{ij}B_{ji}$ and $(\mathbf{A} \cdot \mathbf{B})_{ij} = A_{ik}B_{kj}$, respectively, where repeated indices assume Einstein's summation, and A_{ij} and B_{ij} are the components of the tensors in a right handed orthonormal Cartesian basis $\{\mathbf{e}_1, \mathbf{e}_2, \mathbf{e}_3\}$. The Euclidean norm of \mathbf{A} is denoted as $|\mathbf{A}| = (\mathbf{A}^T : \mathbf{A})^{1/2}$; \mathbf{I} is the second order identity tensor; \mathbf{A}^{-1} and \mathbf{A}^T , respectively, denote the inversion and transposition of \mathbf{A} ; $\text{cof } \mathbf{A}$, $\text{dev } \mathbf{A}$, $\text{det } \mathbf{A}$ and $\text{tr } \mathbf{A}$ designate the cofactor, deviatoric part, determinant, and trace of \mathbf{A} , respectively; $\mathbf{a} \otimes \mathbf{b}$ is the dyadic product of two arbitrary vectors \mathbf{a} and \mathbf{b} . The reference, stress-relaxed intermediate, and current configurations are denoted by Ω_0 , Ω_t , and Ω , respectively (script 0 means that the quantity is defined in Ω_0). The symbols ∇_0 and ∇ designate the gradient operators in Ω_0 and Ω , respectively; $\nabla_0^2 := \nabla_0 \cdot \nabla_0$ and $\nabla^2 := \nabla \cdot \nabla$ are the Laplacian operators in Ω_0 and Ω , respectively. The symbol $:=$ stands for equality by definition.

2. Order Parameters

The main desired feature of our model is to decouple the description of $\mathbf{A} \leftrightarrow \mathbf{M}$ PTs from the description of $\mathbf{M}_i \leftrightarrow \mathbf{M}_j$ PTs. This will allow us to avoid the phase equivalence condition (which is mandatory for martensitic variants) in the formulation for $\mathbf{A} \leftrightarrow \mathbf{M}$ PTs and use the same general interpolation functions used for the theories with single order parameter (see e.g. Levitas (2013a); Levitas and Preston (2002a,b)). That is why we introduce a separate order parameter η_0 for the description of the $\mathbf{A} \leftrightarrow \mathbf{M}$ PT, which is equal to 0 in \mathbf{A} and 1 in \mathbf{M} . Clearly there is a similarity between η_0 and the radial order parameter Υ within the hyperspherical order parameters in Levitas et al. (2003, 2013). Martensitic variants are described by N order parameters η_i such that $\eta_i = 1$ in \mathbf{M}_i and $\eta_i = 0$ in \mathbf{M}_j for all $j \neq i$. To focus on the variant-variant transformations we impose the constraint

$$\sum_{i=1}^N \eta_i = 1, \quad (1)$$

which is similar to the one accepted in the multiphase phase field approaches (Bollada et al. (2012); Garcke et al. (1999); Kim et al. (2006); Moelans et al. (2009); Nestler (2005); Steinbach et al. (1996); Tóth et al. (2015)). Geometrically, Eq. (1) describes a plane in the order parameter space η_i (Fig. 1 (f) and (g)) passing through all the martensitic variants. While we wrote in Levitas and Roy (2015, 2016) that accepting the constraint (1) does not allow one to impose the instability conditions, this can however be overcome in the current approach.

Indeed, with the penalizing energy term we will have an option to constrain η_i to the lines $\eta_i + \eta_j = 1$ connecting martensitic variants, and the instability conditions will be applied when this constraint is imposed. In contrast to the hyperspherical order parameters, for which Υ can be naturally presented geometrically along with all other (angular) order parameters (Fig. 1 (c) and (d)), η_0 is independent of η_i and does not belong to the order parameter space η_i . Still we have shown it conventionally in Fig. 1 (f) and (g). The η_0 -line (shown as a vector in those figures) starts at 0 (A) and ends at $\eta_0 = 1$ corresponding to the martensitic plane $\sum_i^N \eta_i = 1$. As it will be seen later, the thermodynamic potential constrain the A \leftrightarrow M PTs to some $\eta_i = 1$ and $\eta_j = 0$ for all $j \neq i$. That is why the η_0 -line may be conventionally directed along the Cartesian axis corresponding to a specific martensitic variant.

We denote the set of the arbitrary order parameters as $\tilde{\eta} = (\eta_0, \eta_1, \dots, \eta_i, \dots, \eta_N)$ with the subset $\tilde{\eta}_M = (\eta_1, \dots, \eta_i, \dots, \eta_N)$ for martensitic variants. Also, denote $\hat{\eta}_0 = (\eta_0 = 0, \eta_1, \dots, \eta_i, \dots, \eta_N)$ for A and $\hat{\eta}_i = (\eta_0 = 1, \eta_1 = 0, \dots, \eta_i = 1, \dots, \eta_N = 0)$ for martensitic variant M_i .

3. Kinematics

Let us denote the position vectors of a particle in the reference configuration Ω_0 and the current configuration Ω by \mathbf{r}_0 and \mathbf{r} , respectively, where $\mathbf{r} = \mathbf{r}(\mathbf{r}_0, t) = \mathbf{r}_0 + \mathbf{u}$, and t and \mathbf{u} are time instance and displacement vector, respectively. In the intermediate configuration Ω_t the body is imagined to be a set of arbitrarily small disjoint pieces which are stress-relaxed. Denoting the mapping from Ω_0 to Ω_t by \mathbf{F}_t and the mapping from Ω_t to Ω by \mathbf{F}_e , the total deformation gradient $\mathbf{F} := \nabla_0 \mathbf{r}$ can be multiplicatively decomposed into (see, e.g. Levitas (2014))

$$\mathbf{F} = \mathbf{F}_e \cdot \mathbf{F}_t = \mathbf{V}_e \cdot \mathbf{R}_e \cdot \mathbf{R}_t \cdot \mathbf{U}_t = \mathbf{V}_e \cdot \mathbf{R}_l \cdot \mathbf{U}_t, \quad (2)$$

where the polar decompositions for the elastic $\mathbf{F}_e = \mathbf{V}_e \cdot \mathbf{R}_e$ and transformational $\mathbf{F}_t = \mathbf{R}_t \cdot \mathbf{U}_t$ deformation gradient have been used. Here, suffixes e and t stand for elastic and transformational parts, respectively; \mathbf{V}_e is the symmetric left elastic stretch tensor; \mathbf{U}_t is the symmetric right transformation stretch tensor; $\mathbf{R}_l = \mathbf{R}_e \cdot \mathbf{R}_t$ is the lattice rotation tensor. Also, we define $J = \det \mathbf{F} := dV/dV_0$, $J_t = \det \mathbf{F}_t := dV_t/dV_0$, and $J_e = \det \mathbf{F}_e := dV/dV_t$, where dV_0 , dV_t , and dV are infinitesimal volume elements in Ω_0 , Ω_t , and Ω , respectively. Hence by Eq.

(2), $J = J_e J_t$. Note that the thermal strains have been neglected here for compactness and can be included in a manner similar to Levitas (2014).

The Lagrangian total and elastic strain tensors are defined as

$$\mathbf{E} := 0.5(\mathbf{F}^T \cdot \mathbf{F} - \mathbf{I}) = 0.5(\mathbf{U}^2 - \mathbf{I}), \quad \text{and} \quad \mathbf{E}_e := 0.5(\mathbf{F}_e^T \cdot \mathbf{F}_e - \mathbf{I}) = 0.5(\mathbf{U}_e^2 - \mathbf{I}). \quad (3)$$

We define the Eulerian total and elastic strain tensors as

$$\mathbf{b} := 0.5(\mathbf{F} \cdot \mathbf{F}^T - \mathbf{I}) = 0.5(\mathbf{V}^2 - \mathbf{I}), \quad \text{and} \quad \mathbf{b}_e := 0.5(\mathbf{F}_e \cdot \mathbf{F}_e^T - \mathbf{I}) = 0.5(\mathbf{V}_e^2 - \mathbf{I}), \quad (4)$$

respectively, where we have used the polar decompositions $\mathbf{F} = \mathbf{V} \cdot \mathbf{R} = \mathbf{R} \cdot \mathbf{U}$ with \mathbf{V} and \mathbf{R} being the total left stretch tensor and the rotation tensor, respectively.

4. Phase field approach: General theory and thermodynamic formalism

In this section a thermodynamically consistent general theory for our multiphase phase field approach will be presented. Our thermodynamic formalism presented here includes the constitutive relations for the observer invariant free energy, the derivation of the dissipation inequality and the Ginzburg-Landau equations, thermodynamic equilibrium conditions of homogeneous phases, an explicit form of the free energy, the constitutive relations for the transformation deformation gradient, and finally, an analysis of the transformation work for the KMs.

4.1. Free energy and dissipation inequality

A thermodynamically consistent general phase field theory for martensitic PT at finite strains was developed in Levitas (2014). While our order parameters here have different meanings than in Levitas (2014), the general formalism is still applicable. That is why we will directly consider the dissipation inequalities from (Levitas, JMPS, 2014), which were derived using the first two laws of thermodynamics (see Section 2 therein):

$$\mathbf{P} : \dot{\mathbf{F}}^T - \rho_0 \dot{\psi} - \rho_0 s \dot{\theta} + \nabla_0 \cdot (\mathbf{Q}_0^\eta \dot{\eta}_0) + \sum_{i=1}^N \nabla_0 \cdot (\mathbf{Q}_i^\eta \dot{\eta}_i) \geq 0; \quad -\frac{1}{\theta} \mathbf{h}_0 \cdot \nabla_0 \theta \geq 0. \quad (5)$$

In inequality (5) \mathbf{P} denotes the first Piola-Kirchhoff stress, ρ_0 is the mass density in Ω_0 , ψ is the Helmholtz free energy per unit mass, s is the specific entropy per unit mass, $\theta > 0$ is the absolute temperature, \mathbf{Q}_0^η and

\mathbf{Q}_i^η are the generalized force vectors in Ω_0 (yet to be determined) which were introduced into the theory for balancing some of the terms from the inequality (5) (see (Levitas, JMPS, 2014) for details), and \mathbf{h}_0 is the heat flux. Eq. (5)₂ is the Fourier's inequality. As usual, we can assume the Fourier's law for the flux $\mathbf{h}_0 = -\mathbf{K}_\theta \cdot \nabla_0 \theta$, where \mathbf{K}_θ is the heat conductivity tensor, which is symmetric positive semi-definite. The evolution equation for temperature at any material point can be obtained using the energy balance equation and the Fourier's law (see (Levitas, JMPS, 2014) for details).

On the other hand, to cast inequality (5)₁ into an amenable form, we need to prescribe a constitutive relation for ψ . We assume the Helmholtz free energy per unit mass in the following form (also see Levitas (2014)):

$$\psi(\mathbf{F}, \eta_0, \eta_i, \theta, \nabla \eta_0, \nabla \eta_i) = \frac{J_t}{\rho_0} \psi_e(\mathbf{F}_e, \eta_0, \eta_i, \theta) + J \check{\psi}^\theta(\eta_0, \eta_i, \theta) + \tilde{\psi}^\theta(\eta_0, \eta_i, \theta) + \psi_p(\eta_0, \eta_i) + J \psi^\nabla(\nabla \eta_0, \nabla \eta_i, \eta_0, \eta_i). \quad (6)$$

In Eq. (6) ψ_e is the strain energy density per unit volume of the intermediate configuration Ω_t ; $\check{\psi}^\theta$ is the free energy related to the barrier heights for $A \leftrightarrow M$ and $M_i \leftrightarrow M_j$ transformations; $\tilde{\psi}^\theta$ is the thermal energy for $A \leftrightarrow M$ transformations (the thermal energy of all the variants is identical); ψ_p is the penalizing free energy term, which allows us to control the transformation paths between variants, and to regulate the coexistence of three or more phases at a single material point; ψ^∇ is the gradient energy which penalizes the interfaces between the phases. Note that $\check{\psi}^\theta$ and ψ^∇ have been multiplied with J , and the gradient of the order parameters is considered in the deformed configuration for yielding the correct expression for the structural stress tensor (see Levitas (2014) for further details).

We now use Eq. (6) in the inequality (5)₁. Using the material time derivative of ψ given by Eq. (A.4) (see Appendix A for the derivation) in the inequality (5)₁ and assuming that the dissipation rate is independent of $\dot{\theta}$, $\overline{\dot{\nabla}_0 \eta_0}$, and all $\overline{\dot{\nabla}_0 \eta_i}$, we get the constitutive relations for the specific entropy and the generalized force vectors:

$$s = -\frac{\partial \psi}{\partial \theta}, \quad \mathbf{Q}_0^\eta = \rho_0 J \mathbf{F}^{-1} \cdot \frac{\partial \psi^\nabla}{\partial \nabla \eta_0}, \quad \text{and} \quad \mathbf{Q}_i^\eta = \rho_0 J \mathbf{F}^{-1} \cdot \frac{\partial \psi^\nabla}{\partial \nabla \eta_i}, \quad (7)$$

respectively, and the dissipation inequality reduces to

$$\mathbf{P}_d : \dot{\mathbf{F}}^T + X_0 \dot{\eta}_0 + \sum_{i=1}^N X_i \dot{\eta}_i \geq 0 \quad \text{in } \Omega_0, \quad (8)$$

where

$$\mathbf{P}_d := \mathbf{P} - \mathbf{P}_e - \mathbf{P}_{st} \quad (9)$$

is the dissipative first Piola-Kirchhoff stress tensor, and \mathbf{P}_e and \mathbf{P}_{st} are the elastic and structural parts of \mathbf{P} , respectively:

$$\mathbf{P}_e = J_t \frac{\partial \psi_e}{\partial \mathbf{F}_e} \cdot \mathbf{F}_t^{-T}, \quad \mathbf{P}_{st} = J \rho_0 (\check{\psi}^\theta + \psi^\nabla) \mathbf{F}^{-T} - J \rho_0 \left(\nabla \eta_0 \otimes \frac{\partial \psi^\nabla}{\partial \nabla \eta_0} + \sum_{i=1}^N \nabla \eta_i \otimes \frac{\partial \psi^\nabla}{\partial \nabla \eta_i} \right) \cdot \mathbf{F}^{-T}. \quad (10)$$

The thermodynamic force X_l , conjugate to the generalized rate $\dot{\eta}_l$ in inequality (8), is

$$X_l = \left(\mathbf{P}_e^T \cdot \mathbf{F}_e - J_t \psi_e \mathbf{F}_t^{-1} \right) : \frac{\partial \mathbf{F}_t}{\partial \eta_l} - J_t \frac{\partial \psi_e}{\partial \eta_l} \Big|_{\mathbf{F}_e} - \rho_0 J \frac{\partial (\check{\psi}^\theta + \psi^\nabla)}{\partial \eta_l} - \rho_0 \frac{\partial (\check{\psi}^\theta + \psi_p)}{\partial \eta_l} + \nabla_0 \cdot \left(\rho_0 J \mathbf{F}^{-1} \cdot \frac{\partial \psi^\nabla}{\partial \nabla \eta_l} \right),$$

for $l = 0, 1, 2, \dots, N$,

(11)

which can also be expressed in the following compact form (also see Levitas (2014))

$$X_l = -\rho_0 \frac{\partial \psi}{\partial \eta_l} + \nabla_0 \cdot \left(\rho_0 J \frac{\partial \psi^\nabla}{\partial \nabla_0 \eta_l} \right) \quad \text{for } l = 0, 1, 2, \dots, N. \quad (12)$$

To obtain the last term in Eq. (12), we have used the relation $\frac{\partial \psi^\nabla}{\partial \nabla_0 \eta_l} = \mathbf{F}^{-1} \cdot \frac{\partial \psi^\nabla}{\partial \nabla \eta_l}$ which can be easily proved using the chain rule of differentiation and $\mathbf{F} := \nabla_0 \mathbf{r}$. We simplify our theory by assuming the dissipation due to viscous stress power and the evolution of all order parameters to be independent, and thus decoupling the inequality (8) into

$$\mathbf{P}_d : \dot{\mathbf{F}}^T \geq 0, \quad \text{and} \quad X_0 \dot{\eta}_0 + \sum_{i=1}^N X_i \dot{\eta}_i \geq 0 \quad \text{in } \Omega_0. \quad (13)$$

Using Eqs. (9), (10), and also the relation between $\boldsymbol{\sigma}$ and \mathbf{P} ,

$$\boldsymbol{\sigma} = J^{-1} \mathbf{P} \cdot \mathbf{F}^T, \quad (14)$$

the following expressions for the dissipative, elastic, and structural Cauchy stress tensors are obtained:

$$\begin{aligned} \boldsymbol{\sigma}_d &:= \boldsymbol{\sigma} - \boldsymbol{\sigma}_e - \boldsymbol{\sigma}_{st}, & \boldsymbol{\sigma}_e &= J_e^{-1} \frac{\partial \psi_e(\mathbf{E}_e)}{\partial \mathbf{F}_e} \cdot \mathbf{F}_e^T = J_t \mathbf{F}_e \cdot \frac{\partial \psi_e(\mathbf{E}_e)}{\partial \mathbf{E}_e} \cdot \mathbf{F}_e^T \\ \boldsymbol{\sigma}_{st} &= \rho_0 (\check{\psi}^\theta + \psi^\nabla) \mathbf{I} - \rho_0 \left(\nabla \eta_0 \otimes \frac{\partial \psi^\nabla}{\partial \nabla \eta_0} + \sum_{i=1}^N \nabla \eta_i \otimes \frac{\partial \psi^\nabla}{\partial \nabla \eta_i} \right). \end{aligned} \quad (15)$$

Our general theory applies to both isotropic and anisotropic materials. For the isotropic elastic materials, which we will consider in applications, Eq. (15)₂ for the Cauchy elastic stress can be reduced to

$$\boldsymbol{\sigma}_e = J_e^{-1} \mathbf{V}_e^2 \cdot \frac{\partial \psi_e(\mathbf{b}_e)}{\partial \mathbf{b}_e}; \quad (16)$$

see any textbook on nonlinear elasticity or Levitas (2014). The thermodynamic driving force given by Eq. (11) can also be expressed in terms of the Cauchy stresses as

$$X_l = (J\mathbf{F}^{-1} \cdot \boldsymbol{\sigma}_e \cdot \mathbf{F} - J_t \psi_e \mathbf{I}) : \mathbf{F}_t^{-1} \cdot \frac{\partial \mathbf{F}_t}{\partial \eta_l} - J_t \left. \frac{\partial \psi_e}{\partial \eta_l} \right|_{\mathbf{F}_e} - \rho_0 J \frac{\partial(\check{\psi}_\theta + \psi^\nabla)}{\partial \eta_l} - \rho_0 \frac{\partial(\tilde{\psi}_\theta + \psi_p)}{\partial \eta_l} + \nabla_0 \cdot \left(\rho_0 J \mathbf{F}^{-1} \cdot \frac{\partial \psi^\nabla}{\partial \nabla \eta_l} \right) \quad \text{for } l = 0, 1, 2, \dots, N. \quad (17)$$

Note that the driving force X_l depends explicitly on the elastic stresses only. Still, the structural stresses contribute to X_l indirectly by changing the elastic stresses through the mechanical equilibrium equation

$$\nabla_0 \cdot \mathbf{P} = \mathbf{0} \quad \text{in } \Omega_0, \quad \text{or equivalently,} \quad \nabla \cdot \boldsymbol{\sigma} = \mathbf{0} \quad \text{in } \Omega, \quad (18)$$

where body and inertial forces have been neglected for simplicity.

4.2. Ginzburg-Landau equations

Using the dissipation inequality (13)₂ we will now derive the kinetic relations for the order parameters, which are also called the Ginzburg-Landau equations. We will perform some transformations and make assumptions which will allow us to write down kinetics equations for PT between each of the two phases independent of other phases. Then all kinetic parameters can be calibrated using the mobilities of interfaces between each of the two phases known from the experiments or atomistic simulations. As the first step, we assume that the dissipation rate due to $\mathbf{A} \leftrightarrow \mathbf{M}$ and $\mathbf{M}_i \leftrightarrow \mathbf{M}_j$ transformations, D_0 and D_M , respectively, are mutually independent, and hence the inequality (13)₂ can be expressed in the following decoupled form:

$$D_0 = \dot{\eta}_0 X_0 \geq 0 \quad \text{and} \quad D_M = \sum_{i=1}^N \dot{\eta}_i X_i \geq 0. \quad (19)$$

Based on the inequality (19)₁, we postulate the kinetic law for η_0

$$\dot{\eta}_0 = L_{0M} X_0, \quad (20)$$

where $L_{0M} \geq 0$ is the kinetic coefficient for an \mathbf{A} - \mathbf{M} interface. To derive the kinetic law for the variants, we use Eq. (19)₂ in combination with the constraint (1)

$$\sum_{i=1}^N \eta_i = 1, \quad \Rightarrow \quad \sum_{i=1}^N \dot{\eta}_i = 0, \quad (21)$$

which enforces the sum of the order parameters η_i (for $i = 1, \dots, N$) to lie on a prescribed plane in the N -dimensional order parameter space; see Figs. 1(f) and 1(g).

We cannot directly write down the kinetic equations for individual $\dot{\eta}_i$ based on the inequality (19)₂, since that will not lead to the physically meaningful evolution laws for the order parameters η_i . That is why we define the new variables $\dot{\eta}_{ij} = \dot{\eta}_i - \dot{\eta}_j$ which signify the rate of transformation between variants M_j and M_i , and also define corresponding driving force $X_{ij} = X_i - X_j$ (see Idesman et al. (2005); Levitas et al. (2004) for a similar treatment for concentration related order parameters). Obviously, $\dot{\eta}_{ij} = -\dot{\eta}_{ji}$, $\dot{\eta}_{ii} = 0$, and $X_{ii} = 0$. Using the definition of $\dot{\eta}_{ij}$ along with the rate equation (21)₂, it can be shown that

$$\dot{\eta}_i = \sum_{j=1}^N \frac{\dot{\eta}_{ij}}{N}. \quad (22)$$

Using the definitions of $\dot{\eta}_{ij}$ and X_{ij} , we write that

$$\begin{aligned} \sum_{i=1}^N \sum_{j=1}^N X_{ij} \frac{\dot{\eta}_{ij}}{N} &= \sum_{i=1}^N \sum_{j=1}^N \frac{X_i \dot{\eta}_i}{N} - \sum_{i=1}^N \sum_{j=1}^N \frac{X_i \dot{\eta}_j}{N} - \sum_{i=1}^N \sum_{j=1}^N \frac{X_j \dot{\eta}_i}{N} + \sum_{i=1}^N \sum_{j=1}^N \frac{X_j \dot{\eta}_j}{N} \\ &= \sum_{i=1}^N X_i \dot{\eta}_i - \sum_{i=1}^N X_i \sum_{j=1}^N \frac{\dot{\eta}_j}{N} - \sum_{j=1}^N X_j \sum_{i=1}^N \frac{\dot{\eta}_i}{N} + \sum_{j=1}^N X_j \dot{\eta}_j. \end{aligned} \quad (23)$$

Now using Eqs. (21)₂ and the definition of D_M from inequality (19)₂ in Eq. (23), we obtain

$$D_M = \frac{1}{2} \sum_{i=1}^N \sum_{j=1}^N X_{ij} \frac{\dot{\eta}_{ij}}{N} = \sum_{i=1}^{N-1} \sum_{j=i+1}^N X_{ij} \frac{\dot{\eta}_{ij}}{N} \geq 0, \quad (24)$$

where we have used $X_{ij}\dot{\eta}_{ij} = X_{ji}\dot{\eta}_{ji}$. This is the desired form of the dissipation rate for variant-variant transformations, which proves that X_{ij} and $\dot{\eta}_{ij}/N$ are the generalized thermodynamic forces and the rates for $M_i \leftrightarrow M_j$ transformations, respectively. In terms of these variables, we can assume that the dissipation rate due to the $M_i \leftrightarrow M_j$ transformations is independent of any other martensitic variant M_k ($k \neq i, j$). Then the inequality (24) can be split into the following independent inequalities

$$X_{ij}\dot{\eta}_{ij} \geq 0 \quad (\text{no summation}) \quad \text{for all } i, j = 1, 2, \dots, N, \text{ and } i \neq j. \quad (25)$$

Based on the inequality (25), we postulate the simplest kinetic relations for the $M_i \leftrightarrow M_j$ transformations which are independent of any other martensitic variant M_k :

$$\frac{\dot{\eta}_{ij}}{N} = L_{ij} X_{ij} \quad (\text{no summation}) \quad \text{for all } i, j = 1, 2, \dots, N, \text{ and } i \neq j, \quad (26)$$

where $L_{ij} \geq 0$ is the kinetic coefficient for the transformations between M_i and M_j . For a convenience of further derivations, the scalar N is not included in L_{ij} , and $L_{ij} = L_{ji}$ follows from the a comparison of Eq. (26) with its equivalent form $\dot{\eta}_{ji}/N = L_{ji}X_{ji}$ (recall that $\dot{\eta}_{ij} = -\dot{\eta}_{ji}$ and $X_{ji} = -X_{ij}$). Equation (26) yields $0.5N(N-1)$ independent equations for $\dot{\eta}_{ij}$ for all $i, j = 1, 2, \dots, N$, and $i \neq j$, and also there are $0.5N(N-1)$ independent interfaces between martensitic variants, i.e. all L_{ij} can be determined in terms of the known mobility of all the variant-variant interfaces. Note that for a given i , we will have $N-1$ equations from Eq. (26) involving $\dot{\eta}_i$. Adding all those $N-1$ equations and then using Eq. (22), we obtain the final form of the evolution equations for the order parameters:

$$\dot{\eta}_i = \sum_{j=1, j \neq i}^N L_{ij} X_{ij} \quad \text{for all } i = 1, 2, \dots, N. \quad (27)$$

Here the kinetic coefficients for all the variant-variant interfaces are independent and not subject to any restriction other than that they must be non-negative, as desired in a robust theory; see Tóth et al. (2015). This is in contrast to several existing multiphase phase field models (Garcke et al. (1999); Nestler (2005); Steinbach et al. (1996); Steinbach and Pezzolla (1999)), where the coefficients were either identical or subjected to some restrictions; see e.g. Tóth et al. (2015) for a more detailed analysis. Note that for the equivalent interfaces between martensitic variants, the corresponding kinetic coefficients are equal. For example, for cubic to tetragonal transformations, all three variants and three variant-variant interfaces are equivalent and thus all the kinetic coefficients L_{ij} are the same.

4.3. Thermodynamic equilibrium conditions for homogeneous states

Elaborating the approach developed in Levitas (2013a); Levitas and Preston (2002a,b), we will now determine the implications of the thermodynamic equilibrium condition on the forms of the dependence of \mathbf{F}_t and various material properties (such as entropy, elastic, and thermal properties etc.) on the order parameters η_0 and η_i . This will impose restrictions on the interpolation functions. Using Eqs. (20) and (27), we see that the stationary solutions of the system of Ginzburg-Landau equations, i.e. $\dot{\eta}_0 = 0$ and $\dot{\eta}_i = 0$, correspond to

$$X_0 = 0, \quad \text{and} \quad X_i - X_j = 0 \quad \text{for all } i \neq j. \quad (28)$$

Here we are interested in obtaining the conditions for the homogeneous phases, i.e. when the gradient terms are neglected, and hence impose the following *conditions*:

The set of the order parameters for \mathbf{A} , $\tilde{\eta} = \hat{\eta}_0$, and for \mathbf{M}_i , $\tilde{\eta} = \hat{\eta}_i$, must satisfy the equilibrium conditions in Eq. (28) at any stress \mathbf{P} , temperature θ , and associated elastic deformation gradient \mathbf{F}_e . The condition (28)₁ thus using Eq. (11) leads to

$$J_t \left. \frac{\partial \psi_e(\mathbf{E}_e, \theta, \hat{\eta}_0)}{\partial \eta_0} \right|_{\mathbf{F}_e} - \rho_0 J \frac{\partial \check{\psi}_\theta(\theta, \hat{\eta}_0)}{\partial \eta_0} - \rho_0 \frac{\partial \check{\psi}_\theta(\theta, \hat{\eta}_0)}{\partial \eta_0} - \frac{\partial \psi_p(\theta, \hat{\eta}_0)}{\partial \eta_0} = 0 \quad \text{and} \\ \frac{\partial \mathbf{F}_t(\hat{\eta}_0)}{\partial \eta_0} = \mathbf{0}, \quad (29)$$

and Eq. (28)₂ yields

$$J_t \left(\left. \frac{\partial \psi_e(\mathbf{E}_e, \theta, \hat{\eta}_i)}{\partial \eta_i} \right|_{\mathbf{F}_e} - \left. \frac{\partial \psi_e(\mathbf{E}_e, \theta, \hat{\eta}_i)}{\partial \eta_j} \right|_{\mathbf{F}_e} \right) - \rho_0 J \left(\frac{\partial \check{\psi}_\theta(\theta, \hat{\eta}_i)}{\partial \eta_i} - \frac{\partial \check{\psi}_\theta(\theta, \hat{\eta}_i)}{\partial \eta_j} \right) - \\ \rho_0 \left(\frac{\partial \check{\psi}_\theta(\theta, \hat{\eta}_i)}{\partial \eta_i} - \frac{\partial \check{\psi}_\theta(\theta, \hat{\eta}_i)}{\partial \eta_j} \right) - \left(\frac{\partial \psi_p(\theta, \hat{\eta}_i)}{\partial \eta_i} - \frac{\partial \psi_p(\theta, \hat{\eta}_i)}{\partial \eta_j} \right) = 0 \quad \text{and} \\ \frac{\partial \mathbf{F}_t(\hat{\eta}_i)}{\partial \eta_i} - \frac{\partial \mathbf{F}_t(\hat{\eta}_i)}{\partial \eta_j} = \mathbf{0} \quad \text{for all } i, j = 1, 2, \dots, N, \text{ but } i \neq j. \quad (30)$$

We determine all the material properties (e.g. transformation strain, elastic moduli, specific heat etc.) using

$$M(\eta_0, \eta_i, \theta, \mathbf{F}) = M_0(1 - \varphi(a, \eta_0)) + \sum_{i=1}^N M_i \phi_i(\eta_i) \varphi(a, \eta_0). \quad (31)$$

where $M_0 = M_0(\theta, \mathbf{F})$ and $M_i = M_i(\theta, \mathbf{F})$ are the properties of \mathbf{A} and \mathbf{M}_i , respectively, $\varphi(a, \eta_0)$ and $\phi_i(\eta_i)$ are the interpolation functions, and a is a parameter. By definition, $M(\hat{\eta}_0, \theta, \mathbf{F}) = M_0$ and $M(\hat{\eta}_i, \theta, \mathbf{F}) = M_i$, which yield

$$\varphi(a, 0) = 0, \quad \varphi(a, 1) = 1; \quad \text{and} \quad \phi_i(0) = 0, \quad \phi_i(1) = 1. \quad (32)$$

When Eq. (31) is used in Eqs. (29) and (30), the following additional conditions for the interpolation functions are yielded:

$$\frac{\partial \varphi(a, 0)}{\partial \eta_0} = \frac{\partial \varphi(a, 1)}{\partial \eta_0} = 0, \quad (33)$$

$$M_i \frac{\partial \phi_i(\eta_i = 0)}{\partial \eta_i} = M_j \frac{\partial \phi_j(\eta_j = 1)}{\partial \eta_j} \quad \text{and} \quad M_i \frac{\partial \phi_i(\eta_i = 1)}{\partial \eta_i} = M_j \frac{\partial \phi_j(\eta_j = 0)}{\partial \eta_j} \quad \text{for all } i \neq j. \quad (34)$$

Since the conditions in Eq. (34) must be satisfied for all i and j ($i \neq j$) with all possible distinct M_i and M_j (since properties of the variants can be different; e.g. the transformation strains), the derivative of the interpolation

functions must satisfy

$$\frac{\partial \phi_i(\eta_i = 0)}{\partial \eta_i} = \frac{\partial \phi_i(\eta_i = 1)}{\partial \eta_i} = 0 \quad \text{for all } i = 1, 2, \dots, N. \quad (35)$$

Within a fourth-degree potential, the general expression for the interpolation functions, which satisfy the criteria (32), (33), and (35) are

$$\varphi(a, \eta_0) = a\eta_0^2 + (4 - 2a)\eta_0^3 + (a - 3)\eta_0^4 = a\eta_0^2(1 - \eta_0)^2 + \eta_0^3(4 - 3\eta_0) \quad \text{and} \quad (36)$$

$$\phi(\eta_i) = \varphi(3, \eta_i) = \eta_i^2(3 - 2\eta_i). \quad (37)$$

The interpolation function $\phi(\eta_i)$ in addition satisfies the antisymmetry condition

$$\phi(1 - \eta_i) = 1 - \phi(\eta_i), \quad (38)$$

and for $\eta_j = 1 - \eta_i$, one has

$$\phi(1 - \eta_i) = \phi(\eta_j) = 1 - \phi(\eta_i). \quad (39)$$

With this function, all the material properties, and thus the entire theory are invariant with respect to the exchange of two martensitic variants, i.e. $(M_i, \eta_i) \leftrightarrow (M_j, \eta_j)$ for $\eta_i + \eta_j = 1$; see Levitas and Roy (2016). This means that all variants are equivalent, which cannot be achieved with a more general interpolation function $\varphi(a, \eta_i)$ for $a \neq 3$. Function $\varphi(a, \eta_0)$ for $A \leftrightarrow M$ PTs should not satisfy the antisymmetry conditions and that is why it contains a free material parameter a as desired.

4.4. Explicit expression for Helmholtz free energy

Using a routine procedure (see Zheng (1994)) one can show that for the interfacial energy, the free energy ψ given by Eq. (6) would be observer invariant, when

$$\psi_e(\mathbf{F}_e, \eta_0, \eta_i, \theta) = \psi_e(\mathbf{E}_e, \eta_0, \eta_i, \theta), \quad \text{and} \quad \psi^\nabla(\nabla\eta_i, \nabla\eta_j) = \hat{\psi}^\nabla(\nabla\eta_i \cdot \nabla\eta_j) \quad \text{for } i, j = 0, 1, \dots, N, \quad (40)$$

where $\hat{\psi}^\nabla$ is isotropic.

4.4.1. Local free energy

Elastic energy can be presented as a Taylor series expansion corresponding to the chosen crystal lattice symmetry group and η_i -dependent elastic properties; see, e.g. Levitas (2013a). Here, for simplicity, we consider a quadratic strain energy density

$$\hat{\psi}_e = 0.5 \mathbf{E}_e : \mathbf{C}(\eta_0, \eta_i) : \mathbf{E}_e, \quad (41)$$

where \mathbf{C} is the fourth order elasticity tensor taken as (see Eq. (31))

$$\mathbf{C}(\eta_0, \eta_i) = (1 - \varphi(a, \eta_0)) \mathbf{C}_0 + \varphi(a, \eta_0) \sum_{i=1}^N \phi_i(\eta_i) \mathbf{C}_i, \quad (42)$$

where \mathbf{C}_0 and \mathbf{C}_i are the elasticity tensors for A and M_i, respectively.

Thermal energy. Rewriting the fourth degree potential related to the thermal energy given by Eq. (36) as $\varphi(a_\theta, \eta_0) = (a_\theta - 3)\eta_0^2(1 - \eta_0)^2 + \eta_0^2(3 - 2\eta_0)$ (also see Levitas (2013b, 2014)), we present the part of the thermal energy which contributes into the interfacial stresses as (see Eqs. (6) and (10)₂)

$$\check{\psi}^\theta = [A(\theta) + (a_\theta - 3)\Delta\psi^\theta(\theta)]\eta_0^2(1 - \eta_0)^2 + \bar{A} \sum_{i=1}^{N-1} \sum_{j=i+1}^N \eta_i^2 \eta_j^2 \varphi(a_b, \eta_0), \quad (43)$$

and the part which does not contribute into the interfacial stresses as

$$\tilde{\psi}^\theta = \psi_0^\theta(\theta) + \eta_0^2(3 - 2\eta_0)\Delta\psi^\theta(\theta), \quad (44)$$

respectively. Such a division of the fourth-degree polynomial in η_0 into $\check{\psi}^\theta$ and $\tilde{\psi}^\theta$ is justified by analytical solution for a propagating A \leftrightarrow M interface in Section 7.1. In Eqs. (43) and (44) the symbols A and \bar{A} denote the barrier heights for A \leftrightarrow M transformations and all M_i \leftrightarrow M_j transformations, respectively; $\Delta\psi^\theta = \psi_M^\theta - \psi_0^\theta$; ψ_0^θ and ψ_M^θ are the thermal energy of A and M, respectively (note that thermal energy of all the variants is identical), see, e.g. Levitas (2000):

$$\psi_l^\theta = \psi_r^\theta - s_l(\theta - \theta_r) - c_l^\sigma \theta \ln(\theta/\theta_r) + c_l^\sigma(\theta - \theta_r) \quad \text{for } l = 0, M, \quad (45)$$

where s_l is the entropy of the corresponding phase and $c_l^\sigma = \theta(\partial s/\partial \theta)_\sigma$ is the specific heat of phases at constant Cauchy stresses, θ_r and ψ_r^θ are the chosen reference temperature and corresponding energy. We assume $\theta_r = \theta_e$, where θ_e is the thermodynamic equilibrium temperature between A and M. Thus, we have

$$\Delta\psi^\theta = \psi_M^\theta - \psi_0^\theta = -\Delta s(\theta - \theta_e) - \Delta c^\sigma \theta \ln(\theta/\theta_e) + \Delta c^\sigma(\theta - \theta_e), \quad (46)$$

where $\Delta s = s_M - s_0$ and $\Delta c^\sigma = c_M^\sigma - c_0^\sigma$. Obviously, if the specific heats of A and M are identical,

$$\Delta\psi^\theta = -\Delta s(\theta - \theta_e). \quad (47)$$

The barrier function and its first derivative are zero in A and in all the martensitic variants M_i , i.e. it does not violate the thermodynamic equilibrium conditions given by Eqs. (29)₁ and (30)₁. For A \leftrightarrow M transformations, the second term in Eq. (43) disappears, and we are left with the traditional double-well barrier function. For $M_i \leftrightarrow M_j$ transformations, $\eta_0 = 1$, and by choosing the proper penalizing terms we impose that the transformation path represents straight line $\eta_j + \eta_i = 1$ (see below); hence $\check{\psi}^\theta = \bar{A}(\theta)\eta_i^2(1 - \eta_i)^2$, i.e. it has the same functional form as for A \leftrightarrow M PTs.

The *penalty terms* are accepted in the form:

$$\begin{aligned} \psi_p = & \sum_{i=1}^{N-1} \sum_{j=i+1}^N K_{ij}(\eta_i + \eta_j - 1)^2 \eta_i^2 \eta_j^2 + \sum_{i=1}^{N-1} \sum_{j=i+1}^N K_{0ij} \eta_0^2 \eta_i^2 \eta_j^2 (1 - \varphi(a_K, \eta_0)) + \sum_{i=1}^{N-2} \sum_{j=i+1}^{N-1} \sum_{k=j+1}^N K_{ijk} \eta_i^2 \eta_j^2 \eta_k^2 \\ & + \sum_{i=1}^{N-2} \sum_{j=i+1}^{N-1} \sum_{k=j+1}^N K_{0ijk} \eta_0^2 \eta_i^2 \eta_j^2 \eta_k^2 (1 - \varphi(a_K, \eta_0)) + \sum_{i=1}^{N-3} \sum_{j=i+1}^{N-2} \sum_{k=j+1}^{N-1} \sum_{l=k+1}^N K_{ijkl} \eta_i^2 \eta_j^2 \eta_k^2 \eta_l^2, \end{aligned} \quad (48)$$

where the coefficients satisfy the symmetry relations

$$\begin{aligned} K_{ij} &= K_{ji}; \quad K_{0ij} = K_{0ji}; \quad K_{ijk} = K_{jik} = K_{jki} = K_{kji} = K_{kij} = K_{ikj}; \quad K_{0ijk} = K_{0jik} = K_{0jki} = K_{0kji} \\ &= K_{0kij} = K_{0ikj}; \quad K_{ijkl} = K_{jikl} = K_{kjil} = K_{ljki} = K_{ikjl} = K_{ilkj} = K_{ijlk}; \end{aligned} \quad (49)$$

and also they satisfy

$$K_{ii} = K_{0ii} = K_{iik} = K_{iji} = K_{iii} = K_{0iik} = K_{0iji} = K_{0iii} = K_{iikl} = K_{ijil} = K_{ijki} = K_{ijjl} = K_{ijkk} = 0. \quad (50)$$

Obviously, the penalty function ψ_p is zero in A and all martensitic variants M_i and has zero first derivatives therein, i.e. it also does not violate the thermodynamic equilibrium conditions Eqs. (29)₁ and (30)₁. The coefficient $K_{ij} \geq 0$ is a control parameter for penalizing the deviation of the $M_i \leftrightarrow M_j$ transformation path from the straight line $\eta_i + \eta_j = 1$ for $\eta_k = 0$ and $k \neq i, j$. Note that when $K_{ij} \rightarrow \infty$, η_i and η_j strictly follow the straight line, and hence no third phase M_k (for all $k \neq i, j$) can nucleate within the interface between M_i and M_j . However, a third phase can nucleate when K_{ij} is small.

The second and third terms in Eq. (48) penalize the coexistence of any three phases at a single material point. Namely, the term with K_{0ij} penalizes triple junctions between austenite and any two martensitic variants. This term has been multiplied by $1 - \varphi(a, \eta_0)$ to restrict the contribution of the penalty term in a small neighborhood of the triple junctions only. Had this multiplication factor not been there, this term would have been nonzero in M and have a similar contribution as the second term (with \bar{A}) in Eq. (43), which should be avoided. The term with K_{ijk} penalizes triple junctions between any three martensitic variants. Similarly, the terms with coefficients K_{0ijk} and K_{ijkl} penalize the quadruple junctions. All other higher junctions, e.g. those in wedge microstructures (Bhattacharya (2004)) and considered in Ruddock (1994), can be penalized in an analogous way.

4.4.2. Nonlocal free energy

The *gradient energy* satisfying the observer invariance condition Eq. (40)₂ is assumed to be

$$\begin{aligned}\psi^\nabla &= \frac{1}{2\rho_0} \left[\beta_{0M} |\nabla\eta_0|^2 + \sum_{i=1}^N \sum_{j=1, \neq i}^N \frac{\beta_{ij}}{8} |\nabla\eta_{ij}|^2 \tilde{\varphi}(\eta_0, a_\beta, a_0) \right] \\ &= \frac{\beta_{0M}}{2\rho_0} |\nabla\eta_0|^2 + \frac{1}{8\rho_0} \sum_{i=1}^{N-1} \sum_{j=i+1}^N \beta_{ij} (|\nabla\eta_i|^2 + |\nabla\eta_j|^2 - 2\nabla\eta_i \cdot \nabla\eta_j) \tilde{\varphi}(\eta_0, a_\beta, a_0),\end{aligned}\quad (51)$$

where $\beta_{0M} \geq 0$ is the gradient energy coefficient for the A-M interface, $\beta_{ij} = \beta_{ji} > 0$ ($i \neq j$) is the gradient energy coefficient for the M_i - M_j interface, and we have taken $\beta_{ii} = 0$ for all i . The energy ψ^∇ is obviously quadratic and positive. When only two variants are present in a system, using the constraint (21)₁, we express the gradient energy in terms of the order parameters η_0 and η_i :

$$\psi^\nabla = \frac{1}{2\rho_0} \left(\beta_{0M} |\nabla\eta_0|^2 + \beta_{ij} |\nabla\eta_i|^2 \tilde{\varphi}(\eta_0, a_\beta, a_0) \right), \quad (52)$$

which explains the factor 1/8 in Eq. (51). For a three-variant system the gradient energy takes the following form:

$$\begin{aligned}\psi^\nabla &= \frac{\beta_{0M}}{2\rho_0} |\nabla\eta_0|^2 + \frac{1}{8\rho_0} \left[(\beta_{ij} + \beta_{ik}) |\nabla\eta_i|^2 + (\beta_{ij} + \beta_{jk}) |\nabla\eta_j|^2 + (\beta_{ik} + \beta_{jk}) |\nabla\eta_k|^2 - \right. \\ &\quad \left. 2(\beta_{ij} \nabla\eta_i \cdot \nabla\eta_j + \beta_{jk} \nabla\eta_j \cdot \nabla\eta_k + \beta_{ik} \nabla\eta_i \cdot \nabla\eta_k) \right] \tilde{\varphi}(\eta_0, a_\beta, a_0).\end{aligned}\quad (53)$$

Several other constitutive models for the gradient energy were used within the multiphase phase field models in Garcke et al. (1999); Nestler (2005); Steinbach et al. (1996); Steinbach and Pezzolla (1999), however, they possess some thermodynamical issues; see Tóth et al. (2015) for analysis. In contrast, the gradient energy within the present model is fully consistent.

Also, note that in Eq. (51) we have considered a different interpolation function:

$$\tilde{\varphi}(a_\beta, a_0, \eta_0) = a_\beta \eta_0^2 - 2[a_\beta - 2(1 - a_0)]\eta_0^3 + [a_\beta - 3(1 - a_0)]\eta_0^4 + a_0, \quad (54)$$

where a_β and a_0 are constant parameters. Obviously,

$$\tilde{\varphi}(a_\beta, 0, \eta_0) = \varphi(a_\beta, \eta_0); \quad \tilde{\varphi}(a_\beta, a_0, 0) = a_0; \quad \frac{\partial \tilde{\varphi}(a_\beta, a_0, 0)}{\partial \eta_0} = \frac{\partial \tilde{\varphi}(a_\beta, a_0, 1)}{\partial \eta_0} = 0. \quad (55)$$

The interpolation function $\tilde{\varphi}$ is used in order to penalize M_i - M_j interfaces within A ($\eta_0 = 0$). Clearly, A may nucleate at the interface between martensitic variants, see experiments in Xu et al. (1998), 1D models in Falk (1983); Levitas et al. (2003), and a 2D model in Levitas and Javanbakht (2011). For this case, in our phase field model the M_i - M_j interface passes through the region with $\eta_0 = 0$. If $a_0 = 0$, the contribution of the gradient coefficient for M_i - M_j within A vanishes, which leads to zero M_i - M_j interface width and energy and an ill-posed problem formulation. In simulations the variant-variant interface will thus be localized within one computational cell producing a mesh-dependent solution. However, a nonzero a_0 prevents this issue. A similar problem arises for nucleation of any third phase at the interface between two other phases, e.g. nucleation of melt at a solid-solid interface (Levitas and Momeni (2014); Momeni and Levitas (2014, 2015)).

4.5. Explicit form for generalized forces for phase transformations and structural stresses

4.5.1. General case

We will now obtain the explicit expressions for the generalized forces X_i . Using the local and nonlocal energy terms listed in Eqs. (41), (43), (44), (48), and (51) into Eq. (11), we obtain

$$\begin{aligned}
X_0 = & (\mathbf{P}_e^T \cdot \mathbf{F}_e - J_t \psi_e \mathbf{F}_t^{-1}) : \frac{\partial \mathbf{F}_t}{\partial \eta_0} - \frac{J_t}{2} \mathbf{E}_e : \frac{\partial \mathcal{C}}{\partial \eta_0} : \mathbf{E}_e - \rho_0 (6\eta_0 - 6\eta_0^2) \Delta \psi^\theta - J \rho_0 \bar{A} \sum_{i=1}^{N-1} \sum_{j=i+1}^N \eta_i^2 \eta_j^2 \frac{\partial \varphi(a_b, \eta_0)}{\partial \eta_0} \\
& - \rho_0 J [A(\theta) + (a_\theta - 3) \Delta \psi^\theta(\theta)] (2\eta_0 - 6\eta_0^2 + 4\eta_0^3) - \frac{J}{8} \frac{\partial \tilde{\varphi}(a_\beta, a_0, \eta_0)}{\partial \eta_0} \sum_{i=1}^{N-1} \sum_{j=i+1}^N \beta_{ij} |\nabla \eta_i - \nabla \eta_j|^2 - \\
& \rho_0 \left(\sum_{i=1}^{N-1} \sum_{j=i+1}^N K_{0ij} \eta_i^2 \eta_j^2 + \sum_{i=1}^{N-2} \sum_{j=i+1}^{N-1} \sum_{k=j+1}^N K_{0ijk} \eta_i^2 \eta_j^2 \eta_k^2 \right) \left[2\eta_0 (1 - \varphi(a_K, \eta_0)) - \eta_0^2 \frac{\partial \varphi(a_K, \eta_0)}{\partial \eta_0} \right] + \\
& \nabla_0 \cdot (\beta_{0M} J \mathbf{F}^{-1} \cdot \nabla \eta_0); \tag{56}
\end{aligned}$$

$$\begin{aligned}
X_i = & (\mathbf{P}_e^T \cdot \mathbf{F}_e - J_t \psi_e \mathbf{F}_t^{-1}) : \frac{\partial \mathbf{F}_t}{\partial \eta_i} - \frac{J_t}{2} \mathbf{E}_e : \frac{\partial \mathcal{C}}{\partial \eta_i} : \mathbf{E}_e - 2\rho_0 J \bar{A} \sum_{j=1, \neq i}^N \eta_i \eta_j^2 \varphi(a_b, \eta_0) - \\
& 2\rho_0 \sum_{j=1}^N K_{ij} (\eta_i + \eta_j - 1) (2\eta_i + \eta_j - 1) \eta_i \eta_j^2 - 2\rho_0 \left(\sum_{j=1}^N K_{0ij} \eta_j^2 + \sum_{j=1}^{N-1} \sum_{k=j+1}^N K_{0ijk} \eta_j^2 \eta_k^2 \right) \times \\
& \eta_i \eta_0^2 (1 - \varphi(a_K, \eta_0)) - 2\rho_0 \left(\sum_{j=1}^{N-1} \sum_{k=j+1}^N K_{ijk} \eta_j^2 \eta_k^2 + \sum_{j=1}^{N-2} \sum_{k=j+1}^{N-1} \sum_{l=k+1}^N K_{ijkl} \eta_j^2 \eta_k^2 \eta_l^2 \right) \eta_i + \\
& \nabla_0 \cdot \left(J \tilde{\varphi}(a_\beta, a_0, \eta_0) \sum_{j=1}^N \frac{\beta_{ij}}{4} \mathbf{F}^{-1} \cdot (\nabla \eta_i - \nabla \eta_j) \right) \quad \text{for all } i = 1, 2, \dots, N. \tag{57}
\end{aligned}$$

The first terms on the right hand side of both Eqs. (56) and (57) are related to the transformation work. The elastic, barrier, thermal, gradient, and local penalization energies also contribute to the forces. In Eq. (56) the terms with penalty coefficients K_{0ij} and K_{0ijk} are nonvanishing only within the regions where A and the variants coexists, which is the desired condition. Since in austenite $\eta_0 = 0$ and $\partial \varphi(a_K, 0)/\partial \eta_0 = 0$, and in martensite $\varphi(a_K, 1) = 1$ and $\partial \varphi(a_K, 1)/\partial \eta_0 = 0$, all the terms with K_{0ij} and K_{0ijk} disappear therein. Also, note that the penalty terms contribute to the microstructure evolutions only if the coefficients K_{0ij} and K_{0ijk} are comparable with or larger than the double-well barrier heights and the thermal energy. For example, in NiAl alloy which

undergoes cubic to tetragonal PT, A_{0M} , \bar{A} and $\Delta\psi^\theta$ (at a temperature far from the thermodynamic equilibrium temperature) are at the level of several GPa; see e.g. Levitas and Preston (2002a,b). In view of that, K_{0ij} and K_{0ijk} should also be several GPas, and then only the system will avoid coexistence of A and the variants at a single material point to minimize the total energy. However, if these coefficients are less than a GPa, their contribution will be negligible and the multiphase junctions will not be penalized. Similarly, the penalty coefficients (including K_{ij}) must also be at least of the order of GPa or higher to enforce the variant \leftrightarrow variant transformation paths close to the straight lines $\eta_i + \eta_j = 1$; see Figs. 1(f) and 1(g). Smaller K_{ij} would yield the transformation paths similar to the dashed curves shown in those figures. The last terms in Eqs. (56) and (57) appear due to the gradient energy, and they determine the structure of the interfaces.

The exact expressions for the structural stresses \mathbf{P}_{st} and $\boldsymbol{\sigma}_{st}$ given by Eqs. (10)₂ and (15)₃, respectively, are rewritten using Eq. (51) as

$$\begin{aligned}\mathbf{P}_{st} &= J\rho_0(\check{\psi}^\theta + \psi^\nabla)\mathbf{F}^{-T} - J\beta_{0M}\nabla\eta_0 \otimes \nabla\eta_0 \cdot \mathbf{F}^{-T} - J\tilde{\varphi}(a_\beta, a_0, \eta_0) \sum_{i=1}^N \sum_{j=1}^N \frac{\beta_{ij}}{4} \nabla\eta_i \otimes (\nabla\eta_i - \nabla\eta_j) \cdot \mathbf{F}^{-T}; \\ \boldsymbol{\sigma}_{st} &= \rho_0(\check{\psi}^\theta + \psi^\nabla)\mathbf{I} - \beta_{0M}\nabla\eta_0 \otimes \nabla\eta_0 - \tilde{\varphi}(a_\beta, a_0, \eta_0) \sum_{i=1}^N \sum_{j=1}^N \frac{\beta_{ij}}{4} \nabla\eta_i \otimes (\nabla\eta_i - \nabla\eta_j).\end{aligned}\quad (58)$$

When there is just a single interface between A and M_i or between M_i and M_j , the stress $\boldsymbol{\sigma}_{st}$ can be easily proved to be biaxial (a tangential tensor), and its magnitude is equal to the corresponding interfacial energy (see below and Levitas (2014)). If in A gradient of some η_i is not zero, this corresponds to a complex M_i - A - M_j interface, or triple and multiple junction, and the stresses have a more complex structure, which does not have counterparts for a sharp interface. Some examples of interfacial stresses for complex interfaces can be found in Momeni and Levitas (2016).

4.5.2. Explicit form of the equations for a system with two variants

Let us assume $K_{ij} \rightarrow \infty$ for the chosen i and j , i.e. the constraint $\eta_j + \eta_i = 1$ is imposed, and we will obtain the explicit forms of the Ginzburg-Landau equations for a system with austenite A and two martensitic variants M_i and M_j . When η_j is replaced by $1 - \eta_i$ in Eq. (37), we have

$$\phi_j(\eta_j) = 1 - \phi_i(\eta_i), \quad \text{and} \quad \frac{\partial\phi_j(\eta_j)}{\partial\eta_j} = \frac{\partial\phi_i(\eta_i)}{\partial\eta_i}.\quad (59)$$

Obviously, we can express the kinetics of this system just in terms of two independent order parameters η_0 and η_i . Substituting $\eta_j = 1 - \eta_i$ and using Eq. (59) and the material property given by Eq. (31) into Eq. (20) and Eq. (27), the Ginzburg-Landau equations are finally simplified to

$$\begin{aligned}
\dot{\eta}_0 &= L_{0M} X_{0M} \\
&= L_{0M} \left[(\mathbf{P}_e^T \cdot \mathbf{F} - J_t \psi_e \mathbf{I}) : \mathbf{F}_t^{-1} \cdot \frac{\partial \mathbf{F}_t}{\partial \eta_0} - 0.5 J_t \frac{\partial \varphi(a_\varepsilon, \eta_0)}{\partial \eta_0} \mathbf{E}_e : \{\mathbf{C}_j + (\mathbf{C}_i - \mathbf{C}_j) \phi_i - \mathbf{C}_0\} : \mathbf{E}_e - \right. \\
&\quad \rho_0 \Delta \psi^\theta (6\eta_0 - 6\eta_0^2) - \rho_0 \bar{A} J \frac{\partial \varphi(a_b, \eta_0)}{\partial \eta_0} \eta_i^2 (1 - \eta_i)^2 - J \rho_0 \{A(\theta) + (a_\theta - 3) \Delta \psi^\theta(\theta)\} (2\eta_0 - 6\eta_0^2 + 4\eta_0^3) - \\
&\quad \rho_0 K_{0ij} \left(2\eta_0 \{1 - \varphi(a_K, \eta_0)\} - \eta_0^2 \frac{\partial \varphi(a_K, \eta_0)}{\partial \eta_0} \right) \eta_i^2 (1 - \eta_i)^2 - 0.5 J \beta_{ij} |\nabla \eta_i|^2 \frac{\partial \tilde{\varphi}(a_\beta, a_0, \eta_0)}{\partial \eta_0} + \\
&\quad \left. \nabla_0 \cdot (\beta_{0M} J \mathbf{F}^{-1} \cdot \nabla \eta_0) \right] \quad \text{and} \tag{60}
\end{aligned}$$

$$\begin{aligned}
\dot{\eta}_i &= L_{ij} (X_i - X_j) \\
&= L_{ij} \left[(\mathbf{P}_e^T \cdot \mathbf{F} - J_t \psi_e \mathbf{I}) : \mathbf{F}_t^{-1} \cdot \left(\frac{\partial \mathbf{F}_t}{\partial \phi(\eta_i)} - \frac{\partial \mathbf{F}_t}{\partial \phi(1 - \eta_i)} \right) \frac{\partial \phi_i}{\partial \eta_i} - \right. \\
&\quad 0.5 J_t \varphi(a_\varepsilon, \eta_0) \frac{\partial \phi_i(\eta_i)}{\partial \eta_i} \mathbf{E}_e : (\mathbf{C}_i - \mathbf{C}_j) : \mathbf{E}_e - \rho_0 J \bar{A} \varphi(a_b, \eta_0) (2\eta_i - 6\eta_i^2 + 4\eta_i^3) - \\
&\quad \left. \rho_0 K_{0ij} \eta_0^2 (2\eta_i - 6\eta_i^2 + 4\eta_i^3) (1 - \varphi(a_K, \eta_0)) + \nabla_0 \cdot (J \tilde{\varphi}(a_\beta, a_0, \eta_0) \beta_{ij} \mathbf{F}^{-1} \cdot \nabla \eta_i) \right], \tag{61}
\end{aligned}$$

respectively. Note that in the first term of Eq. (61)₂ the derivatives of $\mathbf{F}_t(\phi(\eta_i), \phi(1 - \eta_i))$ are with respect to $\phi(\eta_i)$ and $\phi(1 - \eta_i)$, respectively.

The derivatives of \mathbf{F}_t and ψ_e in Eq. (61) with respect to η_i should be determined considering η_j to be a constant and vice versa. All other terms in Eq. (61) have been expressed after applying $\eta_j = 1 - \eta_i$. Since the only possible triple junctions in this system are those made by A, and variants M_i and M_j , only the penalizing term with coefficient K_{0ij} is nontrivial.

The structural first Piola-Kirchhoff and Cauchy stress tensors in Eq. (58) simplify to

$$\begin{aligned}
\mathbf{P}_{st} &= J \rho_0 (\check{\psi}^\theta + \psi^\nabla) \mathbf{F}^{-T} - J \beta_{0M} \nabla \eta_0 \otimes \nabla \eta_0 \cdot \mathbf{F}^{-T} - \beta_{ij} J \tilde{\varphi}(a_\beta, a_0, \eta_0) (\nabla \eta_i \otimes \nabla \eta_i) \cdot \mathbf{F}^{-T} \quad \text{and} \\
\boldsymbol{\sigma}_{st} &= \rho_0 (\check{\psi}^\theta + \psi^\nabla) \mathbf{I} - \beta_{0M} \nabla \eta_0 \otimes \nabla \eta_0 - \beta_{ij} \tilde{\varphi}(a_\beta, a_0, \eta_0) \nabla \eta_i \otimes \nabla \eta_i, \tag{62}
\end{aligned}$$

respectively, where

$$\begin{aligned}\check{\psi}^\theta &= [A(\theta) + (a_\theta - 3)\Delta\psi^\theta(\theta)]\eta_0^2(1 - \eta_0)^2 + \bar{A}\varphi(a_b, \eta_0)\eta_i^2(1 - \eta_i)^2 \quad \text{and} \\ \psi^\nabla &= \frac{1}{2\rho_0}(\beta_{0M}|\nabla\eta_0|^2 + \beta_{ij}\tilde{\varphi}(a_\beta, a_0, \eta_0)|\nabla\eta_i|^2).\end{aligned}\quad (63)$$

In particular, for the A-M and $M_i - M_j$ interfaces, Eqs. (62) and (63) reduce to (see Levitas (2014) for details)

$$\begin{aligned}\boldsymbol{\sigma}_{st} &= \sigma_{st}^{0M}(\mathbf{I} - \mathbf{k}_{0M} \otimes \mathbf{k}_{0M}), \quad \text{where } \sigma_{st}^{0M} = \beta_{0M}|\nabla\eta_0|^2 = 2\rho_0\check{\psi}^\theta \quad \text{and } \mathbf{k}_{0M} = \nabla\eta_0/|\nabla\eta_0|, \quad \text{and,} \\ \boldsymbol{\sigma}_{st} &= \sigma_{st}^{ij}(\mathbf{I} - \mathbf{k}_{ij} \otimes \mathbf{k}_{ij}), \quad \text{where } \sigma_{st}^{ij} = \beta_{ij}|\nabla\eta_i|^2 = 2\rho_0\check{\psi}^\theta \quad \text{and } \mathbf{k}_{ij} = \nabla\eta_i/|\nabla\eta_i|,\end{aligned}\quad (64)$$

respectively. Clearly, the structural Cauchy stress tensor is biaxial within interfaces between each pair of phases.

4.5.3. Explicit form of the equations for a system with three variants

For a more complex system with austenite and three martensitic variants M_i , M_j , and M_k , using Eq. (27) the kinetic equations can be expressed as

$$\begin{aligned}\dot{\eta}_i &= L_{ij}(X_i - X_j) + L_{ik}(X_i - X_k), \\ \dot{\eta}_j &= L_{ji}(X_j - X_i) + L_{jk}(X_j - X_k), \\ \dot{\eta}_k &= L_{ki}(X_k - X_i) + L_{kj}(X_k - X_j) = -\dot{\eta}_i - \dot{\eta}_j,\end{aligned}\quad (65)$$

where the driving forces are expressed in terms of all the order parameters η_0 , η_i , η_j , and η_k :

$$\begin{aligned}X_0 &= (\mathbf{P}_e^T \cdot \mathbf{F}_e - J_t\psi_e\mathbf{F}_t^{-1}) : \frac{\partial\mathbf{F}_t}{\partial\eta_0} - J_t\frac{\partial\psi_e}{\partial\eta_0}\Big|_{\mathbf{F}_e} - \rho_0J\bar{A}(\eta_i^2\eta_j^2 + \eta_j^2\eta_k^2 + \eta_i^2\eta_k^2)\frac{\partial\varphi(a_\beta, \eta_0)}{\partial\eta_0} - \\ &(6\eta_0 - 6\eta_0^2)\rho_0\Delta\psi^\theta - J\rho_0\{A(\theta) + (a_\theta - 3)\Delta\psi^\theta(\theta)\}(2\eta_0 - 6\eta_0^2 + 4\eta_0^3) - \rho_0(K_{0ij}\eta_i^2\eta_j^2 + K_{0jk}\eta_j^2\eta_k^2 + \\ &K_{0ki}\eta_k^2\eta_i^2 + K_{0ijk}\eta_i^2\eta_j^2\eta_k^2) \left(2\eta_0\{1 - \varphi(a_K, \eta_0)\} - \eta_0^2\frac{\partial\varphi(a_K, \eta_0)}{\partial\eta_0}\right) - \\ &\frac{J}{8}\frac{\partial\tilde{\varphi}(a_\beta, a_0, \eta_0)}{\partial\eta_0} [(\beta_{ij} + \beta_{ik})|\nabla\eta_i|^2 + (\beta_{ij} + \beta_{jk})|\nabla\eta_j|^2 + (\beta_{jk} + \beta_{ik})|\nabla\eta_k|^2 - \\ &2(\beta_{ij}\nabla\eta_i \cdot \nabla\eta_j + \beta_{jk}\nabla\eta_j \cdot \nabla\eta_k + \beta_{ki}\nabla\eta_k \cdot \nabla\eta_i)] + \nabla_0 \cdot (J\beta_{0M}\mathbf{F}^{-1} \cdot \nabla\eta_0),\end{aligned}\quad (66)$$

$$\begin{aligned}
X_i = & (\mathbf{P}_e^T \cdot \mathbf{F}_e - J_t \psi_e \mathbf{F}_t^{-1}) : \frac{\partial \mathbf{F}_t}{\partial \eta_i} - J_t \frac{\partial \psi_e}{\partial \eta_i} \Big|_{\mathbf{F}_e} - 2\rho_0 J \bar{A} \eta_i (\eta_j^2 + \eta_k^2) \varphi(a_b, \eta_0) - \\
& 2\rho_0 K_{ij} \eta_i \eta_j^2 (\eta_i + \eta_j - 1)(2\eta_i + \eta_j - 1) - 2\rho_0 K_{ik} \eta_i \eta_k^2 (\eta_i + \eta_k - 1)(2\eta_i + \eta_k - 1) - \\
& 2\rho_0 \eta_0^2 \eta_i (K_{0ij} \eta_j^2 + K_{0ik} \eta_k^2 + K_{0ijk} \eta_j^2 \eta_k^2) (1 - \varphi(a_K, \eta_0)) - 2\rho_0 K_{ijk} \eta_i \eta_j^2 \eta_k^2 + \\
& \nabla_0 \cdot \left[\frac{J}{4} \tilde{\varphi}(a_\beta, a_0, \eta_0) \mathbf{F}^{-1} \cdot \{(\beta_{ij} + \beta_{ik}) \nabla \eta_i - (\beta_{ij} \nabla \eta_j + \beta_{ik} \nabla \eta_k)\} \right]. \tag{67}
\end{aligned}$$

For calculating the derivatives $\partial \mathbf{F}_t / \partial \eta_i$ and $\partial \psi_e / \partial \eta_i$ in Eq. (67), the other order parameters η_j and η_k are taken to be constant. The expressions for X_j and X_k can be obtained just by interchanging i and j , and i and k , respectively, in Eq. (67). Evidently, among the three kinetic relations in Eq. (65), only two are independent. Hence one can solve any two equations in conjunction with the constraint $\eta_i + \eta_j + \eta_k = 1$ for determining all the order parameters related to the variants.

The structural stress tensors given in Eq. (58) are expressed as

$$\begin{aligned}
\mathbf{P}_{st} = & J\rho_0(\check{\psi}^\theta + \psi^\nabla) \mathbf{F}^{-T} - J\beta_{0M} \nabla \eta_0 \otimes \nabla \eta_0 \cdot \mathbf{F}^{-T} - \frac{J}{4} \tilde{\varphi}(a_\beta, a_0, \eta_0) [\beta_{ij} (\nabla \eta_i \otimes \nabla \eta_i + \nabla \eta_j \otimes \nabla \eta_j - \\
& \nabla \eta_i \otimes \nabla \eta_j - \nabla \eta_j \otimes \nabla \eta_i) + \beta_{jk} (\nabla \eta_j \otimes \nabla \eta_j + \nabla \eta_k \otimes \nabla \eta_k - \nabla \eta_j \otimes \nabla \eta_k - \nabla \eta_k \otimes \nabla \eta_j) + \\
& \beta_{ki} (\nabla \eta_i \otimes \nabla \eta_i + \nabla \eta_k \otimes \nabla \eta_k - \nabla \eta_k \otimes \nabla \eta_i - \nabla \eta_i \otimes \nabla \eta_k)] \cdot \mathbf{F}^{-T}, \text{ and} \\
\boldsymbol{\sigma}_{st} = & \rho_0(\check{\psi}^\theta + \psi^\nabla) \mathbf{I} - \beta_{0M} \nabla \eta_0 \otimes \nabla \eta_0 - \frac{1}{4} \tilde{\varphi}(a_\beta, a_0, \eta_0) [\beta_{ij} (\nabla \eta_i \otimes \nabla \eta_i + \nabla \eta_j \otimes \nabla \eta_j - \\
& \nabla \eta_i \otimes \nabla \eta_j - \nabla \eta_j \otimes \nabla \eta_i) + \beta_{jk} (\nabla \eta_j \otimes \nabla \eta_j + \nabla \eta_k \otimes \nabla \eta_k - \nabla \eta_j \otimes \nabla \eta_k - \nabla \eta_k \otimes \nabla \eta_j) + \\
& \beta_{ki} (\nabla \eta_i \otimes \nabla \eta_i + \nabla \eta_k \otimes \nabla \eta_k - \nabla \eta_k \otimes \nabla \eta_i - \nabla \eta_i \otimes \nabla \eta_k)], \tag{68}
\end{aligned}$$

respectively, where we can eliminate, say, η_k using the constraint Eq. (21)₁. The barrier energy and interfacial energy thus take the forms

$$\begin{aligned}
\check{\psi}^\theta = & [A(\theta) + (a_\theta - 3)\Delta\psi^\theta(\theta)] \eta_0^2 (1 - \eta_0)^2 + \bar{A} (\eta_i^2 \eta_j^2 + \eta_j^2 \eta_k^2 + \eta_k^2 \eta_i^2) \varphi(a_b, \eta_0), \quad \text{and} \\
\psi^\nabla = & \frac{\beta_{0M}}{2\rho_0} |\nabla \eta_0|^2 + \frac{1}{8\rho_0} \tilde{\varphi}(a_\beta, a_0, \eta_0) [(\beta_{ij} + \beta_{ik}) |\nabla \eta_i|^2 + (\beta_{ij} + \beta_{jk}) |\nabla \eta_j|^2 + (\beta_{ik} + \beta_{jk}) |\nabla \eta_k|^2 - \\
& 2(\beta_{ij} \nabla \eta_i \cdot \nabla \eta_j + \beta_{jk} \nabla \eta_j \cdot \nabla \eta_k + \beta_{ki} \nabla \eta_k \cdot \nabla \eta_i)], \tag{69}
\end{aligned}$$

respectively.

The kinetic relations, structural stresses, barrier energy, and interfacial energy for a system with any number of variants can be derived in a similar manner.

4.6. Transformation deformation gradient

The transformation deformation gradient for any intermediate state will be defined in terms of the transformation strains for the phases and the interpolation functions. Three different kinematic models KM-I, KM-II, and KM-III will be discussed.

KM-I. In this model we assume \mathbf{F}_t as a linear function of the transformation strain tensors related to the variants M_i and the interpolation functions φ and ϕ_i :

$$\mathbf{F}_t = \mathbf{U}_t = \mathbf{I} + \sum_{i=1}^N \boldsymbol{\varepsilon}_{ti} \phi_i \varphi(a_\varepsilon, \eta_0), \quad (70)$$

where $\boldsymbol{\varepsilon}_{ti} = \mathbf{U}_{ti} - \mathbf{I}$ is the transformation strain tensor and \mathbf{U}_{ti} is the transformation stretch tensor (Bain tensor) for the variant M_i . Obviously, $\varphi(a_\varepsilon, 0) = 0$ and so $\mathbf{F}_t = \mathbf{I}$ in A. In martensitic phase M, $\varphi(a_\varepsilon, 1) = 1$ and hence $\mathbf{F}_t = \mathbf{I} + \sum_{i=1}^N \boldsymbol{\varepsilon}_{ti} \phi_i$; in variant M_i , $\phi_i = 1$ and $\phi_j = 0$ for all $j \neq i$, and thus $\mathbf{F}_t = \mathbf{U}_{ti}$. This model was earlier used for studying multiphase martensitic PTs in Levitas (2013a); Levitas and Roy (2015); Levitas et al. (2013). Using the relation (see Chapter 1 of Jog (2007))

$$\det(\mathbf{A} + \mathbf{B}) = \det \mathbf{A} + \text{cof} \mathbf{A} : \mathbf{B}^T + \mathbf{A} : (\text{cof} \mathbf{B})^T + \det \mathbf{B}, \quad (71)$$

which holds for arbitrary second order tensors \mathbf{A} and \mathbf{B} , we get from Eq. (70) for $\mathbf{A} = \mathbf{I}$ and $\mathbf{B} = \sum_{i=1}^N \boldsymbol{\varepsilon}_{ti} \phi_i$

$$\det \mathbf{F}_t = 1 + \varphi(a_\varepsilon, \eta_0) I_1 + (\varphi(a_\varepsilon, \eta_0))^2 I_2 + (\varphi(a_\varepsilon, \eta_0))^3 I_3, \quad (72)$$

where I_1 , I_2 , and I_3 , respectively, are the first, second, and third invariants of $\sum_{i=1}^N \boldsymbol{\varepsilon}_{ti} \phi_i$. For any martensitic variant M_i ($\varphi(a_\varepsilon, 1) = 1$, $\phi_i = 1$ and $\phi_j = 0$ for all $i \neq j$) one obtains from Eq. (72)

$$\det \mathbf{F}_t = 1 + I_1(\boldsymbol{\varepsilon}_{ti}) + I_2(\boldsymbol{\varepsilon}_{ti}) + I_3(\boldsymbol{\varepsilon}_{ti}) = \det(\mathbf{I} + \boldsymbol{\varepsilon}_{ti}) = \det \mathbf{U}_{ti}. \quad (73)$$

Since $\det \mathbf{U}_{ti}$ is identical for all $i = 1, \dots, N$ (Bhattacharya (2004)), according to Eq. (73) the volume of all the stress-free variants is also the same. However, $\det \mathbf{F}_t$ given by Eq. (72) varies along the entire variant-variant transformation path $0 < \eta_i < 1$ when $\varphi = 1$. This implies that although the specific volume of a particle is the same for all variants, the variant-variant transformation process (when $\varphi = 1$) described by Eq. (70) is not isochoric. According to the crystallographic theory for a sharp interface, variant-variant transformations which

form twin boundaries, are obtained through simple shear deformation (a volume preserving deformation) of one variant with respect to the other. But whether the entire transformation path is indeed isochoric in reality, is not yet well-known to the best of our knowledge. In an attempt to study dislocation dynamics (known to be a volume preserving process) using atomistic simulations Bulatov et al. (1999) observed that the entire shearing path between two stable atomic configurations is not isochoric. Therefore, we consider the conservation of volume during variant-variant transformation to be a plausible condition, but not a mandatory one. In any case, we think that there should be a basic model in which this condition is met.

KM-II. Recently, an exponential-logarithmic transformation deformation gradient was suggested for studying twinning in the phase field model (Tůma and Stupkiewicz (2016); Tůma et al. (2016)). This theory was developed for the microscale, with volume fraction of phases as the order parameters. A simple linear mixture rule for interpolation functions was used. The motivation in Tůma and Stupkiewicz (2016); Tůma et al. (2016) for considering an exp-ln transformation rule was to achieve volume-preserving variant-variant transformations along the entire path of transformation. Being motivated by this idea of volume conservation, we develop the KM-II for our nanoscale phase field model.

We consider the natural logarithms of the transformation deformation gradient as a linear combination of the natural logarithm of the Bain tensors multiplied with the interpolation functions:

$$\ln \mathbf{F}_t = \sum_{i=1}^N \ln(\mathbf{U}_{ti}) \phi_i \varphi(a_\varepsilon, \eta_0); \Rightarrow \mathbf{F}_t = \exp \left[\sum_{i=1}^N \ln(\mathbf{U}_{ti}) \phi_i \varphi(a_\varepsilon, \eta_0) \right], \quad (74)$$

see, for example, Chapter 1 of Jog (2007) for the definitions of exponential and logarithm of second order tensors. In pure A, $\varphi = 0$, and hence $\mathbf{F}_t = \mathbf{I}$. In pure M, $\varphi = 1$, and hence $\mathbf{F}_t = \exp[\sum_{i=1}^N \ln(\mathbf{U}_{ti}) \phi_i]$. Since $\exp(\ln \mathbf{A}) = \mathbf{A}$ for any second order tensor \mathbf{A} , we have $\mathbf{F}_t = \mathbf{U}_{ti}$ for the variant M_i (note that $\phi_i = 1$ and $\phi_j = 0$ for all $j \neq i$ therein).

If the transformation strains ε_{ti} are small, i.e. $|\varepsilon_{ti}| \ll 1$, by expanding Eq. (74) into series we can show that it coincides with Eq. (70) when the higher order terms are neglected. Using the identities (see Chapter 1 of Jog (2007) and Clayton (2014))

$$\det(\exp \mathbf{U}_{ti}) = \exp(\text{tr} \mathbf{U}_{ti}) \quad \text{and} \quad \ln(\det \mathbf{U}_{ti}) = \text{tr}(\ln \mathbf{U}_{ti}), \quad (75)$$

we now prove the isochoric nature of the transformation rule Eq. (74) along the entire $M_i \leftrightarrow M_j$ transformation path. Here

$$\begin{aligned} \det \mathbf{F}_t &= \det [\exp(\varphi\phi_i \ln \mathbf{U}_{ti} + \varphi\phi_j \ln \mathbf{U}_{tj})] = \exp[\varphi\phi_i \text{tr}(\ln \mathbf{U}_{ti}) + \varphi\phi_j \text{tr}(\ln \mathbf{U}_{tj})] \\ &= \exp[\varphi\phi_i \ln(\det \mathbf{U}_{ti}) + \varphi\phi_j \ln(\det \mathbf{U}_{tj})] = (\det \mathbf{U}_{ti})^{\varphi\phi_i} (\det \mathbf{U}_{tj})^{\varphi\phi_j} = (\det \mathbf{U}_{ti})^{\varphi\phi_i + \varphi\phi_j}, \end{aligned} \quad (76)$$

where we took into account that for martensitic variants $\det \mathbf{U}_{ti} = \det \mathbf{U}_{tj}$ for all $i, j (\neq i)$ (see Chapter 4 of Bhattacharya (2004)). Along the $M_i \leftrightarrow M_j$ transformation path, we have $\varphi = 1$, $\eta_i + \eta_j = 1$, and $\eta_k = 0$ for all $k \neq i, j$. According to Eq. (39), $\phi_i + \phi_j = 1$. As a consequence, (76) yields $\det \mathbf{F}_t = \det \mathbf{U}_{ti} = \text{constant}$, which completes the proof.

We have just seen that KM-II has an advantage over KM-I in that the entire variant-variant transformation path is isochoric, which is, of course, a plausible condition, but may not be a mandatory one. The authors have recently shown that both KM-I and KM-II generate excess elastic stresses within the variant-variant boundaries, including the twin boundaries (Basak and Levitas (2017)). In fact, KM-II results in much larger elastic stresses compared to KM-I; we will show this in the present paper as well. The question is whether this large excess elastic stress is real or an artifact of our transformation rules. Such question arises because, according to the crystallographic theory of martensitic PTs, sharp twin boundaries are compatible and do not generate internal elastic stresses. Thus, it was believed that the diffuse variant-variant interfaces also will not produce elastic interfacial stresses. Again, this is yet to be verified using either the molecular dynamics or the first principle simulations, which, to the best of our knowledge, has not yet been done.

Furthermore, it is necessary to note that when the phase field model is combined with the either phenomenological or plasticity model or dislocation based plasticity models (Gröger et al. (2016); Javanbakht and Levitas (2015); Levitas and Javanbakht (2015)), such high interfacial stresses might cause spurious plastic flow within the interface, which is not geometrically necessary for the compatible sharp interface. It was recently reported in Gröger et al. (2016), where high dislocation density was observed within variant-variant interfaces. We believe that this is an artifact of large elastic stresses within the interfaces in that model in Gröger et al. (2016). This motivated us to consider the KM-III which yields excess elastic stress-relaxed twin boundaries.

KM-III. In this kinematic model we propose a relaxation method for an interfacial elastic stress within the twin boundaries, which arises due to incompatible transformation deformation gradients in KM-I and KM-II. Our proposal is to let a system evolve until all the twin boundaries are fully developed, using \mathbf{F}_t either from KM-I or KM-II. Then we switch \mathbf{F}_t for the entire domain to

$$\mathbf{F}_t = \mathbf{I} + \varphi(a_\varepsilon, \eta_0)[\phi_i(\mathbf{Q}_t \cdot \mathbf{U}_{ti} - \mathbf{I}) + \phi_j(\mathbf{U}_{tj} - \mathbf{I})], \quad (77)$$

which is motivated from the crystallographic theory of martensite with sharp interfaces (see Chapter 5 of Bhattacharya (2004)). Here \mathbf{Q}_t is a rotation tensor which is known from the crystallographic solutions. A comparison between Eqs. (70), (74), and (77) shows that in KM-III, the relative rotation between the variants \mathbf{Q}_t has been taken into account in the transformation deformation gradient, which was otherwise neglected (i.e. assumed $\mathbf{Q}_t = \mathbf{I}$) in KM-I and KM-II. Obviously, if one assumes $\mathbf{Q}_t = \mathbf{I}$, both KM-I and KM-III would coincide for a two variant system. Also, KM-II coincides with KM-I and KM-III in this case when the transformation strains are small, i.e. $|\varepsilon_{ti}| \ll 1$.

We can express Eq. (77) in an alternative and more convenient form

$$\mathbf{F}_t = \mathbf{I} + \varphi(a_\varepsilon, \eta_0)[\varepsilon_{tj} + \phi_i \mathbf{m}_t \otimes \mathbf{n}_t] \quad (78)$$

using the twinning equation (see Chapter 5 of Bhattacharya (2004))

$$\mathbf{Q}_t \cdot \mathbf{U}_{ti} - \mathbf{U}_{tj} = \mathbf{m}_t \otimes \mathbf{n}_t, \quad (79)$$

where we have used $\phi_i + \phi_j = 1$ in deriving Eq. (78); \mathbf{n}_t is the unit normal to the twin boundary and \mathbf{m}_t is a vector related to the simple shear direction. Both \mathbf{n}_t and \mathbf{m}_t are known from the crystallographic solutions, which depend on the constant components of the complete (after transformation) Bain tensors. Along an $M_i \leftrightarrow M_j$ transformation path (substituting $\varphi = 1$), we derive from Eq. (78) that

$$\begin{aligned} \det \mathbf{F}_t &= \det(\mathbf{U}_{tj} + \phi_i \mathbf{m}_t \otimes \mathbf{n}_t) = \det \mathbf{U}_{tj} \det(\mathbf{I} + \phi_i \mathbf{U}_{tj}^{-1} \cdot \mathbf{m}_t \otimes \mathbf{n}_t) \\ &= \det \mathbf{U}_{tj} (1 + \phi_i \mathbf{U}_{tj}^{-1} : \mathbf{m}_t \otimes \mathbf{n}_t) = \det \mathbf{U}_{tj}, \end{aligned} \quad (80)$$

where we have used Eq. (71), and also, applied the facts that the second and the third invariants of the rank-one tensor $\mathbf{U}_{tj}^{-1} \cdot \mathbf{m}_t \otimes \mathbf{n}_t$ are identically zero, and the vectors $\mathbf{U}_{tj}^{-1} \cdot \mathbf{m}_t$ and \mathbf{n}_t are mutually perpendicular

(see Chapter 5 of Bhattacharya (2004)). Obviously, \mathbf{F}_t in Eq. (78) yields isochoric transformation between the variants. We have shown in Basak and Levitas (2017) that the transformation rule Eq. (78) does not generate interfacial excess elastic stresses within twin boundaries when $\varphi = 1$. In summary, Eq. (78) would yield isochoric variant-variant transformations with internal stress-free twin boundaries. However, there are difficulties in using this model for simulating complex microstructures such as zigzag twins and twins within twins between a single pair of variants just with a single order parameter (see Levitas et al. (2013) for details). For more than two variants, the scenario is even more complicated. On the other hand, KM-I and II can be easily used to produce such complex solutions; say, for two variants one needs single independent order parameter related to the variants, and for three variants two independent order parameters are needed within our present approach.

4.6.1. \mathbf{F}_t for a system with austenite and two variants

We will write down the explicit forms of \mathbf{F}_t for all kinematic models when there is austenite and two variants M_i and M_j in a system. The order parameters for the variants η_i and η_j follow the constraint $\eta_i + \eta_j = 1$ and the corresponding interpolation functions satisfy the conditions in Eq. (59). Using these relations in the transformation deformation gradient tensors Eqs. (70), (74), and (78) we obtain

$$\begin{aligned}
\text{for KM-I:} \quad & \mathbf{F}_t = \mathbf{I} + \boldsymbol{\varepsilon}_{tj}\varphi(a_\varepsilon, \eta_0) + (\boldsymbol{\varepsilon}_{ti} - \boldsymbol{\varepsilon}_{tj})\phi_i\varphi(a_\varepsilon, \eta_0), \\
\text{for KM-II:} \quad & \mathbf{F}_t = \exp[\ln \mathbf{U}_{tj}\varphi(a_\varepsilon, \eta_0) + (\ln \mathbf{U}_{ti} - \ln \mathbf{U}_{tj})\phi_i\varphi(a_\varepsilon, \eta_0)], \text{ and} \\
\text{for KM-III:} \quad & \mathbf{F}_t = \mathbf{I} + [\boldsymbol{\varepsilon}_{tj} + \phi_i \mathbf{m}_t \otimes \mathbf{n}_t]\varphi(a_\varepsilon, \eta_0).
\end{aligned} \tag{81}$$

4.6.2. \mathbf{F}_t for a system with austenite and three variants

We now consider a three-variant system with M_i , M_j , and M_k . Since KM-III can accommodate only two variants, in this case we will write the explicit form for \mathbf{F}_t for KM-I and II only:

$$\begin{aligned}
\text{for KM-I:} \quad & \mathbf{F}_t = \mathbf{I} + \varphi(a_\varepsilon, \eta_0)(\boldsymbol{\varepsilon}_{ti}\phi_i + \boldsymbol{\varepsilon}_{tj}\phi_j + \boldsymbol{\varepsilon}_{tk}\phi_k), \\
\text{for KM-II:} \quad & \mathbf{F}_t = \exp[\varphi(a_\varepsilon, \eta_0)(\phi_i \ln \mathbf{U}_{ti} + \phi_j \ln \mathbf{U}_{tj} + \phi_k \ln \mathbf{U}_{tk})],
\end{aligned} \tag{82}$$

respectively. Here the expressions have been written in terms of all three order parameters for the variants η_i , η_j , and η_k . However, one can always express them in terms of any two order parameters using the constraint

Eq. (1).

4.7. Analysis of the transformation work for KM-I, KM-II, and KM-III

Let us now analyze the transformation work term in the driving forces X_0 and X_i given by Eqs. (56) and (57), and make a comparative study for all three kinematic models. For simplicity, we consider a two variant system without loss of generality, and hence use the \mathbf{F}_t listed in Eq. (81). Using Eqs. (14) and (2), the transformation work terms are rewritten as a function of the elastic Cauchy stress:

$$\begin{aligned} W &= (J\mathbf{F}^{-1} \cdot \boldsymbol{\sigma}_e \cdot \mathbf{F} - J_t\psi_e\mathbf{I}) : \mathbf{F}_t^{-1} \cdot \frac{\partial \mathbf{F}_t}{\partial \eta} \\ &= (J\sigma_{e0} - J_t\psi_e) \text{tr} \left(\mathbf{F}_t^{-1} \cdot \frac{\partial \mathbf{F}_t}{\partial \eta} \right) + J\mathbf{F}^{-1} \cdot \text{dev} \boldsymbol{\sigma}_e \cdot \mathbf{F} : \text{dev} \left(\mathbf{F}_t^{-1} \cdot \frac{\partial \mathbf{F}_t}{\partial \eta} \right), \end{aligned} \quad (83)$$

where $\boldsymbol{\sigma}_e$ has been decomposed into $\boldsymbol{\sigma}_e = \sigma_{0e}\mathbf{I} + \text{dev} \boldsymbol{\sigma}_e$, and σ_{0e} is the mean part of $\boldsymbol{\sigma}_e$. Also, we have used the fact that $\mathbf{F}^{-1} \cdot \text{dev} \boldsymbol{\sigma}_e \cdot \mathbf{F}$ is a deviatoric tensor, which can be proved by showing that its trace is zero: $\text{tr}(\mathbf{F}^{-1} \cdot \text{dev} \boldsymbol{\sigma}_e \cdot \mathbf{F}) = \mathbf{I} : \mathbf{F}^{-1} \cdot \text{dev} \boldsymbol{\sigma}_e \cdot \mathbf{F} = \mathbf{F} \cdot \mathbf{F}^{-1} : \text{dev} \boldsymbol{\sigma}_e = \text{tr}(\text{dev} \boldsymbol{\sigma}_e) = 0$.

Analysis for KM-II: At first we consider Eq. (81)₂ for KM-II and analyze Eq. (83). To this end, we use Eqs. (B.4) and (B.6) in Eq. (83) and obtain the transformation work for $\mathbf{A} \leftrightarrow \mathbf{M}$ transformations (denoted by W_0), and for $\mathbf{M}_i \leftrightarrow \mathbf{M}_j$ transformations (denoted by W_i):

$$\begin{aligned} W_0 &= \frac{(J\sigma_{e0} - J_{ti}\psi_e)}{\varphi(a_\varepsilon, \eta_0)} \frac{\partial \varphi(a_\varepsilon, \eta_0)}{\partial \eta_0} \text{tr}(\ln \mathbf{F}_t) + \frac{J}{\varphi(a_\varepsilon, \eta_0)} \frac{\partial \varphi(a_\varepsilon, \eta_0)}{\partial \eta_0} \mathbf{F}^{-1} \cdot \text{dev} \boldsymbol{\sigma}_e \cdot \mathbf{F} : \text{dev}(\ln \mathbf{F}_t), \\ W_i &= J\varphi(a_\varepsilon, \eta_0) \frac{\partial \phi_i}{\partial \eta_i} \mathbf{F}^{-1} \cdot \text{dev} \boldsymbol{\sigma}_e \cdot \mathbf{F} : \text{dev}(\ln \mathbf{U}_{ti} - \ln \mathbf{U}_{tj}). \end{aligned} \quad (84)$$

Note that in obtaining the expression for $\partial \mathbf{F}_t / \partial \eta_i$ for KM-II, $\ln \mathbf{U}_{ti}$ and $\ln \mathbf{U}_{tj}$ were assumed to be commutative, which is true only for some specific kind of PTs such as cubic to tetragonal PT. For a general case where $\ln \mathbf{U}_{ti}$ and $\ln \mathbf{U}_{tj}$ are not commutative, a similar analysis can be carried out. For $\eta_0 = 0$ the limit transition in Eq. (84)₁ gives $W_0 = 0$. Note that $\text{tr}(\ln \mathbf{F}_t)$ and $\text{dev}(\ln \mathbf{F}_t)$ represent the volumetric part of $\ln \mathbf{F}_t$ and the isochoric change in shape of the material particle. Thus, Eq. (84)₁ represents an additive split of the work of the generalized mean stress into the volumetric part of the logarithmic transformation strain and work of the generalized deviatoric stress on the deformation describing the isochoric change in shape, both along the entire $\mathbf{A} \leftrightarrow \mathbf{M}$ transformation path. For variant-variant transformations, the volumetric part of the transformation

strain measure is zero, and that is why the mean stress does not contribute to the transformation work. Both these results are desired.

Analysis for KM-III: Considering the relations for \mathbf{F}_t^{-1} and $\partial\mathbf{F}_t/\partial\eta_i$ from Eqs. (B.8) and (B.9), respectively, we see that it is not possible to decompose the transformation work additively into the work of the generalized mean stress on the volumetric part of the transformation strain and work of the generalized deviatoric stress on the deformation describing the isochoric change in shape. However, considering $\varphi = 1$ and noticing that $\mathbf{U}_{tj}^{-1} \cdot \mathbf{m}_t$ and \mathbf{n}_t are mutually perpendicular (hence $\mathbf{U}_{tj}^{-1} \cdot \mathbf{m}_t \otimes \mathbf{n}_t$ is a deviatoric tensor) in Eqs. (B.8)₃ and (B.9), the transformation work W_i becomes

$$W_i = J\varphi(a_\varepsilon, \eta_0) \frac{\partial\phi_i}{\partial\eta_i} \mathbf{F}^{-1} \cdot \text{dev } \boldsymbol{\sigma}_e \cdot \mathbf{F} : \mathbf{U}_{tj}^{-1} \cdot \mathbf{m}_t \otimes \mathbf{n}_t, \quad (85)$$

i.e. variant-variant transformation work depends on $\text{dev } \boldsymbol{\sigma}_e$ and is independent of the mean stress, as desired.

Analysis for KM-I: Using Eqs. (81)₁ and (B.1)_{1,3} in Eq. (83) we can show that both spherical and deviatoric parts of $\boldsymbol{\sigma}_e$ contributes in the transformation work for the variant-variant transformation W_i .

5. Thermodynamic instability criteria for $\mathbf{A} \leftrightarrow \mathbf{M}$ and $\mathbf{M}_i \leftrightarrow \mathbf{M}_j$ transformations

We will now analyze the stability of homogeneous phases under prescribed stresses and temperature, and establish the instability criteria for homogeneous transformation between the phases. We will also show that our instability criteria actually do not depend on which stress (e.g. the first Piola-Kirchhoff or Cauchy stress tensor) is prescribed. Although, the prescribed stress is constant, the elastic deformation gradient \mathbf{F}_e may vary along the transformation path due to variation of the elastic constants.

We define the instability criterion as follows. If for a thermodynamic equilibrium state ($\hat{\eta}_j$ for $j = 0, 1, 2, \dots, N$) a spontaneous perturbation $\Delta\eta$ of the order parameters is thermodynamically admissible under prescribed stresses and temperature, i.e. the dissipation rate is positive, then the equilibrium is unstable (Levitas (2013a); Levitas and Roy (2015)):

$$X_i(\mathbf{T}, \mathbf{F}_e(\hat{\eta}_j + \Delta\eta_j), \hat{\eta}_j + \Delta\eta_j, \theta) \dot{\eta}_i \geq 0 \quad \text{for } i = 0, 1, 2, \dots, N \quad (86)$$

implies that the thermodynamic equilibrium $\hat{\eta}_j$ is unstable under arbitrary prescribed stress \mathbf{T} ($= \mathbf{P}$ or $\boldsymbol{\sigma}$) and temperature θ , where \mathbf{F}_e has been considered as a function of the order parameters. Based on the definition Eq.

(86) we now determine the instability criterion for $\mathbf{A} \leftrightarrow \mathbf{M}$ and $\mathbf{M}_i \leftrightarrow \mathbf{M}_j$ transformations for all the kinematic models. Expanding X_i in Taylor series about the equilibrium $\hat{\eta}_j$ we have

$$X_i(\mathbf{T}, \mathbf{F}_e(\hat{\eta}_j), \hat{\eta}_j + \Delta\eta, \theta) = \left. \frac{\partial X_i(\mathbf{T}, \mathbf{F}_e(\hat{\eta}_j), \hat{\eta}_j, \theta)}{\partial \eta_k} \right|_{\mathbf{T}} \Delta\eta_k + o(\Delta\eta_k), \quad (87)$$

where $o(\Delta\eta_k)$ is such that $o(\Delta\eta_k)/\Delta\eta_k \rightarrow 0$ as $\Delta\eta_k \rightarrow 0$ and we have considered $X_i(\mathbf{T}, \mathbf{F}_e(\hat{\eta}_j), \hat{\eta}_j, \theta) = 0$. Using Eq. (87) in Eq. (86) the instability criterion is finally obtained as

$$\left. \frac{\partial X_i(\mathbf{T}, \mathbf{F}_e(\hat{\eta}_j), \hat{\eta}_j, \theta)}{\partial \eta_k} \right|_{\mathbf{T}} \hat{\eta}_i \hat{\eta}_k \geq 0. \quad (88)$$

$\mathbf{A} \leftrightarrow \mathbf{M}$ transformation:

In obtaining the instability criteria for $\mathbf{A} \leftrightarrow \mathbf{M}$ transformations, we assume without loss of generality that $\eta_i = 1$ and $\eta_j = 0$ for all $j \neq i$, i.e. $\mathbf{M} = \mathbf{M}_i$. The instability criteria for $\mathbf{A} \rightarrow \mathbf{M}$ and $\mathbf{M} \rightarrow \mathbf{A}$ transformations are

$$\begin{aligned} \mathbf{A} \rightarrow \mathbf{M} & \quad \left. \frac{\partial X_0(\mathbf{T}, \mathbf{F}_e(\eta_0 = 0), \eta_0 = 0, \theta)}{\partial \eta_0} \right|_{\mathbf{T}} \geq 0, \\ \mathbf{M} \rightarrow \mathbf{A} & \quad \left. \frac{\partial X_0(\mathbf{T}, \mathbf{F}_e(\eta_0 = 1), \eta_0 = 1, \theta)}{\partial \eta_0} \right|_{\mathbf{T}} \geq 0. \end{aligned} \quad (89)$$

We evaluate $\partial X_0/\partial \eta_0$ by differentiating Eq. (56) with respect to η_0 and substituting $\eta_i = 1$ and $\eta_j = 0$ for all $j \neq i$:

$$\begin{aligned} \left. \frac{\partial X_0}{\partial \eta_0} \right|_{\mathbf{T}} &= \left. \frac{\partial(\mathbf{P}_e^T \cdot \mathbf{F}_e - J_t \psi_e \mathbf{F}_t^{-1})}{\partial \eta_0} \right|_{\mathbf{T}} : \frac{\partial \mathbf{F}_t}{\partial \eta_0} + (\mathbf{P}_e^T \cdot \mathbf{F}_e - J_t \psi_e \mathbf{F}_t^{-1}) : \frac{\partial^2 \mathbf{F}_t}{\partial \eta_0^2} - J_t \left. \frac{\partial \psi_e}{\partial \eta_0} \right|_{\mathbf{F}_e} \mathbf{F}_t^{-1} : \frac{\partial \mathbf{F}_t}{\partial \eta_0} - \\ & J_t \frac{\partial}{\partial \eta_0} \left(\left. \frac{\partial \psi_e}{\partial \eta_0} \right|_{\mathbf{F}_e} \right)_{\mathbf{T}} - \rho_0 \Delta \psi^\theta (6 - 12\eta_0) - J \rho_0 [A(\theta) + (a_\theta - 3) \Delta \psi^\theta(\theta)] (2 - 12\eta_0 + 12\eta_0^2) - \\ & \rho_0 [A(\theta) + (a_\theta - 3) \Delta \psi^\theta(\theta)] (2\eta_0 - 6\eta_0^2 + 4\eta_0^3) \left. \frac{\partial J}{\partial \eta_0} \right|_{\mathbf{T}} + \left. \frac{\partial(\mathbf{P}_e^T \cdot \mathbf{F}_e - J_t \psi_e \mathbf{F}_t^{-1})}{\partial \mathbf{F}_e^T} \right|_{\mathbf{T}} : \left. \frac{\partial \mathbf{F}_e}{\partial \eta_0} \right|_{\mathbf{T}} : \left. \frac{\partial \mathbf{F}_t}{\partial \eta_0} \right|_{\mathbf{T}} - \\ & J_t \left. \frac{\partial}{\partial \mathbf{F}_e^T} \left(\left. \frac{\partial \psi_e}{\partial \eta_0} \right|_{\mathbf{F}_e} \right) \right|_{\mathbf{T}} : \left. \frac{\partial \mathbf{F}_e}{\partial \eta_0} \right|_{\mathbf{T}} - \left. \frac{\partial f_l}{\partial \mathbf{F}_e^T} \right|_{\mathbf{T}} : \left. \frac{\partial \mathbf{F}_e}{\partial \eta_0} \right|_{\mathbf{T}}, \quad \text{where} \end{aligned} \quad (90)$$

$$f_l = J \rho_0 [A(\theta) + (a_\theta - 3) \Delta \psi^\theta(\theta)] (2\eta_0 - 6\eta_0^2 + 4\eta_0^3). \quad (91)$$

Due to the properties of interpolation functions for any material properties (Eqs. (31) and (33)), $\partial \mathbf{F}_t(\hat{\eta}_0)/\partial \eta_0 =$

$\mathbf{0}$. Furthermore, using Eq. (41), we have

$$\left. \frac{\partial}{\partial \eta_0} \left(\left. \frac{\partial \psi_e}{\partial \eta_0} \right|_{\mathbf{F}_e} \right) \right|_{\mathbf{T}} = \left. \frac{\partial \mathbf{E}_e}{\partial \eta_0} \right|_{\mathbf{T}} : \left. \frac{\partial \mathcal{C}}{\partial \eta_0} \right|_{\mathbf{T}} : \mathbf{E}_e + 0.5 \mathbf{E}_e : \left. \frac{\partial^2 \mathcal{C}}{\partial \eta_0^2} \right|_{\mathbf{T}} : \mathbf{E}_e, \quad (92)$$

where the elastic modulus \mathbf{C} has been assumed to be independent of \mathbf{F}_e . Using the same Eqs. (31) and (33) we readily see that $\frac{\partial \mathbf{C}(\hat{\eta}_0)}{\partial \eta_0} = \mathbf{0}$ and the first term of Eq. (92) vanishes at $\eta_0 = 0$ and 1.

Also, it can be proved that $(\partial \mathbf{F}_e(\hat{\eta}_0)/\partial \eta_0)_{\mathbf{T}} = \mathbf{0}$, and hence $(\partial \mathbf{E}_e(\hat{\eta}_0)/\partial \eta_0)_{\mathbf{T}} = \mathbf{0}$ whether $\mathbf{T} = \mathbf{P}$ or $\mathbf{T} = \boldsymbol{\sigma}_e$ (see Levitas (2013a) for the proof). Using all these condition in Eq. (90), the expression is simplified to

$$\begin{aligned} \left. \frac{\partial X_0}{\partial \eta_0} \right|_{\mathbf{T}} &= (J\sigma_{e0} - J_t\psi_e)tr \left(\mathbf{F}_t^{-1} \cdot \frac{\partial^2 \mathbf{F}_t}{\partial \eta_0^2} \right) + J\mathbf{F}^{-1} \cdot dev(\boldsymbol{\sigma}_e) \cdot \mathbf{F} : dev \left(\mathbf{F}_t^{-1} \cdot \frac{\partial^2 \mathbf{F}_t}{\partial \eta_0^2} \right) - (6 - 12\eta_0)\rho_0\Delta\psi^\theta(\theta) \\ &\quad - 0.5J_t\mathbf{E}_e : \frac{\partial^2 \mathbf{C}}{\partial \eta_0^2} : \mathbf{E}_e - J\rho_0[A(\theta) + (a_\theta - 3)\Delta\psi^\theta(\theta)](2 - 12\eta_0 + 12\eta_0^2) \quad \text{for } \eta_0 = 0, 1, \end{aligned} \quad (93)$$

where we have used Eq. (14) for expressing the transformation work related term as a function of the Cauchy stress. It is clear from Eq. (93) that the instability criteria does not depend on which stress was kept constant (also see Levitas (2013a)). Using Eq. (93) and expressions for derivatives of \mathbf{F}_t corresponding to all the kinematic models from Appendix B into Eq. (89), we finally establish the following criteria for $\mathbf{A} \rightarrow \mathbf{M}$ and $\mathbf{M} \rightarrow \mathbf{A}$ transformations:

$\mathbf{A} \rightarrow \mathbf{M}$:

$$\begin{aligned} \text{for KM-I: } & a_\varepsilon(J_e\sigma_{e0} - \psi_e)tr(\boldsymbol{\varepsilon}_{ti}) + a_\varepsilon J_e \mathbf{F}^{-1} \cdot dev(\boldsymbol{\sigma}_e) \cdot \mathbf{F} : dev(\boldsymbol{\varepsilon}_{ti}) - \rho_0[3 + J_e(a_\theta - 3)]\Delta\psi^\theta + \\ & 0.5a_\varepsilon \mathbf{E}_e : (\mathbf{C}_0 - \mathbf{C}_i) : \mathbf{E}_e \geq \rho_0 J_e A(\theta); \\ \text{for KM-II: } & a_\varepsilon(J_e\sigma_{e0} - \psi_e)tr(\ln \mathbf{U}_{ti}) + a_\varepsilon J_e \mathbf{F}^{-1} \cdot dev(\boldsymbol{\sigma}_e) \cdot \mathbf{F} : dev(\ln \mathbf{U}_{ti}) - \rho_0[3 + J_e(a_\theta - 3)]\Delta\psi^\theta + \\ & 0.5a_\varepsilon \mathbf{E}_e : (\mathbf{C}_0 - \mathbf{C}_i) : \mathbf{E}_e \geq \rho_0 J_e A(\theta); \\ \text{for KM-III: } & a_\varepsilon(J_e\sigma_{e0} - \psi_e)tr(\boldsymbol{\varepsilon}_{ti}) + a_\varepsilon J_e \mathbf{F}^{-1} \cdot dev(\boldsymbol{\sigma}_e) \cdot \mathbf{F} : dev(\boldsymbol{\varepsilon}_{tj} + \mathbf{m}_t \otimes \mathbf{n}_t) - \\ & \rho_0[3 + J_e(a_\theta - 3)]\Delta\psi^\theta + 0.5a_\varepsilon \mathbf{E}_e : (\mathbf{C}_0 - \mathbf{C}_i) : \mathbf{E}_e \geq \rho_0 J_e A(\theta); \end{aligned} \quad (94)$$

$M \rightarrow A$:

for KM-I: $(6 - a_\varepsilon)(J\sigma_{e0} - J_{ti}\psi_e) \text{tr}(\mathbf{U}_{ti}^{-1} \cdot \boldsymbol{\varepsilon}_{ti}) + (6 - a_\varepsilon)J\mathbf{F}^{-1} \cdot \text{dev}(\boldsymbol{\sigma}_e) \cdot \mathbf{F} : \text{dev}(\mathbf{U}_{ti}^{-1} \cdot \boldsymbol{\varepsilon}_{ti}) +$

$$[J(a_\theta - 3) - 3]\rho_0\Delta\psi^\theta + 0.5J_{ti}(6 - a_\varepsilon)\mathbf{E}_e : (\mathbf{C}_0 - \mathbf{C}_i) : \mathbf{E}_e \leq -\rho_0JA;$$

for KM-II: $(6 - a_\varepsilon)(J\sigma_{e0} - J_{ti}\psi_e) \text{tr}(\ln \mathbf{U}_{ti}) + (6 - a_\varepsilon)J\mathbf{F}^{-1} \cdot \text{dev}(\boldsymbol{\sigma}_e) \cdot \mathbf{F} : \text{dev}(\ln \mathbf{U}_{ti}) +$

$$[J(a_\theta - 3) - 3]\rho_0\Delta\psi^\theta + 0.5(6 - a_\varepsilon)J_{ti}\mathbf{E}_e : (\mathbf{C}_0 - \mathbf{C}_i) : \mathbf{E}_e \leq -\rho_0JA;$$

for KM-III: $(6 - a_\varepsilon)(J\sigma_{e0} - J_{ti}\psi_e) \text{tr} \left[\mathbf{U}_{tj}^{-1} \cdot \boldsymbol{\varepsilon}_{tj} - \mathbf{U}_{tj}^{-1} \cdot (\mathbf{m}_t \otimes \mathbf{n}_t) \cdot \mathbf{U}_{tj}^{-1} \cdot (\boldsymbol{\varepsilon}_{tj} + \mathbf{m}_t \otimes \mathbf{n}_t) \right] +$

$$(6 - a_\varepsilon)J\mathbf{F}^{-1} \cdot \text{dev}(\boldsymbol{\sigma}_e) \cdot \mathbf{F} : \text{dev} \left[\left(\mathbf{U}_{tj}^{-1} - \mathbf{U}_{tj}^{-1} \cdot (\mathbf{m}_t \otimes \mathbf{n}_t) \cdot \mathbf{U}_{tj}^{-1} \right) \cdot (\boldsymbol{\varepsilon}_{tj} + \mathbf{m}_t \otimes \mathbf{n}_t) \right] +$$

$$[J(a_\theta - 3) - 3]\rho_0\Delta\psi^\theta + 0.5(6 - a_\varepsilon)J_{ti}\mathbf{E}_e : (\mathbf{C}_0 - \mathbf{C}_i) : \mathbf{E}_e \leq -\rho_0JA. \quad (95)$$

All the criteria for KM-I, II, and KM-III coincide when the transformation strains $\boldsymbol{\varepsilon}_{ti}$ are small, i.e. $|\boldsymbol{\varepsilon}_{ti}| \ll 1$, both for Eq. (94) and Eq. (95), where we have used the fact for KM-III that $|\boldsymbol{\varepsilon}_{ti}|$ and $|\mathbf{m}_t \otimes \mathbf{n}_t|$ are of the same order (Bhattacharya (2004)).

$M_i \leftrightarrow M_j$ *transformations*:

In obtaining the instability criteria for $M_i \leftrightarrow M_j$ transformations, we consider a fully martensitic region with variants M_i and M_j , and hence $\eta_0 = 1$. The transformation path follows the straight line $\eta_i + \eta_j = 1$, which is provided by large penalizing terms, $K_{ij} \rightarrow \infty$. The criteria for $M_i \rightarrow M_j$ and $M_j \rightarrow M_i$ transformations are thus

$$\begin{aligned} M_i \rightarrow M_j & \quad \left. \frac{\partial X_i(\mathbf{T}, \mathbf{F}_e(\hat{\eta}_i), \hat{\eta}_i, \theta)}{\partial \eta_i} \right|_{\mathbf{T}} \geq 0, \quad \text{and} \\ M_j \rightarrow M_i & \quad \left. \frac{\partial X_i(\mathbf{T}, \mathbf{F}_e(\hat{\eta}_j), \hat{\eta}_j, \theta)}{\partial \eta_i} \right|_{\mathbf{T}} \geq 0, \end{aligned} \quad (96)$$

respectively.

Using $\eta_j = 1 - \eta_i$ and $\eta_k = 0$ for $k \neq i, j$ in Eq. (57) and differentiating it with respect to η_i we get

$$\begin{aligned} \left. \frac{\partial X_i}{\partial \eta_i} \right|_{\mathbf{T}} &= \left. \frac{\partial}{\partial \eta_i} (\mathbf{P}_e^T \cdot \mathbf{F}_e - J_t \psi_e \mathbf{F}_t^{-1}) \right|_{\mathbf{T}} : \left. \frac{\partial \mathbf{F}_t}{\partial \eta_i} \right|_{\mathbf{T}} + (\mathbf{P}_e^T \cdot \mathbf{F}_e - J_t \psi_e \mathbf{F}_t^{-1}) : \left. \frac{\partial^2 \mathbf{F}_t}{\partial \eta_i^2} \right|_{\mathbf{T}} - J_t \left. \frac{\partial}{\partial \eta_i} \left(\left. \frac{\partial \psi_e}{\partial \eta_i} \right|_{\mathbf{F}_e} \right) \right|_{\mathbf{T}} - \\ & \rho_0 \bar{A} J (2 - 12\eta_i + 12\eta_i^2) + \left. \frac{\partial}{\partial \mathbf{F}_e^T} (\mathbf{P}_e^T \cdot \mathbf{F}_e - J_t \psi_e \mathbf{F}_t^{-1}) \right|_{\mathbf{T}} : \left. \frac{\partial \mathbf{F}_e}{\partial \eta_i} \right|_{\mathbf{T}} : \left. \frac{\partial \mathbf{F}_t}{\partial \eta_i} \right|_{\mathbf{T}} - \\ & J_t \left. \frac{\partial}{\partial \mathbf{F}_e^T} \left(\left. \frac{\partial \psi_e}{\partial \eta_i} \right|_{\mathbf{F}_e} \right) \right|_{\mathbf{T}} : \left. \frac{\partial \mathbf{F}_e}{\partial \eta_i} \right|_{\mathbf{T}} - \rho_0 \bar{A} (2\eta_i - 6\eta_i^2 + 4\eta_i^3) \left. \frac{\partial J}{\partial \mathbf{F}_e^T} \right|_{\mathbf{T}} : \left. \frac{\partial \mathbf{F}_e}{\partial \eta_i} \right|_{\mathbf{T}}. \end{aligned} \quad (97)$$

When we differentiate \mathbf{F}_t in Eq. (81) with respect to η_i and use that $\partial\phi_i/\partial\eta_i = 0$ at $\eta_i = 0, 1$ therein, we note that all the terms on the right hand side of Eq. (97) with $\partial\mathbf{F}_t/\partial\eta_i$ vanish at $\eta_i = 0$ and 1. Also, using a relation similar to Eq. (92) where the derivatives are now taken with respect to η_i and considering $(\partial\mathbf{F}_e(\hat{\eta}_i)/\partial\eta_i)_{\mathbf{T}} = \mathbf{0}$ for $\mathbf{T} = \mathbf{P}$ or $\mathbf{T} = \boldsymbol{\sigma}_e$ (see Levitas (2013a) for the proof), we simplify Eq. (97) to

$$\left. \frac{\partial X_i}{\partial \eta_i} \right|_{\mathbf{T}} = (\mathbf{P}_e^T \cdot \mathbf{F}_e - J_t \psi_e \mathbf{F}_t^{-1}) : \frac{\partial^2 \mathbf{F}_t}{\partial \eta_i^2} - J_t \frac{\partial}{\partial \eta_i} \left(\left. \frac{\partial \psi_e}{\partial \eta_i} \right|_{\mathbf{F}_e} \right)_{\mathbf{T}} - \rho_0 \bar{A} J (2 - 12\eta_i + 12\eta_i^2) \text{ at } \eta_i = 0 \text{ and } 1. \quad (98)$$

Finally, using Eqs. (98) and the required derivatives from Appendix B in Eq. (96), the instability criteria for variant-variant transformations are obtained:

$M_i \rightarrow M_j$:

$$\begin{aligned} \text{for KM-I: } & (J\sigma_{e0} - J_{ti}\psi_e) \text{tr}(\mathbf{U}_{ti}^{-1} \cdot (\boldsymbol{\varepsilon}_{ti} - \boldsymbol{\varepsilon}_{tj})) + J\mathbf{F}^{-1} \cdot \text{dev } \boldsymbol{\sigma}_e \cdot \mathbf{F} : \text{dev}(\mathbf{U}_{ti}^{-1} \cdot (\boldsymbol{\varepsilon}_{ti} - \boldsymbol{\varepsilon}_{tj})) - \\ & 0.5J_{ti}\mathbf{E}_e : (\mathbf{C}_i - \mathbf{C}_j) : \mathbf{E}_e \geq \frac{\rho_0 J \bar{A}}{3}; \\ \text{for KM-II: } & J\mathbf{F}^{-1} \cdot \text{dev } \boldsymbol{\sigma}_e \cdot \mathbf{F} : \text{dev}(\ln \mathbf{U}_{ti} - \ln \mathbf{U}_{tj}) - 0.5J_{ti}\mathbf{E}_e : (\mathbf{C}_i - \mathbf{C}_j) : \mathbf{E}_e \geq \frac{\rho_0 J \bar{A}}{3}; \\ \text{for KM-III: } & J\mathbf{F}^{-1} \cdot \text{dev } \boldsymbol{\sigma}_e \cdot \mathbf{F} : \text{dev}(\mathbf{U}_{tj}^{-1} \cdot \mathbf{m}_t \otimes \mathbf{n}_t) - 0.5J_{ti}\mathbf{E}_e : (\mathbf{C}_i - \mathbf{C}_j) : \mathbf{E}_e \geq \frac{\rho_0 J \bar{A}}{3}. \end{aligned} \quad (99)$$

$M_j \rightarrow M_i$:

$$\begin{aligned} \text{for KM-I: } & (J\sigma_{e0} - J_{ti}\psi_e) \text{tr}(\mathbf{U}_{ti}^{-1} \cdot (\boldsymbol{\varepsilon}_{ti} - \boldsymbol{\varepsilon}_{tj})) + J\mathbf{F}^{-1} \cdot \text{dev } \boldsymbol{\sigma}_e \cdot \mathbf{F} : \text{dev}(\mathbf{U}_{ti}^{-1} \cdot (\boldsymbol{\varepsilon}_{ti} - \boldsymbol{\varepsilon}_{tj})) - \\ & 0.5J_{ti}\mathbf{E}_e : (\mathbf{C}_i - \mathbf{C}_j) : \mathbf{E}_e \leq -\frac{\rho_0 J \bar{A}}{3} \\ \text{for KM-II: } & J\mathbf{F}^{-1} \cdot \text{dev } \boldsymbol{\sigma}_e \cdot \mathbf{F} : \text{dev}(\ln \mathbf{U}_{ti} - \ln \mathbf{U}_{tj}) - 0.5J_{ti}\mathbf{E}_e : (\mathbf{C}_i - \mathbf{C}_j) : \mathbf{E}_e \leq -\frac{\rho_0 J \bar{A}}{3}; \\ \text{for KM-III: } & J\mathbf{F}^{-1} \cdot \text{dev } \boldsymbol{\sigma}_e \cdot \mathbf{F} : \text{dev}(\mathbf{U}_{tj}^{-1} \cdot \mathbf{m}_t \otimes \mathbf{n}_t) - 0.5J_{ti}\mathbf{E}_e : (\mathbf{C}_i - \mathbf{C}_j) : \mathbf{E}_e \leq -\frac{\rho_0 J \bar{A}}{3}, \end{aligned} \quad (100)$$

where we recall that while calculating $\partial^2\mathbf{F}_t/\partial^2\eta_i$ for KM-II, $\ln \mathbf{U}_{ti}$ and $\ln \mathbf{U}_{tj}$ were assumed to be commutative, and also, we have used that $\text{tr}(\ln \mathbf{U}_{ti} - \ln \mathbf{U}_{tj}) = \ln(J_{ti}) - \ln(J_{tj}) = 0$ and $\mathbf{U}_{tj}^{-1} \cdot \mathbf{m}_t \cdot \mathbf{n}_t = 0$. As desired, the volumetric part of the Cauchy stress does not contribute to the variant-variant transformation criteria for KM-II and III, only the deviatoric part does. However, that is not the case for KM-I. There both the volumetric and deviatoric parts of $\boldsymbol{\sigma}_e$ contribute to the criteria.

6. List of governing equations

Here we collect the entire system of equations presented above, first for a general 3D system with N variants (Box-I), and then a specialized form of the system of equations for a system with austenite and two variants in isotropic elastic solids under plane stress condition (Box-II). We assume that the temperature is constant in space and time; hence the heat flux $\mathbf{h}_0 = \mathbf{0}$ in Ω_0 (see Section 4.1) and $\dot{\theta} = 0$ for all $t \geq 0$.

Box-I. List of governing equations in the general form

- Order parameters for the martensitic variants satisfy

$$\sum_{i=1}^N \eta_i = 1. \quad (101)$$

- Kinematics: strains and kinematic models for \mathbf{F}_t

$$\begin{aligned} \mathbf{F} &= \mathbf{V}_e \cdot \mathbf{R}_l \cdot \mathbf{U}_t; \quad \mathbf{E} = 0.5(\mathbf{F}^T \cdot \mathbf{F} - \mathbf{I}); \quad \mathbf{E}_e := 0.5(\mathbf{F}_e^T \cdot \mathbf{F}_e - \mathbf{I}); \quad \mathbf{b} = 0.5(\mathbf{F} \cdot \mathbf{F}^T - \mathbf{I}); \\ \mathbf{b}_e &= 0.5(\mathbf{F}_e \cdot \mathbf{F}_e^T - \mathbf{I}). \end{aligned} \quad (102)$$

$$\begin{aligned} \text{KM-I: } \mathbf{F}_t &= \mathbf{U}_t = \mathbf{I} + \sum_{i=1}^N \varepsilon_{ti} \phi_i \varphi(a_\varepsilon, \eta_0); \\ \text{KM-II: } \mathbf{F}_t &= \exp \left[\sum_{i=1}^N \ln(\mathbf{U}_{ti}) \phi_i \varphi(a_\varepsilon, \eta_0) \right]; \\ \text{KM-III: } \mathbf{F}_t &= \mathbf{I} + \varphi(a_\varepsilon, \eta_0) [\phi_i (\mathbf{Q}_t \cdot \mathbf{U}_{ti} - \mathbf{I}) + \phi_j (\mathbf{U}_{tj} - \mathbf{I})], \quad \text{where} \\ \varphi(a_\varepsilon, \eta_0) &= a_\varepsilon \eta_0^2 (1 - \eta_0)^2 + \eta_0^3 (4 - 3\eta_0), \quad \text{and} \quad \phi_i = \eta_i^2 (3 - 2\eta_i). \end{aligned} \quad (103)$$

- Helmholtz's free energy

$$\begin{aligned} \psi(\mathbf{F}, \eta_0, \eta_i, \theta, \nabla \eta_0, \nabla \eta_i) &= \frac{J_t}{\rho_0} \psi_e(\mathbf{F}_e, \eta_0, \eta_i, \theta) + J \check{\psi}^\theta(\eta_0, \eta_i, \theta) + \tilde{\psi}^\theta(\eta_0, \eta_i, \theta) + \psi_p(\eta_0, \eta_i) + \\ &J \psi^\nabla(\nabla \eta_0, \nabla \eta_i, \eta_i), \quad \text{where} \end{aligned} \quad (104)$$

$$\psi_e = 0.5 \mathbf{E}_e : \mathbf{C}(\eta_0, \eta_i) : \mathbf{E}_e, \quad \text{where } \mathbf{C}(\eta_0, \eta_i) = (1 - \varphi(a, \eta_0)) \mathbf{C}_0 + \varphi(a, \eta_0) \sum_{i=1}^N \phi_i(\eta_i) \mathbf{C}_i; \quad (105)$$

$$\check{\psi}^\theta = [A(\theta) + (a_\theta - 3) \Delta \psi^\theta(\theta)] \eta_0^2 (1 - \eta_0)^2 + \bar{A} \sum_{i=1}^{N-1} \sum_{j=i+1}^N \eta_i^2 \eta_j^2 \varphi(a_b, \eta_0); \quad (106)$$

$$\tilde{\psi}^\theta = \psi_0^\theta(\theta) + \Delta \psi^\theta(\theta) \eta_0^2 (3 - 2\eta_0) \quad \text{with } \Delta \psi^\theta = -\Delta s(\theta - \theta_e) - \Delta c^\sigma \theta \ln(\theta/\theta_e) + \Delta c^\sigma (\theta - \theta_e); \quad (107)$$

$$\begin{aligned} \psi_p = & \sum_{i=1}^{N-1} \sum_{j=i+1}^N K_{ij} (\eta_i + \eta_j - 1)^2 \eta_i^2 \eta_j^2 + \sum_{i=1}^{N-1} \sum_{j=i+1}^N K_{0ij} \eta_0^2 \eta_i^2 \eta_j^2 (1 - \varphi(a_K, \eta_0)) + \\ & \sum_{i=1}^{N-2} \sum_{j=i+1}^{N-1} \sum_{k=j+1}^N K_{ijk} \eta_i^2 \eta_j^2 \eta_k^2 + \sum_{i=1}^{N-2} \sum_{j=i+1}^{N-1} \sum_{k=j+1}^N K_{0ijk} \eta_0^2 \eta_i^2 \eta_j^2 \eta_k^2 (1 - \varphi(a_K, \eta_0)) + \\ & \sum_{i=1}^{N-3} \sum_{j=i+1}^{N-2} \sum_{k=j+1}^{N-1} \sum_{l=k+1}^N K_{ijkl} \eta_i^2 \eta_j^2 \eta_k^2 \eta_l^2, \quad \text{where} \\ & K_{ii} = K_{0ii} = K_{iik} = K_{iji} = K_{iii} = K_{0iik} = K_{0iji} = K_{0iii} = K_{iikl} = K_{ijil} = K_{ijk i} = K_{ijjl} = \\ & K_{ijkk} = 0; \end{aligned} \quad (108)$$

$$\psi^\nabla = \frac{\beta_{0M}}{2\rho_0} |\nabla \eta_0|^2 + \frac{1}{8\rho_0} \sum_{i=1}^{N-1} \sum_{j=i+1}^N \beta_{ij} (|\nabla \eta_i|^2 + |\nabla \eta_j|^2 - 2\nabla \eta_i \cdot \nabla \eta_j) \tilde{\varphi}(\eta_0, a_\beta, a_0); \quad (109)$$

$$\tilde{\varphi}(a_\beta, a_0, \eta_0) = a_\beta \eta_0^2 - 2[a_\beta - 2(1 - a_0)] \eta_0^3 + [a_\beta - 3(1 - a_0)] \eta_0^4 + a_0. \quad (110)$$

- Total, elastic, and structural stresses

$$\mathbf{P} = \mathbf{P}_e + \mathbf{P}_{st}, \quad \boldsymbol{\sigma} = \boldsymbol{\sigma}_e + \boldsymbol{\sigma}_{st}; \quad (111)$$

$$\mathbf{P}_e = J_e^{-1} \mathbf{V}_e \cdot \mathbf{R}_e \cdot \frac{\partial \psi_e(\mathbf{E}_e)}{\partial \mathbf{E}_e} \cdot \mathbf{R}_e^T \cdot \mathbf{V}_e \cdot \mathbf{F}^T; \quad (112)$$

$$\boldsymbol{\sigma}_e = J_e^{-1} \mathbf{V}_e \cdot \mathbf{R}_e \cdot \frac{\partial \psi_e(\mathbf{E}_e)}{\partial \mathbf{E}_e} \cdot \mathbf{R}_e^T \cdot \mathbf{V}_e; \quad (113)$$

$$\begin{aligned} \mathbf{P}_{st} = & J \rho_0 (\check{\psi}^\theta + \psi^\nabla) \mathbf{F}^{-T} - J \beta_{0M} \nabla \eta_0 \otimes \nabla \eta_0 \cdot \mathbf{F}^{-T} - \\ & J \tilde{\varphi}(a_\beta, a_0, \eta_0) \sum_{i=1}^N \sum_{j=1}^N \frac{\beta_{ij}}{4} \nabla \eta_i \otimes (\nabla \eta_i - \nabla \eta_j) \cdot \mathbf{F}^{-T}; \end{aligned} \quad (114)$$

$$\boldsymbol{\sigma}_{st} = \rho_0 (\check{\psi}^\theta + \psi^\nabla) \mathbf{I} - \beta_{0M} \nabla \eta_0 \otimes \nabla \eta_0 - \tilde{\varphi}(a_\beta, a_0, \eta_0) \sum_{i=1}^N \sum_{j=1}^N \frac{\beta_{ij}}{4} \nabla \eta_i \otimes (\nabla \eta_i - \nabla \eta_j). \quad (115)$$

- Mechanical equilibrium equations (body forces and inertia are neglected)

$$\nabla_0 \cdot \mathbf{P} = \mathbf{0} \quad \text{in } \Omega_0 \quad \text{or equivalently,} \quad \nabla \cdot \boldsymbol{\sigma} = \mathbf{0} \quad \text{in } \Omega. \quad (116)$$

- Ginzburg-Landau equations

$$\dot{\eta}_0 = L_{0M} X_0, \quad \dot{\eta}_i = \sum_{j:j \neq i} L_{ij} (X_i - X_j) \quad (\text{no summation over } i), \quad \text{where} \quad (117)$$

$$\begin{aligned} X_0 = & (\mathbf{P}_e^T \cdot \mathbf{F}_e - J_t \psi_e \mathbf{F}_t^{-1}) : \frac{\partial \mathbf{F}_t}{\partial \eta_0} - \frac{J_t}{2} \mathbf{E}_e : \frac{\partial \mathcal{C}}{\partial \eta_0} : \mathbf{E}_e - \rho_0 (6\eta_0 - 6\eta_0^2) \Delta \psi^\theta - \\ & J \rho_0 \bar{A} \sum_{i=1}^{N-1} \sum_{j=i+1}^N \eta_i^2 \eta_j^2 \frac{\partial \varphi(a_b, \eta_0)}{\partial \eta_0} - \rho_0 J [A(\theta) + (a_\theta - 3) \Delta \psi^\theta(\theta)] (2\eta_0 - 6\eta_0^2 + 4\eta_0^3) - \\ & \frac{J}{8} \frac{\partial \tilde{\varphi}(a_\beta, a_0, \eta_0)}{\partial \eta_0} \sum_{i=1}^{N-1} \sum_{j=i+1}^N \beta_{ij} |\nabla \eta_i - \nabla \eta_j|^2 - \rho_0 \left(\sum_{i=1}^{N-1} \sum_{j=i+1}^N K_{0ij} \eta_i^2 \eta_j^2 + \right. \\ & \left. \sum_{i=1}^{N-2} \sum_{j=i+1}^{N-1} \sum_{k=j+1}^N K_{0ijk} \eta_i^2 \eta_j^2 \eta_k^2 \right) \left[2\eta_0 (1 - \varphi(a_K, \eta_0)) - \eta_0^2 \frac{\partial \varphi(a_K, \eta_0)}{\partial \eta_0} \right] + \\ & \nabla_0 \cdot (\beta_{0M} J \mathbf{F}^{-1} \cdot \nabla \eta_0); \end{aligned} \quad (118)$$

$$\begin{aligned} X_i = & (\mathbf{P}_e^T \cdot \mathbf{F}_e - J_t \psi_e \mathbf{F}_t^{-1}) : \frac{\partial \mathbf{F}_t}{\partial \eta_i} - \frac{J_t}{2} \mathbf{E}_e : \frac{\partial \mathcal{C}}{\partial \eta_i} : \mathbf{E}_e - 2\rho_0 J \bar{A} \sum_{j=1, \neq i}^N \eta_i \eta_j^2 \varphi(a_b, \eta_0) - \\ & 2\rho_0 \sum_{j=1}^N K_{ij} (\eta_i + \eta_j - 1) (2\eta_i + \eta_j - 1) \eta_i \eta_j^2 - 2\rho_0 \left(\sum_{j=1}^N K_{0ij} \eta_j^2 + \sum_{j=1}^{N-1} \sum_{k=j+1}^N K_{0ijk} \eta_j^2 \eta_k^2 \right) \times \\ & \eta_i \eta_0^2 (1 - \varphi(a_K, \eta_0)) - 2\rho_0 \left(\sum_{j=1}^{N-1} \sum_{k=j+1}^N K_{ijk} \eta_j^2 \eta_k^2 + \sum_{j=1}^{N-2} \sum_{k=j+1}^{N-1} \sum_{l=k+1}^N K_{ijkl} \eta_j^2 \eta_k^2 \eta_l^2 \right) \eta_i + \\ & \nabla_0 \cdot \left(J \tilde{\varphi}(a_\beta, a_0, \eta_0) \sum_{j=1}^N \frac{\beta_{ij}}{4} \mathbf{F}^{-1} \cdot (\nabla \eta_i - \nabla \eta_j) \right) \quad \text{for all } i = 1, 2, \dots, N. \end{aligned} \quad (119)$$

- Boundary conditions for the order parameters

$$\nabla_0 \eta_0 \cdot \mathbf{n}_0 = 0, \quad \text{and} \quad \nabla_0 \eta_i \cdot \mathbf{n}_0 = 0 \quad \text{on } \partial \Omega_0. \quad (120)$$

We now enlist the system of equations for a system with austenite and two martensitic variants (denoted by M_1 and M_2) under the plane stress condition in Box-II which have been derived from the system of equations for a 3D system enlisted in Box-I. The independent order parameter corresponding to the variants is here denoted by η_1 . Under the plane stress condition $\sigma_{13} = \sigma_{23} = \sigma_{33} = 0$, and consequently, $\sigma_{e13} = \sigma_{e23} = \sigma_{e33} = \sigma_{13}^{st} = \sigma_{23}^{st} = \sigma_{33}^{st} = 0$. All the out-of-plane components of \mathbf{P} , \mathbf{P}_e , and \mathbf{P}_{st} (i.e. 13, 31, 23, 32, and 33 components), and all the off-diagonal out-of-plane components (i.e. 13, 31, 23, and 32 components) of \mathbf{F} , \mathbf{F}_e , \mathbf{V}_e , \mathbf{E}_e , \mathbf{b}_e , \mathbf{R} , and \mathbf{F}_t are identically zero. δ_{ij} denotes the Kronecker delta. The phases have been assumed to have an isotropic elastic response of St. Venant-Kirchhoff type (see Eq. (124)), where λ and μ are the Lamé constants, and $\lambda' = 2\lambda\mu/(\lambda + 2\mu)$ (see Chapter 7 of Slaughter (2002) for a similar treatment with infinitesimal strains). The Cauchy elastic stresses are obtained using Eq. (16) and the elastic first Piola-Kirchhoff by Eq. (10)₁. Their explicit forms are expressed in Eqs. (130) and (131), respectively. Also, the 33 components of various stretch and strain tensors are given in Eq. (121). The structural stresses, free energy, interpolation functions, mechanical equilibrium equations, Ginzburg-Landau equations, and Neumann boundary conditions for the order parameters are also listed in Box-II. The subscripts with lowercase letters $i, j, k, l = 1, 2$ etc. have been used to denote the components of the tensors in our plane stress problem. For example, F_{ij} denotes the components for the total deformation gradient, where $i, j = 1, 2$. Nonzero out-of-plane 33 component is denoted by F_{33} . We assume that the specific heat of A and M are identical for all the simulations, i.e. $\Delta c^\sigma = 0$.

Box-II. List of governing equations for a two variant system under plane stress condition and isotropic elasticity

- Components of elastic and total strains, and the transformation deformation gradient

$$\begin{aligned}
b_{ij} &= 0.5 \left(\sum_{k=1}^2 V_{ik} V_{kj} - \delta_{ij} \right); & b_{(e)ij} &= 0.5 \left(\sum_{k=1}^2 V_{(e)ik} V_{(e)kj} - \delta_{ij} \right); \\
b_{(e)33} &= -\frac{\lambda}{\lambda + 2\mu} (b_{(e)11} + b_{(e)22}); & F_{(e)33} = V_{(e)33} &= \sqrt{1 - \frac{\lambda' (b_{(e)11} + b_{(e)22})}{\mu}}; & b_{33} &= 0.5(F_{33}^2 - 1); \\
F_{33} &= V_{(e)33} U_{(e)33}, & \text{where } \lambda \text{ and } \mu & \text{ are the Lamé constants, and } \lambda' = 2\lambda\mu/(\lambda + 2\mu). & & (121)
\end{aligned}$$

$$J = (F_{11}F_{22} - F_{12}F_{21})F_{33}; \quad J_e = (F_{(e)11}F_{(e)22} - F_{(e)12}F_{(e)21})F_{(e)33}; \quad J_t = (F_{(t)11}F_{(t)22} - F_{(t)12}F_{(t)21})F_{(t)33}. \quad (122)$$

$$\begin{aligned} \text{KM-I:} \quad & F_{(t)ij} = \delta_{ij} + \varepsilon_{(t2)ij}\varphi(a_\varepsilon, \eta_0) + (\varepsilon_{(t1)ij} - \varepsilon_{(t2)ij})\phi_1(\eta_1)\varphi(a_\varepsilon, \eta_0); \\ \text{KM-II:} \quad & F_{(t)ij} = \exp[(\ln U_{t2})_{ij}\varphi(a_\varepsilon, \eta_0) + ((\ln U_{t1})_{ij} - (\ln U_{t2})_{ij})\phi_1(\eta_1)\varphi(a_\varepsilon, \eta_0)]; \\ \text{KM-III:} \quad & F_{(t)ij} = \delta_{ij} + [\varepsilon_{(t2)ij} + \phi_1(\eta_1)m_{(t)i}n_{(t)j}]\varphi(a_\varepsilon, \eta_0). \end{aligned} \quad (123)$$

- Free energy densities

$$\psi_e = 0.5\lambda'(E_{(e)11} + E_{(e)22})^2 + \mu \sum_{i,j=1}^2 E_{(e)ij}E_{(e)ij} = 0.5\lambda'(b_{(e)11} + b_{(e)22})^2 + \mu \sum_{i,j=1}^2 b_{(e)ij}b_{(e)ij}; \quad (124)$$

$$\rho_0\check{\psi}^\theta = \rho_0[A(\theta) + (a_\theta - 3)\Delta\psi^\theta(\theta)]\eta_0^2(1 - \eta_0)^2 + \rho_0\bar{A}\eta_1^2(1 - \eta_1)^2\varphi(a_b, \eta_0); \quad (125)$$

$$\check{\psi}^\theta = \psi_0^\theta(\theta) + \Delta\psi^\theta(\theta)\eta_0^2(3 - 2\eta_0) \quad \text{with} \quad \rho_0\Delta\psi^\theta = -\Delta s(\theta - \theta_e); \quad (126)$$

$$\psi_p = K_{012}\eta_0^2\eta_1^2(1 - \eta_1)^2[1 - \varphi(a_K, \eta_0)]; \quad (127)$$

$$\psi^\nabla = \frac{1}{2\rho_0} \sum_{i=1}^2 \left(\beta_{0M} \frac{\partial\eta_0}{\partial r_i} \frac{\partial\eta_0}{\partial r_i} + \beta_{12} \frac{\partial\eta_1}{\partial r_i} \frac{\partial\eta_1}{\partial r_i} \tilde{\varphi}(a_\beta, a_0, \eta_0) \right); \quad (128)$$

$$\tilde{\varphi}(a_\beta, a_0, \eta_0) = a_\beta\eta_0^2 - 2[a_\beta - 2(1 - a_0)]\eta_0^3 + [a_\beta - 3(1 - a_0)]\eta_0^4 + a_0. \quad (129)$$

- Elastic and structural stresses

$$P_{(e)ij} = J_t \sum_{k,m,n=1}^2 V_{(e)ik}V_{(e)km} [\lambda'(b_{(e)11} + b_{(e)22})\delta_{mn} + 2\mu b_{(e)mn}] F_{jn}^{-1}; \quad (130)$$

$$\sigma_{(e)ij} = J_e^{-1} \sum_{k,m=1}^2 V_{(e)ik}V_{(e)km} [\lambda'(b_{(e)11} + b_{(e)22})\delta_{mj} + 2\mu b_{(e)mj}]; \quad (131)$$

$$P_{(st)ij} = J\rho_0(\check{\psi}^\theta + \psi^\nabla)F_{ji}^{-1} - \sum_{k=1}^2 J\beta_{0M} \frac{\partial\eta_0}{\partial r_i} \frac{\partial\eta_0}{\partial r_k} F_{jk}^{-1} - \sum_{k=1}^2 J\beta_{12} \frac{\partial\eta_1}{\partial r_i} \frac{\partial\eta_1}{\partial r_k} F_{jk}^{-1}; \quad (132)$$

$$\sigma_{(st)ij} = \rho_0(\check{\psi}^\theta + \psi^\nabla)\delta_{ij} - \beta_{0M} \frac{\partial\eta_0}{\partial r_i} \frac{\partial\eta_0}{\partial r_j} - \beta_{12} \frac{\partial\eta_1}{\partial r_i} \frac{\partial\eta_1}{\partial r_j}. \quad (133)$$

- Mechanical equilibrium equations (body forces and inertia are neglected)

$$\sum_{j=1}^2 \frac{\partial P_{ij}}{\partial r_{0j}} = 0 \text{ in } \Omega_0, \quad \text{or equivalently,} \quad \sum_{j=1}^2 \frac{\partial \sigma_{ij}}{\partial r_j} = 0 \text{ in } \Omega. \quad (134)$$

- Ginzburg-Landau equations (see Eqs. (61) and (60))

$$\begin{aligned}
\frac{\dot{\eta}_0}{L_{0M}} = & \sum_{i,j,k,m,n=1}^2 \left(JF_{ik}^{-1} \sigma_{(e)kn} F_{nj} - J_t \psi_e \delta_{ij} \right) F_{(t)jm}^{-1} \frac{\partial F_{(t)mi}}{\partial \eta_0} - J_t \left(0.5 \frac{\partial \lambda'}{\partial \eta_0} (b_{(e)11} + b_{(e)22})^2 + \right. \\
& \left. \sum_{i,j=1}^2 \frac{\partial \mu}{\partial \eta_0} b_{(e)ij} b_{(e)ji} \right) - \rho_0 \bar{A} J \eta_1^2 (1 - \eta_1)^2 \frac{\partial \varphi(a_b, \eta_0)}{\partial \eta_0} - \rho_0 \Delta \psi^\theta (6\eta_0 - 6\eta_0^2) - \\
& J \rho_0 [A(\theta) + (a_\theta - 3) \Delta \psi^\theta(\theta)] (2\eta_0 - 6\eta_0^2 + 4\eta_0^3) - \rho_0 K_{012} [2\eta_0 (1 - \varphi(a_K, \eta_0)) - \\
& \eta_0^2 \frac{\partial \varphi(a_K, \eta_0)}{\partial \eta_0}] \eta_1^2 (1 - \eta_1)^2 - \sum_{j=1}^2 \frac{J \beta_{12}}{2} \frac{\partial \eta_1}{\partial r_j} \frac{\partial \eta_1}{\partial r_j} \frac{\partial \tilde{\varphi}(a_\beta, a_0, \eta_0)}{\partial \eta_0} + \\
& \sum_{i,j=1}^2 \frac{\partial}{\partial r_{0i}} \left(\beta_{0M} J F_{ij}^{-1} \frac{\partial \eta_0}{\partial r_j} \right); \tag{135}
\end{aligned}$$

$$\begin{aligned}
\frac{\dot{\eta}_1}{L_{12}} = & \sum_{i,j,k,m,n=1}^2 \left(JF_{ik}^{-1} \sigma_{(e)kn} F_{nj} - J_t \psi_e \delta_{ij} \right) F_{(t)jm}^{-1} \frac{\partial F_{(t)mi}}{\partial \eta_1} - J_t \left(0.5 \frac{\partial \lambda'}{\partial \eta_1} (b_{(e)11} + b_{(e)22})^2 + \right. \\
& \left. \sum_{i,j=1}^2 \frac{\partial \mu}{\partial \eta_1} b_{(e)ij} b_{(e)ji} \right) - \rho_0 J \bar{A} (2\eta_1 - 6\eta_1^2 + 4\eta_1^3) \varphi(a_b, \eta_0) - \rho_0 K_{012} \eta_0^2 (2\eta_1 - 6\eta_1^2 + 4\eta_1^3) \times \\
& (1 - \varphi(a_K, \eta_0)) + \sum_{i,j=1}^2 \frac{\partial}{\partial r_{0i}} \left(\tilde{\varphi}(a_\beta, a_0, \eta_0) \beta_{12} J F_{ij}^{-1} \frac{\partial \eta_1}{\partial r_j} \right). \tag{136}
\end{aligned}$$

- Boundary conditions for the order parameters

$$\sum_{i=1}^2 \frac{\partial \eta_0}{\partial r_{0i}} n_{0i} = 0, \quad \text{and} \quad \sum_{i=1}^2 \frac{\partial \eta_1}{\partial r_{0i}} n_{0i} = 0 \quad \text{on } \partial \Omega_0. \tag{137}$$

7. Parameter identification

The free energy and the kinetic equations derived above involve several material parameters which need to be calibrated based on the experimental data or atomistic simulation results. Let us consider a simplified situation,

where martensitic transformation is occurring without mechanics, i.e. $\psi_e = 0$ and $J = 1$, which allows us to obtain the analytical solutions to the Ginzburg-Landau equations and calibrate the material parameters such as the barrier heights, gradient energy coefficients, and kinetic coefficients using the known data of interfacial energy, width, and mobility.

7.1. Analytical solutions for order parameters under stress free condition

Assuming that the interfaces are planar and the order parameters spatially vary with r_{01} only, and also that A_{0M} , A_{12} , β_{0M} , and β_{12} are constants, we simplify the Ginzburg-Landau equations (135) and (136) for A-M (with $\eta_1 = 1$) and M₁-M₂ (with $\eta_0 = 1$) interfaces as

$$\begin{aligned}\dot{\eta}_0 &= L_{0M} \left[-\frac{\partial\psi}{\partial\eta_0} + \beta_{0M} \frac{\partial^2\eta_0}{\partial r_{01}^2} \right] \\ &= L_{0M} \left[-\rho_0 \Delta\psi^\theta (6\eta_0 - 6\eta_0^2) - \rho_0 [A(\theta) + (a_\theta - 3)\Delta\psi^\theta(\theta)](2\eta_0 - 6\eta_0^2 + 4\eta_0^3) + \beta_{0M} \frac{\partial^2\eta_0}{\partial r_{01}^2} \right], \quad \text{and(138)}\end{aligned}$$

$$\dot{\eta}_1 = L_{12} \left[-\frac{\partial\psi}{\partial\eta_1} + \beta_{12} \frac{\partial^2\eta_1}{\partial r_{01}^2} \right] = L_{12} \left[-\rho_0 \bar{A}(2\eta_1 - 6\eta_1^2 + 4\eta_1^3) + \beta_{12} \frac{\partial^2\eta_1}{\partial r_{01}^2} \right], \quad (139)$$

respectively, where we have used $K_{012} = 0$. The solutions of Eqs. (138) and (139) for a given a_θ are (Levitas (2013b))

$$\begin{aligned}\eta_0 &= [1 + \exp(-\zeta_{0M})]^{-1} \quad \text{with } \zeta_{0M} = 6(r_{01} - r_{0c} - c_{0M}t)/\delta_{0M} \quad \text{and} \\ \eta_1 &= [1 + \exp(-\zeta_{12})]^{-1} \quad \text{with } \zeta_{12} = 6(r_{01} - r_{0c} - c_{12}t)/\delta_{12},\end{aligned} \quad (140)$$

respectively, where the symbol δ denotes the width of the interface (considered to be the distance between points where $\eta = 0.05$ and $\eta = 0.95$ (Steinbach (2009))), γ denotes the interfacial energy as introduced in Section 1, and c is the speed of interface propagation:

$$\begin{aligned}\delta_{0M} &= \sqrt{\frac{18\beta_{0M}}{\rho_0[A_{0M}(\theta) + (a_\theta - 3)\Delta\psi^\theta(\theta)]}}, \quad \gamma_{0M} = \frac{\beta_{0M}}{\delta_{0M}}, \quad c_{0M} = L_{0M}\delta_{0M}\Delta\psi^\theta(\theta), \\ \delta_{12} &= \sqrt{\frac{18\beta_{12}}{\rho_0\bar{A}}}, \quad \gamma_{12} = \frac{\beta_{12}}{\delta_{12}}, \quad c_{12} = 0,\end{aligned} \quad (141)$$

r_{0c} is the coordinate of a point where $\eta_0 = 0.5$ and $\eta_1 = 0.5$ in the respective expressions, and obviously, the subscripts ‘0M’ and ‘12’ stand for A-M and M₁-M₂ interfaces, respectively. For a real value for the A-M interface width, obviously $A_{0M}(\theta)$, a_θ , and $\Delta\psi^\theta(\theta)$ must be such that $A_{0M}(\theta) + (a_\theta - 3)\Delta\psi^\theta(\theta) > 0$.

It is easy to verify that the solution of η_0 in Eq.(140) satisfies

$$\frac{\partial \eta_0}{\partial \zeta} = \eta_0(1 - \eta_0), \quad (142)$$

using which along with the relations in Eq. (141), we show that for a propagating A-M interface its gradient energy is (see Eq. (52))

$$\psi_{0M}^\nabla = \frac{\beta_{0M}}{2} |\nabla \eta_0|^2 = \frac{\beta_{0M} \chi_{0M}^2}{2} \left(\frac{d\eta_0}{d\zeta} \right)^2 = [A_{0M}(\theta) + (a_\theta - 3)\Delta\psi^\theta] \eta_0^2 (1 - \eta_0)^2 = \check{\psi}_{0M}^\theta. \quad (143)$$

Similar to Levitas (2013b), Eq. (143) justifies a choice of the term $\check{\psi}_{0M}^\theta$ in Eq. (43) that contributes to the interfacial stresses. For $a_\theta = 3$, the energy $\check{\psi}_{0M}^\theta$ reduces to $\check{\psi}_{0M}^\theta = A_{0M}(\theta) \eta_0^2 (1 - \eta_0)^2$. For this case the interfacial width, energy, and stresses are thus independent of the thermal energy $\Delta\psi^\theta$ (also see Levitas and Roy (2016); Steinbach (2009)). On the other hand, for $a_\theta = 0$, ψ_{0M}^∇ reduces to the expression given in Levitas (2013b). The Gibbsian divided surfaces with the propagating interface in that case passes through the point where $\eta_{0M} = 0.5$ (Levitas (2013b, 2014)).

7.2. Parameter values

For all our calculations, we assume the material constants for NiAl alloy, in which A and M_i ($i = 1, 2$) possess cubic and tetragonal lattices, respectively; see Levitas and Preston (2002a,b); Levitas et al. (2003) for the experimental and atomistic simulation based data. The Bain tensors are $diag(\beta, \alpha, \alpha)$, $diag(\alpha, \beta, \alpha)$, and $diag(\alpha, \alpha, \beta)$, where β and α are material constants Bhattacharya (2004). For our computations with two variants, we consider the first two Bain tensors without loss of generality. In all the simulations, we will consider $a_\theta = a_b = a_\beta = 3$, $a_0 = 10^{-4}$ (see Momeni and Levitas (2014)), $\rho_0 A_{0M} = 1744.7$ MPa, $\rho_0 \bar{A} = 5320$ MPa, $\beta_{0M} = 0.97 \times 10^{-10}$ N, and $\beta_{12} = 2.96 \times 10^{-10}$ N. Thus Eqs. (140) and (141) yield $\gamma_{0M} = 0.097$ N/m, $\delta_{0M} = 1$ nm, $\gamma_{12} = 0.297$ N/m, and $\delta_{12} = 0.75$ nm. The other parameters are taken to be $\lambda = 74.6$ GPa, $\mu = 72$ GPa, $\alpha = 0.922$, $\beta = 1.215$, $L_{0M} = L_{12} = 2600$ (Pa-s) $^{-1}$, $\theta = 50$ K, $\theta_e = 215$ K, and $\Delta s = -1.4679$ MPa/K. The elastic constants λ and μ have been taken to be identical for A and all the variants.

8. Numerical results

We now consider some examples showing the formation of complex microstructures under various loading conditions in 2D samples. The coupled mechanical equilibrium equations Eq. (134) and the Ginzburg-Landau

equations (135) and (136) along with all other constitutive relations have been solved simultaneously using the finite element method (Zienkiewicz and Taylor (2000a,b)). We have developed a large strain based finite element code in an open source deal.ii framework (Bangerth et al. (2016)). The governing equations are solved iteratively in a decoupled manner using the Newton's method. The detailed computational algorithm will be presented elsewhere. We have used the quadratic quadrilateral elements for spatial discretization of both the mechanics and phase field equations, and a backward finite difference scheme for time discretization of the Ginzburg-Landau equations. All the plots in this paper are shown in the reference configuration.

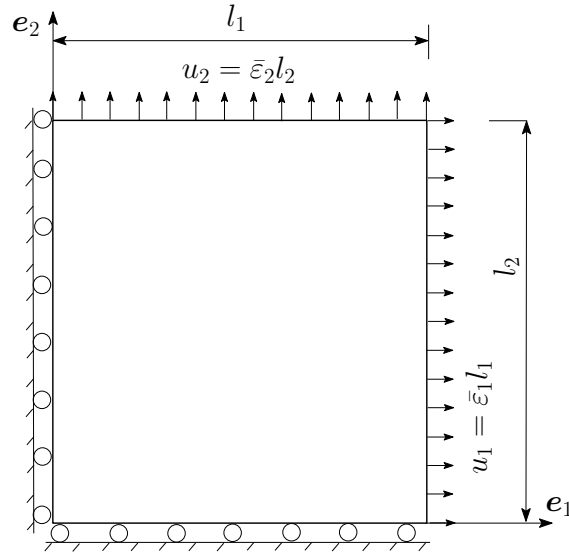


Figure 2: Schematic diagram of the rectangular sample with displacement boundary conditions.

A. Square samples under biaxial strains

Example 1. Large biaxial strain $\bar{\epsilon}_1 = \bar{\epsilon}_2 = 0.06$. We consider an initially square sample of size $l_1 = l_2 = 20$ nm; a schematic of the sample with displacement boundary conditions is depicted in Fig. (2): $u_1 = 0$ on $r_{01} = 0$, and $u_2 = 0$ on $r_{02} = 0$. We assume $\sigma_{12} = 0$ at all external surfaces. Normal displacements corresponding to the homogeneous normal strains $\bar{\epsilon}_1 = \bar{\epsilon}_2 = 0.06$ on two other surfaces are applied at $t = 0$ and then those surfaces are kept fixed for $t > 0$. Here we consider $K_{012} = 0$, i.e. the triple junctions made by A, M_1 , and M_2 are not penalized (the effect of finite K_{012} will be shown in Example 4). We assume $\eta_1 = 0.5$ and randomly distributed $0 \leq \eta_0 \leq 0.4$ in the entire sample at $t = 0$. The Bain tensors are considered to be rotated by $\pi/4$ about e_3 -axis,

i.e.

$$[\mathbf{U}_{t1}] = \begin{bmatrix} 0.5(\alpha + \beta) & 0.5(\alpha - \beta) & 0 \\ 0.5(\alpha - \beta) & 0.5(\alpha + \beta) & 0 \\ 0 & 0 & \alpha \end{bmatrix} \quad \text{and} \quad [\mathbf{U}_{t2}] = \begin{bmatrix} 0.5(\alpha + \beta) & 0.5(\beta - \alpha) & 0 \\ 0.5(\beta - \alpha) & 0.5(\alpha + \beta) & 0 \\ 0 & 0 & \alpha \end{bmatrix}. \quad (144)$$

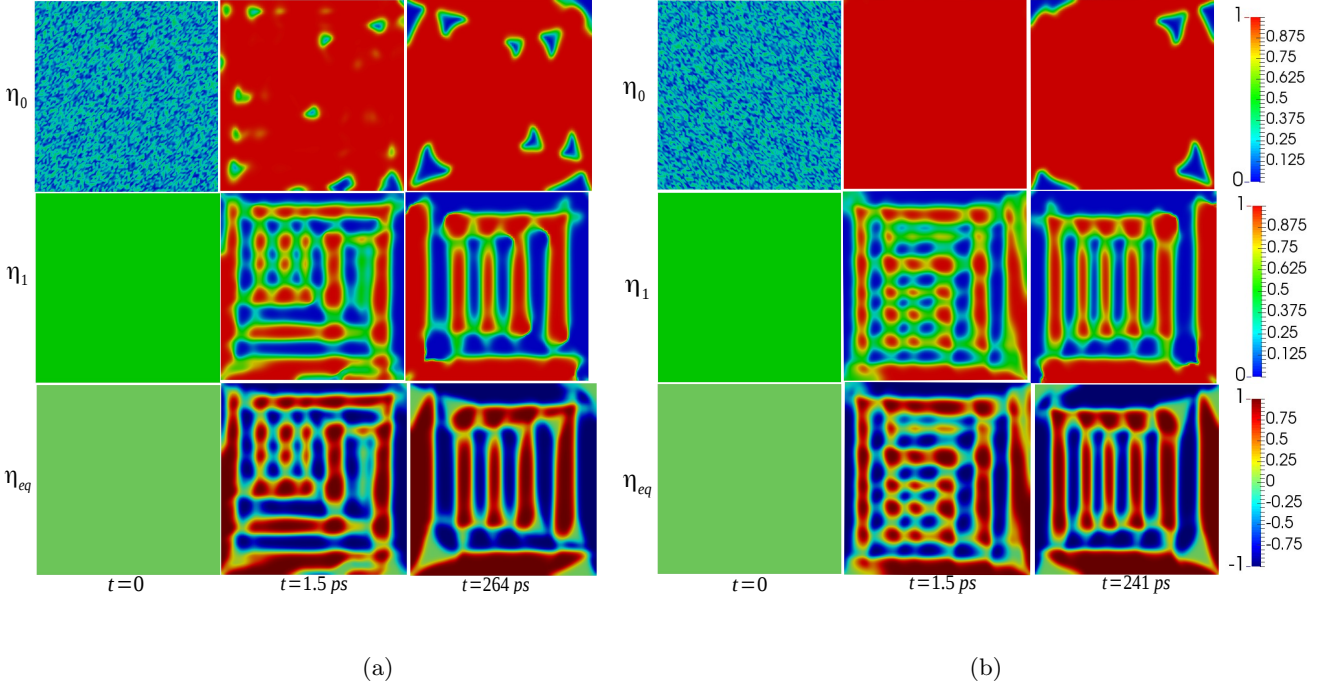


Figure 3: Evolution of order parameters in a square sample of size $20 \text{ nm} \times 20 \text{ nm}$ for $\bar{\varepsilon}_1 = \bar{\varepsilon}_2 = 0.06$ for (a) KM-I and (b) KM-II with $K_{012} = 0$. The last columns in both the figures show the stationary solutions of the Ginzburg-Landau equations.

The evolution of microstructures for KM-I and KM-II are shown in Figs. 3(a) and 3(b), respectively. The first two rows show the evolution of η_0 and η_1 , respectively. The color blue in η_0 plots signifies austenite ($\eta_0 = 0$), red ($\eta_0 = 1$) denotes martensite, and the other colors correspond to the intermediate values $0 < \eta_0 < 1$ and observed within A-M interfaces. In η_1 plots, the color red denotes M_1 ($\eta_1 = 1$), the color blue denotes M_2 ($\eta_1 = 0$), and the other colors correspond to $0 < \eta_1 < 1$ and appear within M_1 - M_2 interfaces. In the third row we have shown the plots for an equivalent order parameter $\eta_{eq} = 2\eta_0(\eta_1 - 0.5)$, which describes a combined distribution of the order parameters η_0 and η_1 . Since both η_0 and η_1 vary between 0 and 1, we have $-1 \leq \eta_{eq} \leq 1$; $\eta_{eq} = 0$

corresponds to the austenite or a point within the M_1 - M_2 interface where $\eta_1 = 0.5$, and $\eta_{eq} = 1$ denotes M_1 and appears in dark red, and $\eta_{eq} = -1$ denotes M_2 and appears in dark blue. In all the subsequent examples also we have used the same color scheme. The last columns in the respective figures show the stationary solutions of the Ginzburg-Landau equations.

A high degree of undercooling, i.e. $\theta - \theta_e = -165$ K and a large biaxial strain yield large volume fraction of martensite and a much smaller fraction of residual austenite. The microstructures consist of two mutually orthogonal sets of martensitic plates of both variants. To explain it, we recall that the twinning equation Eq. (79) in the crystallographic theory has two distinct solutions for the unit normal \mathbf{n}_t (also, for the vector \mathbf{m}_t) which are mutually perpendicular; see Chapter 5 of Bhattacharya (2004) for the analytical solutions. The applied biaxial strain promotes both the solutions of martensitic plates. The plots for η_1 and η_{eq} in Fig. 3 clearly show both the variant-variant solutions for KM-I and KM-II. A certain volume fraction of residual austenite is observed within small near-triangular regions, concentrated mainly within the region where two mutually perpendicular M plates meet. The vertices of these triangular regions where A and two martensitic variants meet are characterized as the triple junctions. Martensitic plates near the external surfaces are larger than those formed inside the samples. The variant-variant interfaces interior of the samples are nearly planar. However, those near the external surfaces are slightly curved. Intermediate structures for both models are quite different. The number of martensitic plates in the stationary state for KM-I and KM-II also differs: for KM-II, there are six pairs of plates aligned in the \mathbf{e}_2 direction, whereas for KM-I, there are five pairs. Obviously, the average widths of these plates are also different. Alternating twins and intersection of two orthogonal twin systems are the typical martensitic microstructures observed experimentally in NiAl (Schryvers (1993)).

Structural and elastic stresses within the sample across the line $r_{02} = 10$ nm have been shown in Fig. 4(a) and (b), respectively. Only the normal stresses have been shown; the shear component σ_{12} is much smaller compared to the normal components, thus not shown here. The distributions of structural stresses for both the models are quite similar, and their maximum values also do not differ much. As expected, they are vanishing within the plates. On the other hand, although the elastic stress σ_{e11} for the two models are comparable, $\max(\sigma_{e22})$ across the variant-variant interfaces for KM-II is significantly larger than that for KM-I across most of the variant-variant interfaces, in accordance with the analytical and FEM solutions for a single variant-

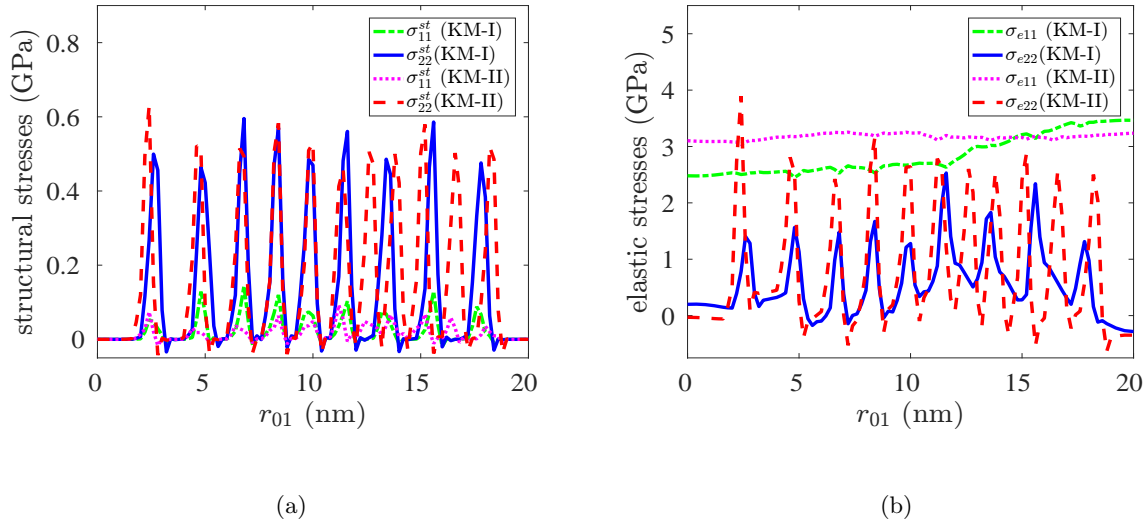


Figure 4: Plots for (a) structural stresses and (b) elastic stresses across $r_{02} = 10$ nm line (passing through the middle of the sample) when stationary solutions are reached in the same $20 \text{ nm} \times 20 \text{ nm}$ sample considered in Fig. 3 (note that $K_{012} = 0$).

variant interface in Basak and Levitas (2017). The small spikes in σ_{11}^{st} and σ_{e11} plots within the interfaces, which should be absent in case of ideal plane infinite interface, appear since the interfaces here deviate from the ideal one, the widths of the interfaces and martensitic plates are comparable, shear stress across the interfaces is heterogeneous, and due to some numerical error. In Fig. 4(b) note that σ_{e22} is very small within the martensitic plates for both KM-I and II. The reason for this is that the normal components of the Bain strains $\varepsilon_{i1}^{11} = \varepsilon_{i2}^{11} = \varepsilon_{i1}^{22} = \varepsilon_{i2}^{22} = 0.0685$ (obtained using Eq. (144)), which are very close to the applied biaxial strains $\bar{\varepsilon}_1 = \bar{\varepsilon}_2 = 0.06$.

Example 2. Sample size effect of the solutions. To investigate the effects of sample size, we have considered three other samples of size $15 \text{ nm} \times 15 \text{ nm}$, $30 \text{ nm} \times 30 \text{ nm}$, and $40 \text{ nm} \times 40 \text{ nm}$. All the initial conditions, boundary conditions for the displacements and order parameters, and all other parameters are identical to those considered for $20 \text{ nm} \times 20 \text{ nm}$ sample in Example 1. The stationary solutions for the order parameters for KM-I and KM-II are shown in Figs. 5(a) and (b), respectively. Residual austenite is observed mainly in regions where two orthogonal martensitic plates meet producing triple junctions. We note that the number of martensitic

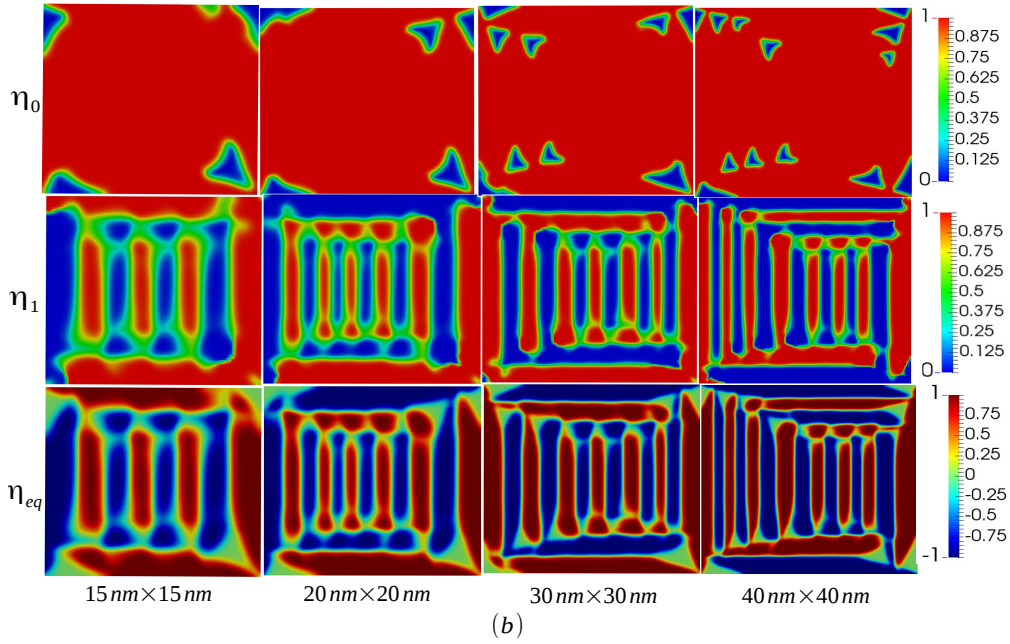
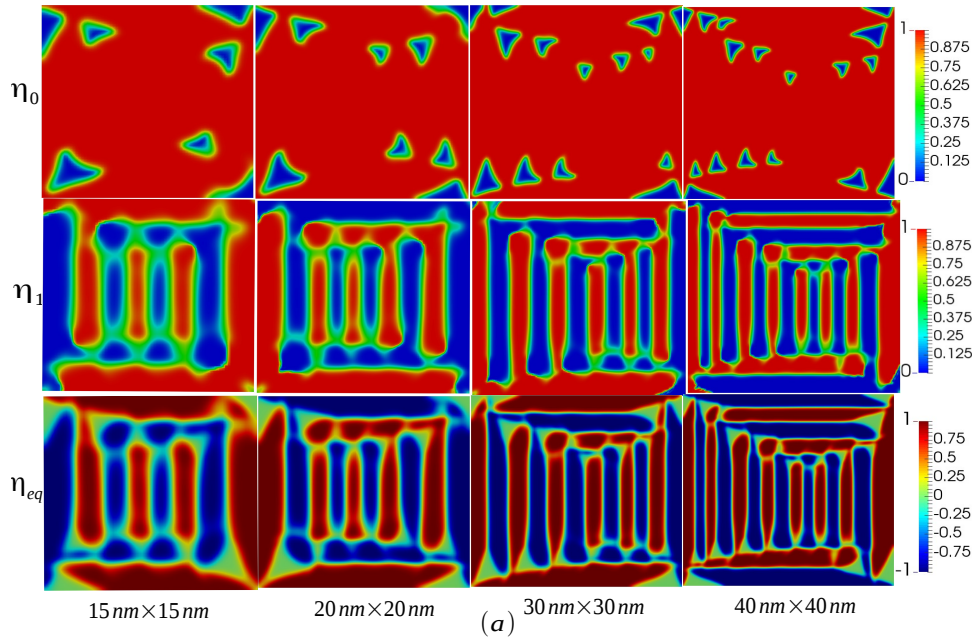


Figure 5: Sample size effect on microstructures in $15 \text{ nm} \times 15 \text{ nm}$, $20 \text{ nm} \times 20 \text{ nm}$, $30 \text{ nm} \times 30 \text{ nm}$, and $40 \text{ nm} \times 40 \text{ nm}$ samples under $\bar{\epsilon}_1 = \bar{\epsilon}_2 = 0.06$ for (a) KM-I and (b) KM-II ($K_{012} = 0$ in both the KMs).

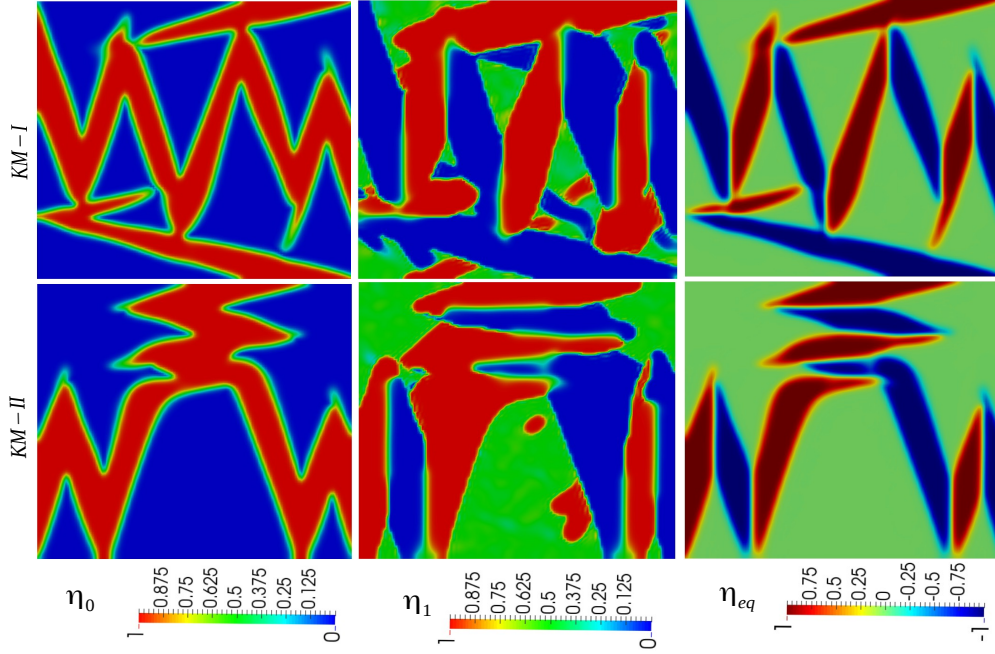


Figure 6: Microstructures in $30 \text{ nm} \times 30 \text{ nm}$ sample under $\bar{\epsilon}_1 = \bar{\epsilon}_2 = 0.02$ for (a) KM-I and (b) KM-II ($K_{012} = 0$ in both the KMs).

plates for both KM-I and KM-II are the same for the sample sizes of $15 \text{ nm} \times 15 \text{ nm}$ and $40 \text{ nm} \times 40 \text{ nm}$. However, the numbers differ in other samples. In all the simulations, the variant-variant interface width has been observed to be close to the stress-free analytical solution $\delta_{12} = 0.75 \text{ nm}$; see Basak and Levitas (2017) for an analysis. The average width of the martensitic plates, which are aligned along e_2 -direction, have been calculated to be 1.22 nm , 1.32 nm , 1.81 nm , and 1.97 nm , within the respective samples (with size in ascending order) shown in Fig. 5(a) for KM-I. Obviously, the average width of the martensitic plates increase with increase in size of the sample. The average width of the similar martensitic plates are 1.22 nm , 0.98 nm , 1.61 nm , and 1.97 nm , in the respective samples for KM-II. The average width of the martensitic plates decreases in the $20 \text{ nm} \times 20 \text{ nm}$ sample because of a larger number of plates (six pairs for KM-II versus five pairs for KM-I), and then the width increases as sample size increases. Also, note that in larger samples the martensitic plates are longer, number of triple junctions are more, and variant-variant interfaces are much planar.

Example 3. Smaller biaxial strain $\bar{\epsilon}_1 = \bar{\epsilon}_2 = 0.02$. We now consider a $30 \text{ nm} \times 30 \text{ nm}$ sample subjected to boundary displacements corresponding to the smaller biaxial strains $\bar{\epsilon}_1 = \bar{\epsilon}_2 = 0.02$. All other boundary and

initial conditions, and parameter values are identical to Example 1. Stationary solutions for η_0 (first column), η_1 (second column), and η_{eq} (third column) are shown in Fig. 6 for both KM-I (first row) and KM-II (second row). The η_0 plots clearly show that due to relatively smaller applied strain as compared to Examples 1 and 2, the volume fraction of the martensite is much smaller. In fact, now the volume fractions of residual austenite and martensitic variants are comparable, and the martensitic variant-austenite interfaces are prominent. Four short vertical variant-variant interfaces are observed for both the models; four short horizontal variant-variant interfaces are visible for KM-II, and very small horizontal variant-variant interfaces are observed for KM-I. Based on the transformation strains, in KM-I the A- M_1 and A- M_2 interfaces are at inclinations of 73.3° and 106.6° , respectively, with the positive e_1 -axis, and in KM-II the same interfaces are at, respectively, 74.4° and 107.5° inclinations with the same axis. [For KM-I the zig-zag structure fills space between two relatively long inclined plates, similar to those observed in some experiments at the microscale \(see Hornbogen \(1999\)\) and nanoscale \(see Kockar et al. \(2008\)\).](#) In real elastoplastic materials such a microstructure is usually arrested by dislocations, and even with decreasing temperature it cannot grow. Instead, a smaller scale zig-zag microstructure fills space between smaller inclined plates producing a fractal microstructure (Hornbogen (1999); [Kockar et al. \(2008\)](#)). One can observe one smaller plate for KM-I. For KM-II, one can see a smooth transition of two martensitic plates within austenite into horizontal contacting variant-variant structure.

Example 4. Effect of penalizing triple junctions. In order to show the effect of penalizing triple junctions, we consider the same $30 \text{ nm} \times 30 \text{ nm}$ sample of Example 1, where all initial and boundary conditions and parameter values are identical to those of Example 1, except that here we penalize the triple junctions. The stationary distribution of the order parameters for $\rho_0 K_{012} = 10 \text{ GPa}$ are shown in Fig. 7(a). We have repeated the plots for $K_{012} = 0$ in Fig. 7(b) for convenience in comparing these two cases (the same figures in the third column of Figs. 5(a) and (b)). Obviously, for both KM-I and II, the microstructures now have a smaller amount of residual austenite as compared to the case with $K_{012} = 0$. It clearly indicates that when triple junctions are penalized, the coexistence of three phases near the tips of the martensitic plates is largely prevented at the interior of the sample, and to some extent near the external surfaces. The triple junctions are still observed near the corners of the samples, but are mostly absent from rest of the domain. For KM-I, an additional horizontal M_2 plate appeared at the bottom of a sample making the M_1 band thinner. For KM-II, a horizontal M_1 plate

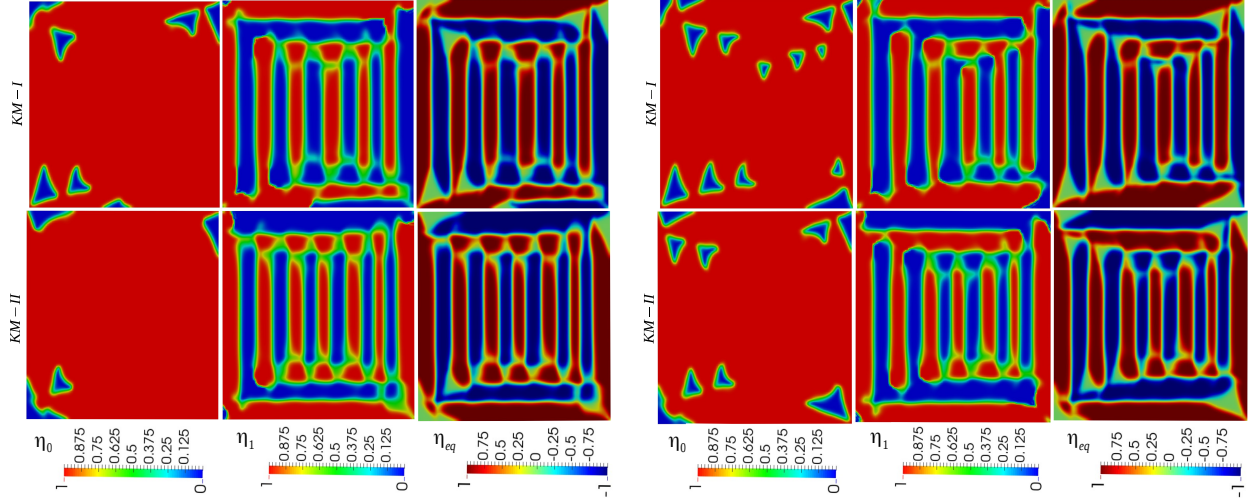


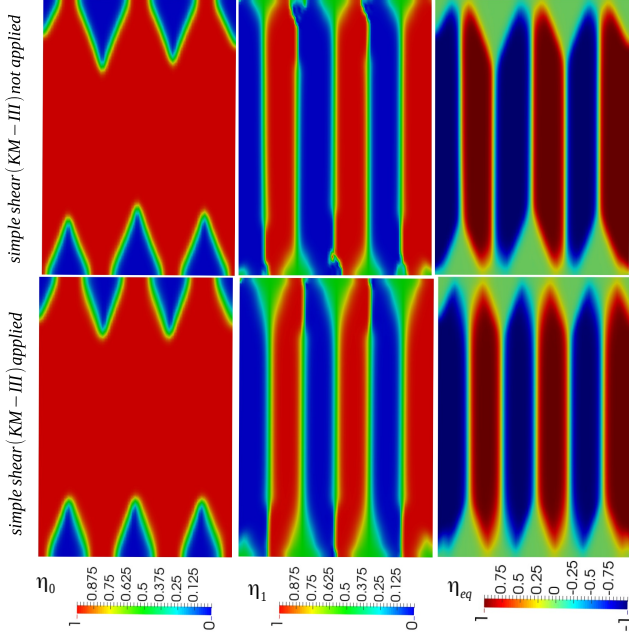
Figure 7: Microstructures in $30 \text{ nm} \times 30 \text{ nm}$ sample under $\bar{\varepsilon}_1 = \bar{\varepsilon}_2 = 0.06$ for KM-I and KM-II, and with (a) $\rho_0 K_{012} = 10 \text{ GPa}$, and (b) $\rho_0 K_{012} = 0$.

at the top of a sample splits into multiple sections leading to an increase in the length of the vertical M_1 plates.

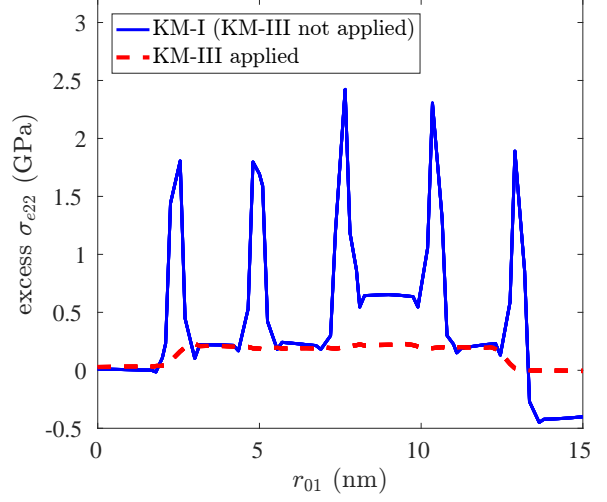
B. Twins under uniaxial strain, and study of a stress relaxation method within twin boundaries

Let us now consider a rectangular sample of size $l_1 = 15 \text{ nm}$ and $l_2 = 20 \text{ nm}$, which is subjected to uniaxial strain corresponding to $\bar{\varepsilon}_2 = 0.1$ at upper boundary $r_{02} = 20 \text{ nm}$ with respect to the lower boundary at $t = 0$ (then fixed at any $t > 0$) and with fixed left and right boundaries in the horizontal directions ($u_1 = 0$). The situation is mostly similar to that depicted in Fig. (2), except we now consider roller support in all the external surfaces except $r_{02} = 20 \text{ nm}$ boundary. For all the boundaries, the shear stress $\sigma_{12} = 0$. The initial conditions and all other parameters and material constants are considered to be identical to Example 1. The large undercooling and uniaxial strain promotes a single twin solution such that the twin plates are aligned vertically. In the first row of Fig. 8(a), the stationary solutions for the order parameters are shown when \mathbf{F}_t is considered from KM-I (i.e. Eq. (81)₁). The fixed boundaries at $r_{02} = 0$ and $r_{02} = 20 \text{ nm}$ act like invariant planes, near which the twin plates end with sharp tips. Although, the tips increase the interfacial area thereby increasing the interfacial energy, such a morphology reduces the elastic energy within the finite A-M interface, and thus reduces the total energy of the system.

The excess elastic stresses across $r_{02} = 10 \text{ nm}$ line of the sample are studied for both KM-I and KM-II. In



(a)



(b)

Figure 8: Microstructures in a $15 \text{ nm} \times 20 \text{ nm}$ rectangular sample with $\bar{\varepsilon}_2 = 0.1$, $\bar{\varepsilon}_1 = 0$, and $K_{012} = 0$ for KM-I (first row) and KM-III (second row). The microstructure shown in the second row was obtained by switching to KM-III, once all the twin boundaries were formed with KM-I. (b) Elastic stress σ_{e22} distribution along $r_{02} = 10 \text{ nm}$ for KM-I (first row) and for KM-III (second row).

KM-I, the average normal elastic stress σ_{e11} is -5.44 GPa across that line, and the maximum value of excess σ_{e11} within the twin boundaries across that line is 0.09 GPa which is small and mainly caused by the numerical error. The shear stress σ_{e12} along that line is an order of magnitude less than a GPa, and hence negligible. The other component σ_{e22} is shown in Fig. 8(b) by the solid blue curve. Evidently, the excess elastic interfacial stress σ_{e22} can reach up to 2.42 GPa (calculated with respect to a reference value 5 GPa), which is significantly large. In reality the magnitude of stresses in twin boundaries is not yet well known, however for sharp coherent twin interfaces they are zero. Thus, to have a parity with the crystallographic theory, as far as the elastic stresses within twin boundaries are concerned, we consider a method of relaxing the excess elastic stress. To this end, we allow the twin boundaries to develop fully from the same initial condition considering \mathbf{F}_t given by Eq. (81)₁

(KM-I). All the boundary conditions and parameters are taken to be identical to those considered for KM-I. Once the twin boundaries are fully formed, we switch \mathbf{F}_t to Eq. (81)₃ (KM-III) in the entire domain. Since \mathbf{F}_t in KM-III is compatible with vanishing excess elastic stresses within twin boundaries (Basak and Levitas (2017)), excess elastic stresses relax from the twin boundaries, which is evident from the red broken curve in Fig. 8(b). In this case the maximum value of the excess interfacial σ_{e22} is 0.23 GPa (calculated with respect to a reference stress 4.6 GPa within the variant plates). Also, we note that the shape of the tips of each twin plate is more ‘V’-shaped in KM-III, and they are sharper than those obtained using KM-I (first row). While KM-III works well for the model problem under consideration, it is not trivial to generalize the method for the more realistic cases with multiple sets of twin boundaries having different orientations. The interfacial stress relaxation method developed in Levitas and Samani (2011) for solid-melt interface may be a possible way to obtain the excess elastic stress-relaxed twin interfaces.

9. Concluding remarks

A thermodynamically consistent novel multi-phase phase field model has been developed for studying stress- and temperature induced martensitic PTs at finite strains. A single order parameter describes austenite to martensitic transformations and another N order parameters have been used to describe the evolution of N martensitic variants. An explicit constraint on the order parameters has been used, which guides in deriving the kinetic laws for the order parameters in a physically consistent manner. The coexistence of three or more phases at a single material point has been penalized in our observer invariant free energy model. Furthermore, to regulate the presence of a third phase and its extent within the interface between any two variants, penalization terms have been considered, which allow one to describe each variant-variant transformation with a single order parameter. This allows to have the analytical solution for each interface, which can be used to calibrate the energy and width of the interface. A comparative study of complex microstructure evolution in various 2-D samples under different loading conditions have been studied under the plane stress condition. The sample size effect on the stationary microstructures and the effect of the triple junction penalization term have been discussed with examples. Three different kinematic models (KMs) for the transformation deformation gradient have been considered. The first two of the models are as follows: in KM-I, it is a linear function of the Bain

tensors of all the variants; in KM-II, it is exponential of a linear combination of the logarithm of the Bain tensors of all the variants. KM-II yields isochoric variant-variant transformations, but KM-I does not.

At this moment it is impossible for the authors to conclude which of the models is to be chosen for the applications. Because to the best of authors' knowledge whether (a) the variant-variant transformations are indeed isochoric or not and (b) the twin boundaries are indeed free of the excess elastic stresses or not are not yet known. They need to be studied using the atomistic simulations. Thus all we can do here is to enumerate the advantages and disadvantages of each of the models:

KM-I: It is simpler and generates lower interfacial stresses than KM-II. However, the volumetric transformation strains across the interfaces are not controlled, and the mechanical part of the thermodynamic driving forces for the order parameters can not be decomposed into volumetric and isochoric parts.

KM-II: It yields isochoric variant-variant transformations and allows to decouple the mechanical part of the driving forces into volumetric and isochoric parts. However, the model is complex and yields significantly higher interfacial stresses.

KM-III: It yields complete relaxation of the excess elastic stresses within the twin boundaries. However, it can be used just for two alternating twin structure, and it is not trivial to generalize the model for the more realistic cases with multiple sets of twin boundaries having different orientations.

Currently, we would choose KM-I as the simplest model, which generates modest interfacial stresses. If it is confirmed through the atomistic simulations that the variant \leftrightarrow variant transformations are indeed isochoric and the twin boundaries are excess elastic stress-free, KM-II supplemented with a stress relaxation mechanism would be the most promising one. A general stress relaxation method within the interfaces is needed, and the method in Levitas and Samani (2011) used for the solid-melt interfaces may be a possible starting point for obtaining the desired interfacial elastic stresses.

Appendix

Appendix A. Time derivative of Helmholtz free energy

In this appendix we derive the material time derivative of the free energy given by Eq. (6) which has been used in Section 4. Taking material time derivative in Eq. (6) we obtain

$$\begin{aligned} \dot{\psi} = & \frac{J_t}{\rho_0} \frac{\partial \psi_e}{\partial \mathbf{F}_e} \cdot \mathbf{F}_t^{-T} : \dot{\mathbf{F}}^T - \frac{J_t}{\rho_0} \mathbf{F}_e^T \cdot \frac{\partial \psi_e}{\partial \mathbf{F}_e} \cdot \mathbf{F}_t^{-T} : \dot{\mathbf{F}}^T + \frac{J_t \psi_e}{\rho_0} \mathbf{F}_t^{-T} : \dot{\mathbf{F}}^T + J(\check{\psi}^\theta + \psi^\nabla) \mathbf{F}^{-T} : \dot{\mathbf{F}}^T + \\ & \sum_{i=0}^N \left(J \frac{\partial(\check{\psi}^\theta + \psi^\nabla)}{\partial \eta_i} + \frac{\partial(\check{\psi}^\theta + \psi_p)}{\partial \eta_i} + \frac{J_t}{\rho_0} \frac{\partial \psi_e}{\partial \eta_i} \Big|_{\mathbf{F}_e} \right) \dot{\eta}_i + J \sum_{i=0}^N \frac{\partial \psi^\nabla}{\partial \nabla \eta_i} \cdot \dot{\nabla} \eta_i + \frac{\partial \psi}{\partial \theta} \dot{\theta}, \end{aligned} \quad (\text{A.1})$$

where we have used $\overline{\dot{\det \mathbf{A}}} = (\det \mathbf{A}) \mathbf{A}^{-1} : \dot{\mathbf{A}}$, and $\overline{\dot{\mathbf{A}}^{-1}} = -\mathbf{A}^{-1} \cdot \dot{\mathbf{A}} \cdot \mathbf{A}^{-1}$ for any second order invertible tensor $\mathbf{A}(t)$. The following term from Eq. (A.1) is rewritten as

$$\sum_{i=0}^N \frac{\partial \psi^\nabla}{\partial \nabla \eta_i} \cdot \dot{\nabla} \eta_i = \sum_{i=0}^N \frac{\partial \psi^\nabla}{\partial \nabla \eta_i} \cdot \overline{(\mathbf{F}^{-T} \cdot \nabla_0 \eta_i)} = \sum_{i=0}^N \left(\mathbf{F}^{-1} \cdot \frac{\partial \psi^\nabla}{\partial \nabla \eta_i} \cdot \dot{\nabla}_0 \eta_i - \nabla \eta_i \otimes \mathbf{F}^{-1} \cdot \frac{\partial \psi^\nabla}{\partial \nabla \eta_i} : \dot{\mathbf{F}}^T \right), \quad (\text{A.2})$$

where we have used $\nabla \eta_i = \mathbf{F}^{-T} \cdot \nabla_0 \eta_i$. Using (A.2) in (A.1) and rearranging the terms, $\dot{\psi}$ turns out to be

$$\begin{aligned} \dot{\psi} = & \left(\frac{J_t}{\rho_0} \frac{\partial \psi_e}{\partial \mathbf{F}_e} \cdot \mathbf{F}_t^{-T} + J(\check{\psi}^\theta + \psi^\nabla) \mathbf{F}^{-T} - J \sum_{i=0}^N \nabla \eta_i \otimes \mathbf{F}^{-1} \cdot \frac{\partial \psi^\nabla}{\partial \nabla \eta_i} \right) : \dot{\mathbf{F}}^T + \sum_{i=0}^N J \mathbf{F}^{-1} \cdot \frac{\partial \psi^\nabla}{\partial \nabla \eta_i} \cdot \dot{\nabla}_0 \eta_i + \frac{\partial \psi}{\partial \theta} \dot{\theta} + \\ & \sum_{i=0}^N \left(J \frac{\partial(\check{\psi}^\theta + \psi^\nabla)}{\partial \eta_i} + \frac{\partial(\check{\psi}^\theta + \psi_p)}{\partial \eta_i} + \frac{J_t}{\rho_0} \frac{\partial \psi_e}{\partial \eta_i} \Big|_{\mathbf{F}_e} \right) \dot{\eta}_i + \left(\frac{J_t \psi_e}{\rho_0} \mathbf{F}_t^{-T} - \frac{J_t}{\rho_0} \mathbf{F}_e^T \cdot \frac{\partial \psi_e}{\partial \mathbf{F}_e} \cdot \mathbf{F}_t^{-T} \right) : \dot{\mathbf{F}}^T. \end{aligned} \quad (\text{A.3})$$

Since \mathbf{F}_t is considered to be a function of all the order parameters, Eq. (A.3) can further be rewritten as

$$\begin{aligned} \dot{\psi} = & \left(\frac{J_t}{\rho_0} \frac{\partial \psi_e}{\partial \mathbf{F}_e} \cdot \mathbf{F}_t^{-T} + J(\check{\psi}^\theta + \psi^\nabla) \mathbf{F}^{-T} - J \sum_{i=0}^N \nabla \eta_i \otimes \mathbf{F}^{-1} \cdot \frac{\partial \psi^\nabla}{\partial \nabla \eta_i} \right) : \dot{\mathbf{F}}^T + \sum_{i=0}^N J \mathbf{F}^{-1} \cdot \frac{\partial \psi^\nabla}{\partial \nabla \eta_i} \cdot \dot{\nabla}_0 \eta_i + \frac{\partial \psi}{\partial \theta} \dot{\theta} + \\ & \sum_{i=0}^N \left(J \frac{\partial(\check{\psi}^\theta + \psi^\nabla)}{\partial \eta_i} + \frac{\partial(\check{\psi}^\theta + \psi_p)}{\partial \eta_i} + \frac{J_t}{\rho_0} \frac{\partial \psi_e}{\partial \eta_i} \Big|_{\mathbf{F}_e} + \left(\frac{J_t \psi_e}{\rho_0} \mathbf{F}_t^{-T} - \frac{J_t}{\rho_0} \mathbf{F}_e^T \cdot \frac{\partial \psi_e}{\partial \mathbf{F}_e} \cdot \mathbf{F}_t^{-T} \right) : \frac{\partial \mathbf{F}_t^T}{\partial \eta_i} \right) \dot{\eta}_i. \end{aligned} \quad (\text{A.4})$$

Appendix B. Inversions and derivatives of \mathbf{F}_t

In this appendix we derive the explicit expressions for various derivatives of the transformation deformation gradient with respect to the order parameters, for all the kinematic models. These relations have been mainly used in analyzing the transformation work and deriving the instability criteria in Sections 4.7 and 5, and thus

obtained considering two martensitic variants and taking the constraint (21) into account. Under this condition \mathbf{F}_t for all the models is listed in Eq. (81).

For KM-I: The derivatives of \mathbf{F}_t given by Eq. (81)₁ are

$$\begin{aligned}\frac{\partial \mathbf{F}_t}{\partial \eta_0} &= \frac{\partial \varphi(a_\varepsilon, \eta_0)}{\partial \eta_0} (\boldsymbol{\varepsilon}_{tj} + \phi_i(\boldsymbol{\varepsilon}_{ti} - \boldsymbol{\varepsilon}_{tj})), & \frac{\partial^2 \mathbf{F}_t}{\partial \eta_0^2} &= \frac{\partial^2 \varphi(a_\varepsilon, \eta_0)}{\partial \eta_0^2} (\boldsymbol{\varepsilon}_{tj} + \phi_i(\boldsymbol{\varepsilon}_{ti} - \boldsymbol{\varepsilon}_{tj})), \\ \frac{\partial \mathbf{F}_t}{\partial \eta_i} &= \varphi(a_\varepsilon, \eta_0) \frac{\partial \phi_i}{\partial \eta_i} (\boldsymbol{\varepsilon}_{ti} - \boldsymbol{\varepsilon}_{tj}), & \frac{\partial^2 \mathbf{F}_t}{\partial \eta_i^2} &= \varphi(a_\varepsilon, \eta_0) \frac{\partial^2 \phi_i}{\partial \eta_i^2} (\boldsymbol{\varepsilon}_{ti} - \boldsymbol{\varepsilon}_{tj}).\end{aligned}\quad (\text{B.1})$$

For KM-II: Using the definition of exponential of a tensor (see Chapter 1 of Jog (2007)) we express \mathbf{F}_t for KM-II (see Eq. (81)₂) as

$$\mathbf{F}_t = \exp(\varphi(a_\varepsilon, \eta_0) \mathbf{H}) = \mathbf{I} + \mathbf{H} \varphi(a_\varepsilon, \eta_0) + \frac{1}{2!} (\varphi(a_\varepsilon, \eta_0) \mathbf{H})^2 + \frac{1}{3!} (\varphi(a_\varepsilon, \eta_0) \mathbf{H})^3 + \dots, \quad (\text{B.2})$$

where $\mathbf{H} = \ln \mathbf{U}_{tj} + \phi_i(\ln \mathbf{U}_{ti} - \ln \mathbf{U}_{tj})$. Taking the derivative in Eq. (B.2) with respect to η_0 and using Eq. (B.2) we can easily show that

$$\frac{\partial \mathbf{F}_t}{\partial \eta_0} = \frac{\partial \varphi(a_\varepsilon, \eta_0)}{\partial \eta_0} \mathbf{H} \cdot \mathbf{F}_t = \frac{\partial \varphi(a_\varepsilon, \eta_0)}{\partial \eta_0} \mathbf{F}_t \cdot \mathbf{H}, \quad (\text{B.3})$$

where we have used that the tensors $\exp(\varphi(a_\varepsilon, \eta_0) \mathbf{H})$ and \mathbf{H} are commutative. Recalling that $\ln(\exp \mathbf{A}) = \mathbf{A}$ for any second order tensor, we write from Eq. (B.3) that $\mathbf{F}_t^{-1} \cdot \frac{\partial \mathbf{F}_t}{\partial \eta_0} = \mathbf{0}$ if $\eta_0 = 0$ (using Eq. (33)) and

$$\mathbf{F}_t^{-1} \cdot \frac{\partial \mathbf{F}_t}{\partial \eta_0} = \frac{1}{\varphi(a_\varepsilon, \eta_0)} \frac{\partial \varphi(a_\varepsilon, \eta_0)}{\partial \eta_0} \ln \mathbf{F}_t \quad \text{if } \eta_0 > 0. \quad (\text{B.4})$$

Differentiating Eq. (B.3) again with respect to η_0 we have

$$\frac{\partial^2 \mathbf{F}_t}{\partial \eta_0^2} = \left(\frac{\partial \varphi(a_\varepsilon, \eta_0)}{\partial \eta_0} \right)^2 \mathbf{H}^2 \cdot \mathbf{F}_t + \frac{\partial^2 \varphi(a_\varepsilon, \eta_0)}{\partial \eta_0^2} \mathbf{H} \cdot \mathbf{F}_t = \left(\frac{\partial \varphi(a_\varepsilon, \eta_0)}{\partial \eta_0} \right)^2 \mathbf{F}_t \cdot \mathbf{H}^2 + \frac{\partial^2 \varphi(a_\varepsilon, \eta_0)}{\partial \eta_0^2} \mathbf{F}_t \cdot \mathbf{H}. \quad (\text{B.5})$$

We will also need an expression for $\partial \mathbf{F}_t / \partial \eta_i$. When $\ln \mathbf{U}_{ti}$ and $\ln \mathbf{U}_{tj}$ are commutative, which is the case at least for the cubic to tetragonal PTs considered in this paper, a simple expression for $\partial \mathbf{F}_t / \partial \eta_i$ can be obtained. For other PTs the Bain tensors may not have this commutative property; for such cases the expression can be complicated and not considered here. Taking the derivative of \mathbf{F}_t with respect to η_i we get

$$\frac{\partial \mathbf{F}_t}{\partial \eta_i} = \frac{\partial \phi_i}{\partial \eta_i} (\ln \mathbf{U}_{ti} - \ln \mathbf{U}_{tj}) \cdot \mathbf{F}_t = \frac{\partial \phi_i}{\partial \eta_i} \mathbf{F}_t \cdot (\ln \mathbf{U}_{ti} - \ln \mathbf{U}_{tj}), \quad (\text{B.6})$$

where it has been assumed that $\ln \mathbf{U}_{ti}$ and $\ln \mathbf{U}_{tj}$ are commutative. The second derivative is

$$\begin{aligned}\frac{\partial^2 \mathbf{F}_t}{\partial \eta_i^2} &= \left(\frac{\partial \phi_i}{\partial \eta_i} \right)^2 (\ln \mathbf{U}_{ti} - \ln \mathbf{U}_{tj})^2 \cdot \mathbf{F}_t + \frac{\partial^2 \phi_i}{\partial \eta_i^2} (\ln \mathbf{U}_{ti} - \ln \mathbf{U}_{tj}) \cdot \mathbf{F}_t \\ &= \left(\frac{\partial \phi_i}{\partial \eta_i} \right)^2 \mathbf{F}_t \cdot (\ln \mathbf{U}_{ti} - \ln \mathbf{U}_{tj})^2 + \frac{\partial^2 \phi_i}{\partial \eta_i^2} \mathbf{F}_t \cdot (\ln \mathbf{U}_{ti} - \ln \mathbf{U}_{tj}).\end{aligned}\quad (\text{B.7})$$

For *KM-III*: The first and second derivatives of \mathbf{F}_t given by Eq. (81)₃ with respect to η_0 and η_i are

$$\begin{aligned}\frac{\partial \mathbf{F}_t}{\partial \eta_0} &= \frac{\partial \varphi(a_\varepsilon, \eta_0)}{\partial \eta_0} (\boldsymbol{\varepsilon}_{tj} + \phi_i \mathbf{m}_t \otimes \mathbf{n}_t), & \frac{\partial^2 \mathbf{F}_t}{\partial \eta_0^2} &= \frac{\partial^2 \varphi(a_\varepsilon, \eta_0)}{\partial \eta_0^2} (\boldsymbol{\varepsilon}_{tj} + \phi_i \mathbf{m}_t \otimes \mathbf{n}_t), \\ \frac{\partial \mathbf{F}_t}{\partial \eta_i} &= \varphi(a_\varepsilon, \eta_0) \frac{\partial \phi_i}{\partial \eta_i} \mathbf{m}_t \otimes \mathbf{n}_t, & \frac{\partial^2 \mathbf{F}_t}{\partial \eta_i^2} &= \varphi(a_\varepsilon, \eta_0) \frac{\partial^2 \phi_i}{\partial \eta_i^2} \mathbf{m}_t \otimes \mathbf{n}_t.\end{aligned}\quad (\text{B.8})$$

In analyzing the transformation work and deriving the instability criteria, we also need to invert \mathbf{F}_t , which we can obtain in this case explicitly using the Woodbury-Sherman-Morrison formula (see, e.g. Chapter 1 of Strang (2007)) as

$$\mathbf{F}_t^{-1} = \mathbf{W}^{-1} - (\varphi(a_\varepsilon, \eta_0) \phi_i / \xi) \mathbf{W}^{-1} \cdot (\mathbf{m}_t \otimes \mathbf{n}_t) \cdot \mathbf{W}^{-1}, \quad (\text{B.9})$$

where $\mathbf{W} = \mathbf{I} + \varphi(a_\varepsilon, \eta_0) \boldsymbol{\varepsilon}_{tj}$ and $\xi = 1 + \varphi(a_\varepsilon, \eta_0) \phi_i \mathbf{W}^{-1} \cdot \mathbf{m}_t \cdot \mathbf{n}_t$.

Acknowledgments

The support of NSF (CMMI-1536925 and DMR-1434613), ARO (W911NF-17-1-0225), ONR (N00014-16-1-2079), and Iowa State University (Vance Coffman Faculty Chair Professorship) are gratefully acknowledged. Simulations were performed at Extreme Science and Engineering Discovery Environment (XSEDE), allocations TG-MSS140033 and MSS170015.

References

- Ankit, K., Nestler, B., Selzer, M., Reichardt, M., 2013. Phase-field study of grain boundary tracking behavior in crack-seal microstructures. *Contrib. Mineral Petrol.* 166, 1709-1723.
- Artemev, A., Wang, Y., Khachaturyan, A.G., 2000. Three-dimensional phase field model and simulation of martensitic transformation in multilayer systems under applied stresses. *Acta. Mater.* 48, 2503-2518.
- Artemev, A., Jin, Y., Khachaturyan, A.G., 2001. Three-dimensional phase field model of proper martensitic transformation. *Acta. Mater.* 49, 1165-1177.

- Artemev, A., Slutsker J., Roytburd, A.L., 2005. Phase field modeling of self-assembling nanostructures in constrained films. *Acta. Mater.* 53, 3425-3432.
- Ball, J.M., James, R.D., 1987. Fine Phase Mixtures as Minimizers of Energy. *Arch. Ration. Mech. Anal.* 100, 13-52.
- Bangerth, W., Davydov, D., Heister, T., Heltai, L., Kanschat, G., Kronbichler, M., Maier, M., Turcksin, B., Wells, D., 2016. The deal.II library, version 8.4. *J. Numer. Math.* 24, 135-141.
- Barsch, G.R., Krumhansl, J.A., 1984. Twin boundaries in ferroelastic media without interface dislocations. *Phys. Rev. Lett.* 53, 1069.
- Basak, A., Levitas, V.I., 2017. Interfacial stresses within boundary between martensitic variants: Analytical and numerical finite strain solutions for three phase field models. *Acta. Mater.* 139, 174-187.
- Bhattacharya, K., 2004. *Microstructure of Martensite: Why It Forms and How It Gives Rise to the Shape-Memory Effect.* Oxford University Press, Oxford.
- Bollada, P.C., Jimack, P.K., Mullis, A.M., 2012. A new approach to multi-phase formulation for the solidification of alloys. *Physica D* 241, 816-829.
- Bulatov, V., Richmond, O., Glazov, M., 1999. An atomistic dislocation mechanism of pressure-dependent plastic flow in aluminum. *Acta Mater.* 47, 3507-3514.
- Chen, L.Q., 2002. Phase-field models for microstructure evolution. *Annu. Rev. Mater. Res.* 32, 113-140.
- Clayton, J.D., 2014. Analysis of shock compression of strong single crystals with logarithmic thermoelastic-plastic theory. *Int. J. Eng. Sci.* 79, 1-20.
- Clayton, J.D., Knap, J., 2011. A phase field model of deformation twinning: Nonlinear theory and numerical simulations. *Physica D* 240, 841-858.
- Clayton, J.D., Knap, J., 2011. Phase field modeling of twinning in indentation of transparent crystals. *Model. Simul. Mater. Sci. Eng.* 19, 085005.

- Diao, J., Gall, K., Dunn, M.L., 2003. Surface-stress-induced phase transformation in metal nanowires. *Nat. Mater.* 2, 656-660.
- Falk, F., 1983. Ginzburg-Landau theory of static domain walls in shape-memory alloys. *Z. Physik. B - Condensed Matter* 51, 177-185.
- Fischer, F.D., Waitz, T., Vollath, D., Simha, N.K., 2008. On the role of surface energy and surface stress in phase-transforming nanoparticles. *Prog. Mat. Sci.* 53, 481-527.
- Folch, R., Plapp, M., 2003. Towards a quantitative phase-field model of two-phase solidification. *Phys. Rev. E* 68, 010602.
- Folch, R., Plapp, M., 2005. Quantitative phase-field modeling of two-phase growth. *Phys. Rev. E* 72, 011602.
- Levitas, V.I., 2000. Structural changes without stable intermediate state in inelastic material. Part II. Applications to displacive and diffusional-displacive phase transformations, strain-induced chemical reactions and ductile fracture. *Int. J. Plast.* 16, 851-892.
- Garcke, H., Nestler, B., Stoth, B., 1999. A multiphase field concept: Numerical simulations of moving phase boundaries and multiple junctions. *Phys. Rev. B* 78, 024113.
- Gibbs, J.W., 1948. *The collected works of J. Willard Gibbs*. Yale University Press, New Haven.
- Gröger, R., Marchand, B., Lookman, T., 2016. Dislocations via incompatibilities in phase-field models of microstructure evolution. *Phys. Rev. B* 94, 054105.
- Gurtin, M.E., Murdoch, A., 1975. A continuum theory of elastic material surfaces. *Arch. Ration. Mech. Anal.* 57, 291-323.
- Hildebrand, F.E., Miehe, C., 2012. A phase field model for the formation and evolution of martensitic laminate microstructure at finite strains. *Phil. Mag.* 92, 1-41.
- Hornbogen, E.J., 1999. Ausforming of NiTi. *J. Mat. Sci.* 34, 599-606.
- Kockar, B., Karaman, I., Kim, J.I., Chumlyakov, Y.I., Sharp, J., Yu, C.J., 2008. Thermomechanical cyclic response of an ultrafine-grained NiTi shape memory alloy. *Acta Mater.* 56, 3630-3646.

- Idesman, A.V., Levitas, V.I., Preston, D.L., Cho, J.Y., 2005. Finite element simulations of martensitic phase transitions and microstructures based on a strain softening model. *J. Mech. Phys. Solids*. 53, 495-523.
- Idesman, A.V., Cho, J.Y., Levitas, V.I., 2008. Finite element modeling of dynamics of martensitic phase transitions. *Appl. Phys. Lett.* 93, 043102.
- Jacobs, A.E., 1992. Finite-strain solitons of a ferroelastic transformation in two dimensions. *Phys. Rev. B*. 46, 8080-8088.
- Javanbakht, M., Levitas, V.I., 2015. Interaction between phase transformations and dislocations at the nanoscale. Part 2. Phase field simulation examples. *J. Mech. Phys. Solids* 82, 164-185.
- Jin, Y.M., Artemev, A., Khachaturyan A.G., 2001. Three-dimensional phase field model of low-symmetry martensitic transformation in polycrystal: Simulation of ζ'_2 martensite in AuCd alloys. *Acta Mater.* 49, 2309-2320.
- Jog, C.S., 2007. *Foundations and Applications of Mechanics. Volume I: Continuum Mechanics*. Narosa, New Delhi.
- Kim, S.G., Kim, D.I., Kim, W.T., Park, Y.B., 2006. Computer simulations of two-dimensional and three-dimensional ideal grain growth. *Phys. Rev. E*. 74, 061605.
- Lei, J.C.H., Li, L.J., Shu, Y.C., Li, J.Y., 2010. Austenite-martensite interface in shape memory alloys. *Appl. Phys. Lett.* 96, 141910.
- Levin, V.A., Levitas V.I., Zingerman, K.M., Freiman, E.I., 2013. Phase-field simulation of stress-induced martensitic phase transformations at large strains. *Int. J. Solids Struct.* 50, 2914-2928.
- Levitas, V.I., 2013a. Phase-field theory for martensitic phase transformations at large strains. *Int. J. Plast.* 49, 85-118.
- Levitas, V.I., 2013b. Thermodynamically consistent phase field approach to phase transformations with interface stresses. *Acta Mater.* 61, 4305-4319.
- Levitas, V.I., 2014. Phase field approach to martensitic phase transformations with large strains and interface stresses. *J. Mech. Phys. Solids* 70, 154-189.

- Levitas, V.I., Javanbakht, M., 2010. Surface tension and energy in multivariant martensitic transformations: Phase-field theory, simulations, and model of coherent interface. *Phys. Rev. Lett.* 105, 165701.
- Levitas, V.I., Javanbakht, M., 2011. Phase-field approach to martensitic phase transformations: Effect of martensite martensite interface energy. *Int. J. Mater. Res.* 102, 652-665.
- Levitas, V.I., Javanbakht, M., 2015. Interaction between phase transformations and dislocations at the nanoscale. Part 1. General phase field approach. *J. Mech. Phys. Solids* 82, 287-319.
- Levitas, V.I., Lee, D.W., 2007. Athermal resistance to an interface motion in phase field theory of microstructure evolution. *Phys. Rev. Lett.* 99, 245701.
- Levitas, V.I., Momeni, K., 2014. Solid-solid transformations via nanoscale intermediate interfacial phase: Multiple structures, Scale and mechanics effects. *Acta Mater.* 65, 125-132.
- Levitas, V.I., Ozsoy, I.B., 2009. Micromechanical modeling of stress-induced phase transformations. Part 1: Thermodynamics and kinetics of coupled interface propagation and reorientation. *Int. J. Plast.* 25, 239-280.
- Levitas, V.I., Ozsoy, I.B., 2009. Micromechanical modeling of stress-induced phase transformations. Part 2: Computational algorithms and examples. *Int. J. Plast.* 25, 546-583.
- Levitas, V.I., Preston, D.L., 2002a. Three-dimensional Landau theory for multivariant stress-induced martensitic phase transformations. I. Austenite \leftrightarrow Martensite. *Phys. Rev. B.* 66, 134206.
- Levitas, V.I., Preston, D.L., 2002b. Three-dimensional Landau theory for multivariant stress-induced martensitic phase transformations. II. Multivariant phase transformations and stress-space analysis. *Phys. Rev. B* 66, 134207.
- Levitas, V.I., Preston, D.L., 2005. Thermomechanical lattice instability and phase field theory of martensitic phase transformations, twinning and dislocations at large strains. *Phys. Lett. A*, 343, 32-39.
- Levitas, V.I., Roy, A.M., 2015. Multiphase phase field theory for temperature- and stress-induced phase transformations. *Phys. Rev. B* 91, 174109.

- Levitas, V.I., Roy, A.M., 2016. Multiphase phase field theory for temperature-induced phase transformations: formulation and application to interfacial phases. *Acta Mater.* 105, 244-257.
- Levitas, V.I., Samani, K., 2011. Coherent solid-liquid interface with stress relaxation in a phase-field approach to the melting/freezing transition. *Phys. Rev. B* 84, 140103.
- Levitas, V.I., Warren, J.A., 2016. Phase field approach with anisotropic interface energy and interface stresses: large strain formulation. *J. Mech. Phys. Solids* 91, 94-125.
- Levitas, V.I., Chen, H., Xiong, L., 2017. Lattice instability during phase transformations under multiaxial stress: modified transformation work criterion. *Phys. Rev. B* 96, 054118.
- Levitas, V.I., Idesman, A.V., Preston, D.L., 2004. Microscale simulation of martensitic microstructure evolution. *Phys. Rev. Lett.* 93, 105701.
- Levitas, V.I., Preston, D.L., Lee, D.W., 2003. Three-dimensional Landau theory for multivariant stress-induced martensitic phase transformations. III. Alternative potentials, critical nuclei, kink solutions, and dislocation theory. *Phys. Rev. B* 68, 134201.
- Levitas, V.I., Roy, A.M., Preston, D.L., 2013. Multiple twinning and variant-variant transformations in martensite: Phase-field approach. *Phys. Rev. B* 88, 054113.
- Levitas, V.I., Henson, B.F., Smilowitz, L.B., Asay, B.W., 2004. Solid-solid phase transformation via virtual melt, significantly below the melting temperature. *Phys. Rev. Lett.* 92, 235702.
- Levitas, V.I., Levin, V.A., Zingerman, K.M., Freiman, E.I., 2009. Displacive phase transitions at large strains: Phase-field theory and simulations. *Phys. Rev. Lett.* 103, 025702.
- Levitas, V.I., Ren, Z., Zeng, Y., Zhang, Z., Han, G., 2012. Crystal-crystal phase transformation via surface-induced virtual pre-melting. *Phys. Rev. B* 85, 220104.
- Li, Y.L., Hu, S.Y., liu, Z.K., Chen, L.Q., 2001. Phase-field model of domain structures in ferroelectric thin films. *App. Phys. Lett.* 78, 3878-3880.

- Li, S., Ding, X., Li, J., Ren, X., Sun, J., Ma, E., Lookman, T., 2010. Inverse martensitic transformation in Zr nanowires. *Phys. Rev. B* 81, 245433.
- Moelans, N., Blanpain, B., Wollants, P., 2008. Quantitative analysis of grain boundary properties in a generalized phase field model for grain growth in anisotropic systems. *Phys. Rev. B.* 78, 024113.
- Moelans, N., Wendler, F., Nestler, B., 2009. Comparative study of two phase-field models for grain growth. *Physica D* 46, 479-490.
- Momeni, K., Levitas, V.I., 2014. Propagating phase interface with intermediate interfacial phase: Phase field approach. *Phys. Rev. B* 89, 184102.
- Momeni, K., Levitas, V.I., 2016. Phase-field approach to nonequilibrium phase transformations in elastic solids via intermediate phase (melt) allowing for interface stresses. *Phys. Chem. Chem. Phys.* 18, 12183.
- Momeni, K., Levitas, V.I., 2015. A Phase-field approach to solid-solid phase transformations via intermediate interfacial phases under stress tensor. *Int. J. Solids Struct.* 71, 39-56.
- Momeni, K., Levitas, V.I., Warren, J.A., 2015. The strong influence of internal stresses on the nucleation of a nanosized, deeply undercooled melt at a solid-solid interface. *Nano Lett.* 15, 2298.
- Nestler, B., 2005. A 3D parallel simulator for crystal growth and solidification in complex alloy systems. *J. Cryst. Growth* 275, e273-e278.
- Petryk, H., Stupkiewicz, S., 2010. Interfacial energy and dissipation in martensitic phase transformations. Part I: Theory. *J. Mech. Phys. Solids* 58, 390-408.
- Petryk, H., Stupkiewicz, S., 2010. Interfacial energy and dissipation in martensitic phase transformations Part II: Size effects in pseudoelasticity. *J. Mech. Phys. Solids* 58, 373-389.
- Pitteri, M., Zanzotto, G., 2003. *Continuum Models for Phase Transitions and Twinning in Crystals*. Chapman & Hall/CRC, Boca Raton.
- Roytburd, A.L., 1974. Theory of formation of heterophase structure under phase transformation in solid state. *Sov. Phys. Uspekhi* 17, 32-55.

- Roytburd, A.L., Slutsker, J., 2001. Deformation of adaptive materials, Part III: deformation of crystals with polytwin product phases. *J. Mech. Phys. Solids* 49, 1795-1822.
- Ruddock, G., 1994. A microstructure of martensite which is not a minimiser of Energy: the X-interface. *Arch. Rational Mech. Anal.* 127, 1-39.
- Schneider, D., Tschukin, O., Choudhury, A., Selzer, M., Böhlke, T., Nestler, B., 2015. Phase-field elasticity model based on mechanical jump conditions. *Comput. Mech.* 55, 887-901.
- Schryvers, D.N., 1993. Microtwin sequences in thermoelastic $\text{Ni}_x\text{Al}_{100-x}$ martensite studied by conventional and high-resolution transmission electron microscopy. *Phil. Mag. A* 68, 1017-1032.
- Seol, D.J., Hu, S.Y., Li, Y.L., Chen, L.Q., Oh, K.H., 2002. Computer simulation of martensitic transformation in constrained films. *Mater. Sci. Forum* 408-412, 1645-1650.
- Seol, D.J., Hu, S.Y., Li, Y.L., Chen, L.Q., Oh, K.H., 2003. Cubic to tetragonal martensitic transformation in a thin film elastically constrained by a substrate. *Metals Mater. Int.* 9, 221-226
- Slaughter, W.S., 2002. *The Linearized Theory of Elasticity*. Springer, New York.
- Steinbach, I., Pezzolla, F., Nestler, B., Seeßelberg, M., Prieler, R., Schmitz, G.J., Rezende, J.L.L., 1996. A phase field concept for multiphase systems. *Physica D* 94, 135-147.
- Steinbach, I., Pezzolla, F., 1999. A generalized field method for multiphase transformations using interface fields. *Physica D* 134, 385-393.
- Steinbach, I., Apel, M., 2006. Multi phase field model for solid state transformation with elastic strain. *Physica D* 217, 153-160.
- Steinbach, I., 2009. Phase-field models in materials science. *Model. Simul. Mater. Sci. Eng.* 17, 073001.
- Strang, G., 2007. *Computational Science and Engineering*. Wellesley-Cambridge Press, Wellesley.
- Tóth, G.I., Morris, R., Gránási, L., 2011. Ginzburg-Landau-type multiphase field model for competing fcc and bcc nucleation. *Phys. Rev. Lett.* 106, 45701.

- Tóth, G.I., Pusztai, T., Tegze, G., Tóth, G., Gránási, L., 2011. Amorphous nucleation precursor in highly nonequilibrium fluids. *Phys. Rev. Lett.* 107, 175702.
- Tóth, G.I., Pusztai, T., Gránási, L., 2015. Consistent multiphase-field theory for interface driven multidomain dynamics. *Phys. Rev. B* 92, 184105.
- Tűma, K., Stupkiewicz, S., 2016. Phase-field study of size-dependent morphology of austenite-twinned martensite interface in CuAlNi. *Int. J. Solids Struct.* 97-98, 89-100.
- Tűma, K., Stupkiewicz, S., Petryk, H., 2016. Size effects in martensitic microstructures: Finite-strain phase field model versus sharp-interface approach. *J. Mech. Phys. Solids* 95, 284-307.
- Wayman, C.M., 1964. *Introduction to the Crystallography of Martensitic Transformation*. Macmillan, New York.
- Xu, H., Tan, S., Müller, I., 1998. In-situ beobachtung der thermo- und spannungs induzierten martensitischen phasenumwandlung. *Z. Metallkd.*, 89, 59-64.
- Zheng, Q.S., 1994. Theory of representations for tensor functions - A unified invariant approach to constitutive equations. *Appl. Mech. Rev.* 47, 545-587.
- Zienkiewicz, O.C., Taylor, R.L., 2000. *The Finite Element Method: Volume 1- The Basis*. Butterworth-Heinemann, Woburn.
- Zienkiewicz, O.C., Taylor, R.L., 2000. *The Finite Element Method: Volume 2- Solid Mechanics*. Butterworth-Heinemann, Woburn.